FINAL TECHNICAL REPORT

Report Period
(September 27, 1995 to April 30, 2001)

POC-SCALE TESTING OF A DRY TRIBOELECTROSTATIC SEPARATOR FOR FINE COAL CLEANING

By

R.-H. Yoon, G. H. Luttrell, E. S. Yan and A. D. Walters

Center for Coal and Minerals Processing
Virginia Polytechnic Institute & State University
Blacksburg, Virginia 24061-0258

Contract Number:

DE-AC22-95PC95151

Contracting Officer's Representative
Carl Maronde
U.S. Department of Energy
National Energy Technology Laboratory
P.O. Box 10940
Pittsburgh, Pennsylvania 15236

Disclaimer

Table of Contents

List of Figures

List Of Tables

Executive Summary

The National Energy Technology Laboratory (NETL) developed a novel triboelectrostatic separation (TES) process for fine coal cleaning. This process was proven in bench-scale tests to be capable of better than 90% removal of pyritic sulfur and greater than 70% reduction of ash for a number of eastern U.S. coals. Since this technology is a dry process, it offers the advantages of lower ancillary costs and improved environmental acceptability as compared to wet processes. It was considered that the TES process would best be installed in-line at a power station, which allows existing pulverization equipment to be used for size reduction.

In order to demonstrate the merits of the TES process, a 200-250 kg/hr proof-of-concept (POC) separator unit was installed and operated at the Center for Coal and Minerals Processing (CCMP) Pilot Plant at Virginia Tech. The POC circuit was designed using scale–up data obtained from test programs conducted at CCMP using bench-scale test units. These test programs consisted of the development of a triboelectrostatic charging system and an electrostatic separator. Initially both the tribocharger and the separator tests were conducted using equipment designed with a nominal capacity rating of approximately 1 kg/hr. These tests were followed by the design, construction and testing of a tribocharger and a separator both with capacities of approximately 10-40 kg/hr. A variety of feed stocks were tested at both bench-and POC-scale, namely:

- raw and clean coals from a preparation plant,
- grinding mill rejects from power plants,
- grinding mill intermediate products from a power plant,
- pulverized coal from a power plant.

The performance standard set for the triboelectrostatic charger was a minimum standard specific charge of 50μC/ kg. The standard for the triboelectrostatic separator was the rejection of 50% of the feed coal mineral matter while maintaining a combustible recovery of at least 80% by weight.

Charger Design

A variety of materials and charger configurations were studied and a turbocharger made of Plexiglas, which met the standard specific charge density of 50μC/kg and provided the best separator performance efficiency. The superior separator performance was attributed to the charger design maximizing particle-particle and particle-wall interaction.

Separator Design

Three types of separators were constructed and tested, namely:

- Rotating Drums
- Plate-type separators
- Pie configuration separator with interchangeable electrodes-screen, horizontal rod, vertical rod and drum

The separator with pie configuration screen-type electrodes gave the overall best performance. The separator was capable of reducing the ash content from 46.7% to 10% with a combustible recovery of 60% and an ash rejection of 92%. The test data also showed that the performance of the screen-type unit did not deteriorate significantly within the feed rate range of 6-44 kg/hr.

POC Electrostatic Separator Design and Test Results

Design

Data obtained from the separator test program was used to design the charger and separator incorporated into the 200-250 kg/hr. POC test unit. The design consisted of pulverized coal passing through a Triboelectrostatic charger and feeding a separator consisting of screen electrodes set in a pie configuration. The unit was designed to operate under a net positive pressure in a nitrogen atmosphere. The electrical field strength voltage could be varied up to 70 kV between the electrodes (up to 35 kV on each electrode). Clean coal and rejects were removed through an air lock system with provision being made for recirculation of by-pass material (middlings). Carpco Inc., built the unit.

Test Results

The following general conclusions were made.

1. Biasing the feed point or relative electrode position did not make a significant difference to separation efficiency.
2. Combustion recovery and ash rejection remained relatively constant when the relative humidity was held below 50%. Combustible recovery begins to deteriorate as the relative humidity increases to 60% and a further sharp decrease occurs at 70%, with little charge in ash content of the clean coal product.

Electrode Position and Splitter Setting

Tests carried out to evaluate the relative position of the electrodes and the splitter setting showed that as the distance between the cathode and splitter increased, (i) the amount of recycled material decreased, (ii) the ash content of this material decreased (because more of the middlings reported to the clean coal product), (iii) the change in recovery due to recycling was minimal, and (iv) for the coal being tested, there was no benefit to recycling middlings.

Particle Size

Tests carried out on various size fractions indicated that the best results were obtained with 35 meshx0 particles.

Applied Potential

Tests indicated that coal recovery decreased with increasing electrode potential difference. A possible explanation is that the charge on the coal particles was substantially higher than that on the ash forming minerals. At low potentials, highly charged coal particles could have been recovered in preference to weakly charged ash forming minerals, resulting in high recoveries. As the potential difference was increased, weakly charged ash particles and some of the middlings were then pulled towards the cathode causing a decrease in recovery.

Charger

Combustible recovery increased with increasing impeller speed, which suggests that coal recovery increased with increasing charge on the coal particles.

Electrode Type

Shielded or coated electrodes provided a superior level of performance when compared to unshielded electrodes. This improvement in performance is believed to be due to prevention of accidental charge reversal when selectively charged particles collide with uncoated electrodes.

POC Performance

In general the POC unit could not reproduce results obtained in the bench scale and fell well short of the required separation efficiency of 50% combustible recovery and 80% ash rejection.

Introduction

Numerous advanced coal cleaning processes have been developed in recent years that are capable of substantially reducing both ash- and sulfur-forming minerals from coal. However, most of the processes involve fine grinding and use water as the cleaning medium; therefore, the clean coal products must be dewatered before they can be transported and burned. Unfortunately, dewatering fine coal is costly, which makes it difficult to deploy advanced coal cleaning processes for commercial applications.

As a means of avoiding problems associated with the fine coal dewatering, the National Energy Technology Laboratory (NETL) developed a dry coal cleaning process in which mineral matter is separated from coal without using water. In this process, pulverized coal is subjected to triboelectrification before being placed in an electric field for electrostatic separation. The triboelectrification is accomplished by passing a pulverized coal through an in-line mixer made of copper. Copper has a work function that lies between that of carbonaceous material (coal) and mineral matter. Thus, coal particles impinging on the copper wall lose electrons to the metal thereby acquiring positive charges, while mineral matter impinging on the wall gain electrons to acquire negative charges. The charged particles then pass through an electric field where they are separated according to their charges into two or more products depending on the configuration of the separator. The results obtained at NETL showed that it is capable of removing more than 90% of the pyritic sulfur and 70% of the ash-forming minerals from a number of eastern U.S. coals. However, the BTU recoveries were less than desirable.

The laboratory-scale batch triboelectrostatic separator (TES) used by NETL relied on adhering charged particles on parallel electrode surfaces and scraping them off. Therefore, its throughput will be proportional to the electrode surface area. If this laboratory device is scaled-up

as is, it would suffer from low throughput capacities and high maintenance requirements. In general, surface area-based separators (e.g., shaking tables, magnetic drum separator, electrodynamic separator, etc.) have lower throughput capacities than volume-based separators (e.g., flotation cell, dense-medium bath, cyclones, etc.) by an order of magnitude. Furthermore, the electrodes of the laboratory unit need to be cleaned frequently, creating a high maintenance requirement if it is scaled-up to a commercial unit. The bench-scale continuous TES unit developed at NETL, on the other hand, separates positively and negatively charged particles by splitting the gaseous stream containing these particles in an electric field by means of a flow splitter, so that the oppositely charged particles can be directed into different compartments. This device is fundamentally different from the laboratory unit in that the former is a surface area-based separator, while the latter is a volume-based separator. The bench-scale unit is referred to as an *entrained flow* separator by the in-house researchers at NETL. Thus, the entrained flow TES unit is a significant improvement over the laboratory unit with regard to throughput capacity.

In the present work, the entrained flow separator concept will be utilized for developing a proof-of concept (POC) separator that can be scaled-up to commercial size units. To accomplish this, it is necessary to develop a bench-scale separator that can achieve high Btu recoveries while maintaining the high degree of separation efficiencies. It is the objective of the present investigation to develop an efficient separator by studying the mechanisms of triboelectrification and investigating better ways of separating the charged particles. An important criterion for developing efficient separators is that they not only provide high separation efficiencies but also have high throughput capacities, which are essential ingredients for successful commercialization.

Theory

Triboelectrostatic Separation

Triboelectrostatic separation involves charging of particles by contact or friction, either with other particles or with a contact surface, followed then by passing the charged particles through an electric field that separates these particles according to the magnitude and sign of their charge. The principle of this separation technique is based on the difference in the surface charge developed of various components comprising the mixture. Therefore, most of the research and development attempts have been directed at the charging step, i.e. acquiring sufficient selectivity, producing enough magnitude of charge, and solving the aerodynamic problems associated with charging and transporting fine particles. From the literature, most of the triboelectrostatic separation applications involve a metal-insulator contact, although an insulator-insulator contact is also of substantial interest.

Earlier triboelectrostatic separators normally charged the particles by means of sliding particles down, or transporting particles through chutes, pipes or nozzles. Until recently, cyclones and fluidized beds have been developed to serve as the tribocharging devices. It is believed that more frequent and presumably better particle charging from particle-particle and/or particle-wall contacts would enhance the separation efficiency. Grinding has also been reported as an alternative means of particle tribocharging, and it is of interest that simultaneous grinding methods may be capable of sizing and, at the same time, maintaining the triboelectric separation of particles. The other charging device was a *"turbocharge*r" which consists of a rotor provided with radial blades in order to create more intense turbulence and stronger contact forces. An *in-line static mixer* has been introduced for charging particles (Link et al., 1990; Finseth et al., 1992), as it provides a large number of particle-particle and/or particle-wall collisions over a

short period of time. It is suggested, though, that any attempts to achieve reliable particle charging should be solidly involved in the relevance of the charging devices to the characteristics of the particles to be separated, along with the applications.

Probably the most successful application of the triboelectrostatic separation technique is known to be in the potash mineral salt industry. The successful work on electrostatic separation of salt began in 1953 at the Potash Research Institute in Hanover, Germany (Fricke, 1977). It is based on the premise found earlier in the late 1940s that salts, potassium chloride (sylvite) and sodium chloride (halite), would become selectively charged by contact electrification. Later in 1956, the process was improved by using the conditioning reagents (inorganic or organic) to pretreat the mixture prior to charging and separation. In a fluidized bed dryer, the salt particles become charged through heating, controlled humidity and multiple contacts between particles. To date, the free-fall triboelectrostatic separation techniques have been used to treat more than 10 million tons of salts per year.

The applications of triboelectrostatic separation technologies in the beneficiation of various minerals and coals are also of great significant. It appears that Inculet and his group (Inculet and Bergougnou, 1973; Inculet et al., 1979; Inculet et al., 1980) are among the first researchers who have modified the fluidized bed techniques for minerals triboelectrostatic beneficiation, and the results they obtained were very impressive. Most of the early work on fluidized bed techniques in mineral beneficiation merely involved other particle charging mechanisms, such as corona charging. In the fluidized bed techniques, a fluidized bed was used, combined with gravity feeding, to pre-charge the particles triboelectrically, and thereafter the particles were allowed to fall through the separation cells. It is apparent that the fluidization produces an individualized charged particle through its multiple collisions. This creates the selective tribocharge on the particles so that the electrical separation can be efficiently achieved.

Evidently, fluidized bed techniques have drawn relatively more attention to the tribocharging applications for mineral beneficiation when compared to the others, namely, cyclone techniques.

Carta and his group, at the University of Cagliari in Italy (Carta, et al., 1968 and 1970), has developed cyclone tribocharging separators to beneficiate barite, feldspars, fluorspar, and several coals. The separation processes involving the similar device, cyclone tribocharger, have been carried out for various minerals, i.e., dolomite, quartz and apatite, by Pearse and Pope (Pearse and Pope, 1975), while the cyclone tribocharger has also been used for clay and coal beneficiation by Masuda and his colleagues (Masuda et al., 1981 and 1983). The results acquired by these researchers claimed that a satisfactory separation was accomplished by using a triboelectric cyclone separator. The other charging apparatus commonly used for the applications of the triboelectrostatic separation for various minerals and coals beneficiation is a "dilute-phase loop," or a pneumatic conveyer (Kittaka et al., 1979; Nieh and Nguyen, 1987; Schaefer, 1995; Kanazawa et al., 1995). It is used mostly for the very fine particles. The particle charging is accomplished through the contacts of particles with the copper (or other materials) wall of the loop, or with multi-blades within the loop (Link, 1990, Finseth, 1994), as well as the particle-particle contacts. Indeed, the loop is similar in principle to the cyclone, in which the particles acquire a charge largely through the particle-wall collisions.

One of the important applications of the triboelectric separation is in plastics and polymers. Many attempts have been made to separate mixed plastics or polymers based on their triboelectric properties. Many studies of triboelectrification of polymers have been carried out in recent years (Lowell and Rose-Innes, 1980), in order to obtain more knowledge regarding the charging behavior of polymers.

Triboelectrostatic Separation for Coal Beneficiation

For electrostatic beneficiation of coal, many recent studies have focused on utilizing the triboelectrification method for particle charging. The studies have demonstrated various aspects of using triboelectric charging techniques. The earliest experiments were conducted by Blacktin and Robinson in 1931. In their work, the mixture of coal dust and air were blown at high velocities through a large-diameter iron pipe. Later in 1941, Niggermann had his description of a simple free-falling stream separator, in both laboratory and industrial sizes that was tested on several coals. Noticeably, most of the early charging processes for coal triboelectric separation were by sliding particles down, or transporting particles through a pipe or nozzle. These include the work of Von Szantho (1939, 1949), Herzderfer and Krajewski (1951), and Olofinskii (1957). Niggermann's work was performed using an unsized coal containing all the fine dust. On the other hand, Kühlwein (1941) carried out the tests on coals from which the finest dust had been removed. However, both investigators found an agreeable result in which the higher the rank of the treated coal, the more favorable were the electrical characteristics of the coal substance, until an optimum was reached. Turning now to more recent work on coal beneficiation. Singewald (1974) had his patent in 1974 on the process for triboelectrostatic separation of pyrite from crude coal, using a free falling plate-type separator. The process is claimed to be improved by preconditioning substances with selected fatty acid glycerides and recycling the intermediate fraction into the initial state. However, the separation may have to be repeatedly performed for several states. In trying to improve the separation performance, attempts have been made to establish the most effective charging processes. Many charging techniques have been considered to substitute the ordinary way of particle charging. In the past, fluidized beds were used with corona and/or tribocharging combined with extractive electrodes to beneficiate black and brown coals (Koncar-Djurdevic, 1962 and Bendfeldt, 1969). Until recently, Inculet and his co-workers

(1980) have made their effort to study the triboelectrification of coal-clay specimens by using fluidization technique. They concluded that fluidization is a practical way to generate the tribocharge. During the same time, Inculet, et al. (1980), have also reported their studies on the triboelectrification of ultra-finely ground and finely ground Canadian coal using a closed-loop system where the particles can be re-circulated for a more efficient separation. The fluidization technique was also employed by Gidaspow, et al. (1987), for coal desulfurization. They pioneered a design concept called "electrostatic sieve" and measured the average charge on particles using an electrostatic ball probe, with the addition of a Faraday cage. The work on cyclone tribocharging separation of coal by Carta and his group (1968, 1970) has been mainly concerned with pyrite removal. The results were mentioned to be fairly good, with 39-71% ash rejects. Mazuda, et al. (1983) have developed a Cyclone-Tribocharger with a copper wall, and pointed out that it is important to select the wall materials according to composition of the mineral inclusions in coal. Laboratory test work with contact charging of minerals using a lined air cyclone prior to electrostatic separation has been reported with success on laboratory/pilot scale (Carta, et al., 1981).

In 1986, Rich patented a tubular turbocharger and reported the unexpectedly high differential electrical charges to particles in a pulverized mixture of coal and mineral matters. A twin-rotor charging device has been developed by Agus, et al. (1990) to create a more intense turbulence and, consequently, a stronger contact force. In more current research, Schaefer, et al. (1994) have investigated the triboelectrification and electrostatic separation of coal and constituent minerals using two different charger geometries: i.e., a multiple-loop coil system and an in-line static mixer. They have developed a non-intrusive, laser-based, Phase Doppler velocimeter system to monitor the characteristics of particle charging and the motion of individual charged particles through an electric field. Link et al. (1990) have studied the

triboelectrostatic separation for ultra-fine coal cleaning, in which the tribocharging was accomplished by passing finely pulverized coal through a helix formed from a long section of copper tubing. The test results using a parallel plate separator showed good separation for Pittsburgh No.8, Illinois No.6, and Upper Freeport coal samples. Finseth et al. (1994) continued the investigation by using an in-line static mixer charger as a tribocharger.

From the research standpoint, it is interesting to note that the particle charging process plays an important role in the electrical separation for coal beneficiation. The separation efficiency -defined here as the recovery of combustible matter minus the recovery of ash in the same product - depends critically on the surface charge of the components involved. The premise that coal and mineral matter can be triboelectrically charged differently when a third material is appropriately chosen has brought the tribo- or contact electrification into a great deal of attention.

Contact Electrification or Triboelectrification

General

Triboelectrification or contact charging is one of the most practical and economical charging processes by which the selective charging of particulate material can be accomplished for electrostatic separation. The phenomenon occurs when two materials are touched or rubbed together and the electrical charge is transferred from one to another.

Despite the fact that tribo- or contact charging is the oldest studied electrical phenomenon, it is still not clearly known why the charge transfers between the two materials, particularly with regard to insulators. The confusion and difficulties can mainly arise from the definitions of various terms involved (such as “contact,” “rubbing” or “frictional”), the given combination of materials, the different experimental conditions, the experimental limitations, and insufficiently sophisticated experimental techniques. Unfortunately, earlier works relevant to the

triboelectrification phenomenon have been comprehensively reviewed by a relatively small number of authors, compared with those in the other electrical-relating areas. Still, substantial reviews of the early investigations have been well established in considerable work (Vick, 1953; Loeb, 1957; Montgomery, 1959; Harper, 1967; Robinson, 1969; Seanor, 1972; Lowell and Rose-Innes, 1980; and Kelly and Spottiswood, 1989). Many references also include extensive citations to any earlier work in this field that is not listed in this report. In the last few decades, significant progress has been made towards an understanding of the contact electrification, both into the theoretical perception of the charging mechanism and the importance of contact electrification (or static electrification) in industry. The investigations have been spaciously carried out for many combinations of various materials, with great concern in the fundamental processes of triboelectric charging.

A short history of the very early work on contact electrification is well provided by Pounder (1977), while the more recent reviews and discussions which contribute directly to the contact electrification of solids are indicated by Krupp (1971) and Fuhrmann (1977). Pounder surveyed a number of ideas proposed to explain the tribocharging mechanism from the time of 1600 to the end of the 19th century. For the more up-to-date work, the basic concept and recent experimental results dealing with contact electrification of dielectric solids, particularly polymers, were well summarized by Fuhrmann. The review by Krupp mainly included the essential principles involving inorganic materials (i.e., metals and semiconductors, and organic materials), also in particular with polymers. Interestingly enough, in the discussion of the paper by Krupp, the result from the field effect measurement performed on *anthracene crystals* was mentioned by Bauser, one of Krupp's colleagues. The positive space charge was found on the anthracite crystals when they were left exposing to air after cleavage. It was presumably explained that there were negatively charged surface states owing to the dislocation moving

through the lattice. This dislocation would then transport the negative charge to the crystal surface, whereas the positive space charge remained in the bulk of the crystal. However, the surface charging on the anthracene crystals indicated in the discussion was a result of deformation and cleavage, which is a method of generating electric charge on solid surface and does not share the same complete mechanism with the contact charging. Seemingly, the most impressive review concentrating on the theory of contact electrification has been made by Lowell and Rose-Innes (1980). A large number of works contributed to the theoretical understanding have been summarized along with the opinion of the authors and the significant discussions

Theoretical Overview

The theory of the contact electrification or triboelectrification has been researched for many years. Still, there remains a largely unsolved problem and some far-from-conclusive points in such phenomenon, especially about the true nature of charge transfer. In general, tribocharging is the process whereby a charge exists on a material after departing from the contact with a dissimilar material and the two materials can be any combination of conductor, semiconductor, or insulator (dielectric). Although it is thought that contact charging is the result of electron transferring from one body to the other (Rose-Innes, 1980), there is evidence in some cases that the charge transfer in contact charging can occur by ion transfer (Harper, 1967; Gaudin, 1971) and material transfer (Salanek et al., 1976). It is a common observation that the tribocharging process involves at least two physical mechanisms, which are equally vital in determining the electrification. Those two phenomena are: i) the charge transfer during the contact of two materials (across the interface at the point of contact) and ii) the back-tunneling of charge (the charge backflow) during separation. The contact electrification of solids is now generally explained by means of the *work functio*n, whereas some investigators may have controversially

proposed their explanations based on the other hypotheses. It is noted that, when two materials with different work functions come into intimate contact, electrons flow from the one of lower work function to the one of higher work function (Figure 1). Charge will flow in a direction determined by the work function parameters until the Fermi levels at the surface are equal. The magnitude of the final charge will actually be the outcome of two processes: the charge transfer that occurs during the contact and the charge backflow occurring as the materials are separated (Kelly and Spottiswood, 1989).

Before considering the statements above in any detail, it is helpful to state exactly the definitions of the terms that will be using frequently in the further theoretical discussions:

(a) *Work function* is defined as the energy required to remove an electron from its *Fermi Level*, E_F, the level in which the probability of finding an electron is 0.5. If an electron moves from just outside to inside the solid, it loses energy ø, the work function of the solid. The work function of the solid, denoted as ø, depends on the nature of the solid and not on how much charge it carries. It is governed by the energy of the Fermi Level. Nevertheless, work function values have been reported to depend not only on the nature or internal structure of the material

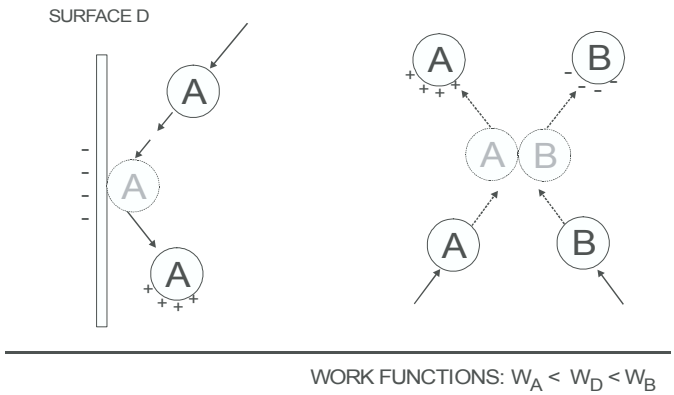

Figure 1 Triboelectrification mechanisms explained by means of the work function

but also on its surface condition, such as bearing of oxides and/or surface contamination (Inculet, 1984).

(b) *Surface Potential*: Suppose that the energy of an electron at an infinite distance from the solid is, by definition, zero. If the solid carries a positive charge, an amount of work eV_s must be done to remove an electron from just outside the solid surface to infinity; V_s is the surface potential, and e is the charge on the electron. Basically, the surface potential depends on the charge carried by the solid, but does not depend on the nature of the solid.

(c) *The electrochemical potential*, ξ, is the energy which must be given to an electron to move it from the Fermi Level to infinity, $\xi = \phi + eV_s$. It is likely that the electrochemical potential has a similar meaning to the work function. But if it is observed more precisely, the electrochemical potential is the free energy of an electron rather than its energy, although the difference is so small for metals at ordinary temperature.

i) Phenomena of Contact Electrification

Practically, all materials acquire a charge when touched or made contact by a dissimilar material. This contact-charging phenomenon can be the result of the combination of any metal (conductor), semiconductor, or dielectric (insulator), which are brought into contact. It is particularly important that the following discussion of the phenomena of contact electrification will begin with a discussion of metal-metal contacts. This is because the theory of the contact electrification of metals has been successfully described with no existing conflict of ideas, and used primarily as a basis for many attempts to explain the contact charging mechanisms of other combinations: i.e., metal-insulator and insulator-insulator.

a) Metal-Metal Contacts

In looking over the theory of the contact electrification, undoubtedly, contact charging of metals is of great significance. It is often thought that the charge transfer between two metals by contact electrification is rather improbable, since the charging of metals is not quite noticeable under most circumstances. Indeed, the charge transfer across the interface between two metals, when the two metals with difference in work functions are brought into contact, may be greater than the charge transfer between a metal and an insulator. However, the high conductivity of the metals allows the charge to run away readily from the region of contact. Moreover, the charge back-flow that usually occurs as the materials are parted happens very quickly in the case of poor insulators (or metals), so that the total charge deposited remains relatively small. Nonetheless, the contact electrification of metals should be carried out in vicinity where there is no electric field or stray alternating fields, because such fields can cause charge transfer by any means but normal contact (for instance, induction). The mechanism of charge transfer in metals is quite crystal-clear, considering the electron states in metals are reasonably simple and well understood. In metals, there is a band of allowed electron states that is filled up to the Fermi energy, E_F. The work function, ϕ, of the metal is the amount of energy by which its Fermi level lies below the vacuum level. When two metals with different work functions, ϕ_A and ϕ_B, are in contact, the charge transfer occurs in such a way that the electrons flow from the metal with the higher Fermi energy into that with the lower Fermi energy (Figure 2). The transfer of these electrons increases the electron potential of B relative to A and terminates when the Fermi energies of A and B equalize. Accordingly, the charge transfer should be proportional to the difference in the work functions between the two metals,

$$Q \propto (\phi_B - \phi_A). \qquad [1]$$

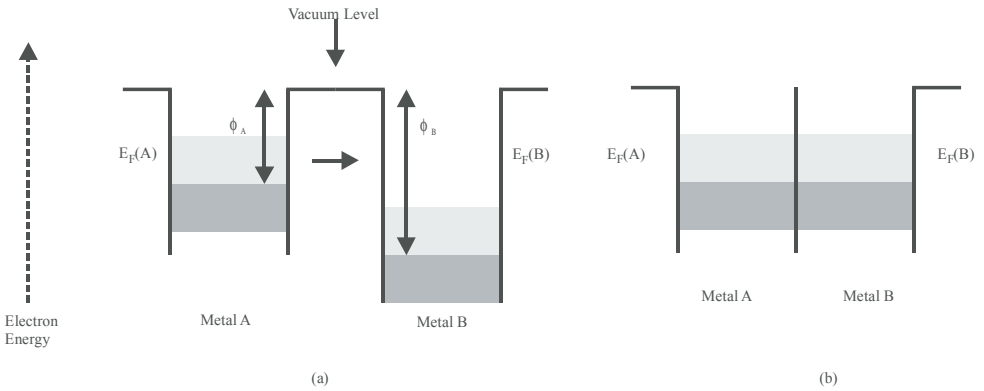

Figure 2 The mechanism of charge transfer in metals, (a) before contact, (b) after contact (after Lowell and Rose-Innes, 1980).

Apparently, the theory of the contact electrification of metals is based on the assumption that when two metals are in contact with each other, charge is transferred between them until their Fermi levels are brought into coincidence. The electrons are exchanged between those two metals so that they come into *thermodynamic equilibriu*m; that is the electrochemical potentials are the same throughout the two metals. Then the difference in the surface potentials of metals will be

$$Vc = (\phi_B - \phi_A) / e, \qquad [2]$$

Where *Vc* is called the *contact potential differenc*e and *e* is the charge on the electron. It seems, therefore, that the charge on the metals during their contacts is given by the aftermath of *Vc* and the effective capacitance between them. The situation when the metals are separated after contact is also of importance in the theory of contact electrification of metals. Harper (1967) pointed out that electrons will tunnel between the metals while they are separating, as long as the distance between them is small enough. As the metals separate, the capacitance between the two metals is found to be decreasing and the surface potential difference for a given charge becomes increasing. In trying to retain the thermodynamic equilibrium, electrons will tend to tunnel

across the gap between the metals, so that the potential difference is maintained equivalently to Vc. Ultimately, the charge on the metals after separation should approximately be

$$Q = C_0 V_c, \qquad [3]$$

where C_0 is the contact capacitance between the bodies at the critical separation z_0, defined as the point whereat the resistance between the two bodies increases very sharply while the capacitance changes relatively slow. According to Harper, C_0 is a constant that depends only on the shape of the contacting bodies and is normally determined by the degree of roughness of the contacting surfaces. It has been experimentally confirmed by many researchers (Lowell and Rose-Innes, 1980) that the charge transfer between two metals is proportional to their contact potential difference (Figure 3). This also includes the finding that the contact charge does not depend on the speed of separation. In summary, the electron back-flow by tunneling has been found not to cause the decrease of the charge on the metals after separation. It may be said that the charge on the metals is entirely determined by the coincidence of the Fermi energies of the two metals on

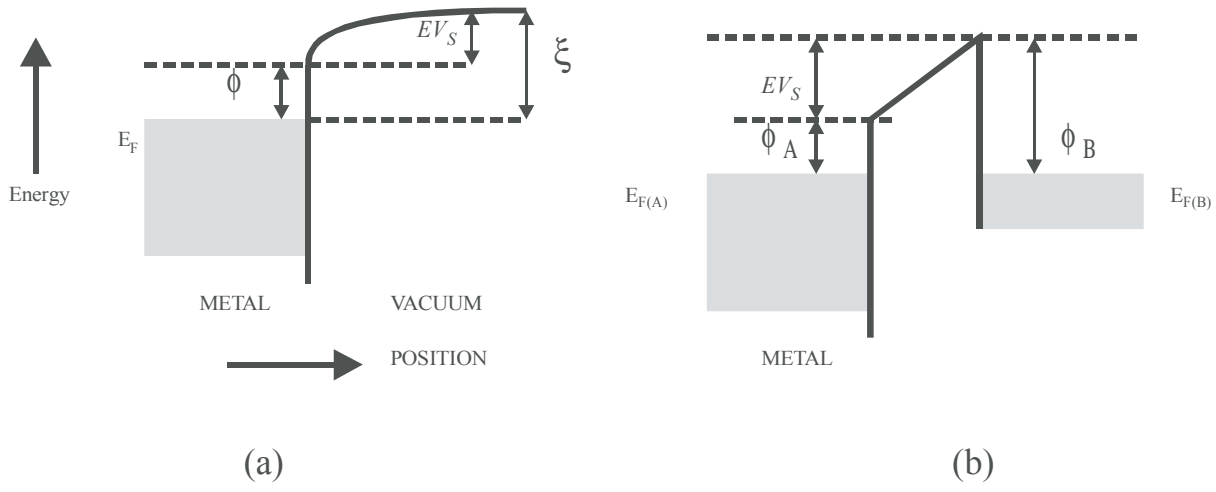

Figure 3 The variation of the energy of an electron inside and outside a metal is shown in (a). V_S is the surface potential and ϕ is the work function. E_F is the minimum energy of an electron added to the metal. Two metals in close proximity (b) exchange charge until, in equilibrium, their Fermi levels are coincident. The transferred charge is such as to cause a different in surface potential equal to $(\phi_B - \phi_A)/e$., i.e. the contact potential difference Vc.

contact, or by the thermodynamic equilibrium**.**

b) Metal-Insulator Contacts

Contact electrification is oftentimes confined to insulators, owing especially to their abilities of accumulating charge in ways that the metals cannot; therefore, the charge on the insulators is usually very observable. The term 'insulator' normally covers a very wide range of materials varying in structure, with only one common feature of being poor conductors of electricity. Work on the contact electrification of insulators is often performed by contacting the insulators with metals since the behavior of a metal in contact electrification has been well understood. In that case, the results can be smoothly interpreted. Still, the contact electrification between insulator and metal does require a good knowledge of the electron states in insulators, which at present falls far short of understanding, specifically at their surface. It is noted that, when an insulator is in contact with a metal, the charge acquired by the insulator may depend not only on the nature of insulator itself, but also, in some cases, on the specific metal and on the type and duration of contact. It has been quantitatively established for a long time that the charge transferred between an insulator and a metal tends to correlate with the difference in work function between the two materials. This correlation suggests that, for the contact electrification of metal and insulator, the charge transfer is by electrons rather than by ions or material. Note that the charge transfer by ions or material has yet been completely excluded. It has also been assumed that the charge is transferred between the metal and the insulator until thermodynamic equilibrium is established. This assumption is based on the same theory as which applicable to metals. It is described that each insulator is supposed to have 'Fermi level', E_F, which, after contact, becomes coincidence with the Fermi level of the metal. After a large number of investigations, it is now recognized that the charging of solids involving the insulators should occur primarily at the surface, and that there are sufficient electron sites in the insulators to

account for the charge. Moreover, it has been suggested that the thermodynamic equilibrium model may not be valid for insulators with a wide energy gap. An alternative mechanism for charge transfer has then been proposed, indicating that the tunneling of electrons between the metal and localized states in the insulator may play an important role in the charge transfer. The detailed mechanism will be discussed in the following section.

ii) Mechanisms of Charge Transfer

According to Harper (1967), the three primary ways in which charge can transfer from one substance to another are i) by electron transfer, ii) ion transfer, and iii) material transfer. There is important evidence suggesting that, in triboelectrification of coal and mineral matter, the charge transfer be often due to electrons. Nonetheless, the other two charging mechanisms may occur in some particular cases, and they are worthwhile to be remarked here, in brief.

a) Material Transfer

There is compelling evidence that the contact of two solids can result in the transfer of material from one to another. Material transfer in some cases (such as, when polymers and metals are brought into contact) is of possible notability to contact electrification, if the number of transferred atoms per unit area exceeds the charge density (in units of e per unit area) observed in the contact electrification (Lowell and Rose-Innes, 1980). As a result of material transfer, charge transfer will occur if the transferred material carries charge. The fact that the conditions at the surface of a material are basically not the same in the interior indicates that the surface of the material may carry a layer of charge. Metals and semiconductors are good examples of such a circumstance. Metals are ordinarily coated with their oxides that usually carry the net charge compensated by charge in the underlying metals. For a semiconductor, charge may reside in its surface states and be compensated by charge of the opposite sign

distributed in the interior. Probably the most convincing evidence of mass transfer is the work of Salanek and his group (Salanek et al., 1976). With the use of ESCA for surface analysis, they showed that some of the metal transferred to the polymer and, likewise, some of the polymer to metal when they were in contact with each other. Moreover, very large amounts of polymer may transfer to the metal during the time that the metal slides over polymer (Pooley and Tabor, 1972). But in spite of what has been reported, those cases where material transfer has been shown taking place were analytically found not to be the first primary cause of charge transfer. As addressed in the work of Salanek et al., the large amounts of material transferred were observed in the first contact between a metal and polymer, but the significant increase in the amount of material transferred did not happen for the second and following contacts. Furthermore, there is the other supporting evidence that material transfer is unlikely to be a primary cause of the contact electrification of metal-insulator. A paper published by Lowell (1977) reported that the same region of polymer surface may be repeatedly charged to approximately the same extent by repeated contacts with a metal. Note that the charge on the surface should be removed between contacts for such case. It is also important to bear in mind that, if a metal charges a polymer because of material transfer, one would expect charge transfer to be practicable only if the two materials have not previously in contact.

b) Ion Transfer

A number of researchers (Shaw, 1917; Henry, 1957; Harper, 1967; Kornfeld, 1976; Ruckdeschel and Hunter, 1977) have suggested that contact electrification may be due to the transferring of ions from one surface to the other. However, it is difficult to accept this suggestion as the mechanism of charge transfer that usually occurs in metal-insulator contacts, although some researchers were influenced to believe so. Only in the case of insulator-insulator contacts, is there a great deal of experimental evidence that ion transfer may be a dominant

mechanism for the charge transfer. Or even two or three mechanisms (electron, ion and material transfer) may contribute simultaneously to the charge transfer in some particular cases. Evidently, the most far-reaching affirmation for the ion transfer model has been made by Kornfeld (1974). He claimed that the circumstances in which the surfaces of the same materials may charge each other, and that the sign of the charge transferred to one surface when it is rubbed by another may eventually change as rubbing continues, can be explained by the ion transfer mechanism. He pointed out that insulators, in general, carry a net internal charge because of charged defects in the crystal lattice; this internal charge is neutralized by ions on the surface. These ions are attracted to the surface from the atmosphere, which is always slightly ionized. It is also suggested that different surfaces have different affinities for a given ion, hence, there will ordinarily be a transfer of ions from one surface to the other when two ion-coated surfaces are brought into contact. Nevertheless, Kornfeld's ion-transfer mechanism has been disputed by the more convincing and nearly overwhelming evidence shown by other workers. Those results controversially indicated that electron transfer should be the dominant mechanism when metal is one of the contacting materials. Moreover, Lowell and Rose-Innes (1980) pointed out that charge transfer between insulators is also attributed to electrons. They included that the electrification of one insulator by another can be predicted from the information on the triboelectrification of each of the insulators by metals. Harper (1967) has several papers contributing to the study of ion transfer mechanism. He found very large charge transfer on quartz and concluded that the charge transfer should be credited to a thick layer of -OH ions which were present on the quartz surface as a result of the manner in which it was prepared. Contrary to what has been reported by Harper, a work performed on quartz by Wagner (1956) indicated electron transfer as the charging mechanism when charging quartz against metals. His indication was attributed to the finding of the relationship between the charging and the work

function of the contacting material. Yet, the ion transfer was not completely denied to be a possible mechanism for the electrification of some substances, such as Al_2O_3, MgO, and the alkali halides. Furthermore, a number of studies in connection with the ionic mechanisms of charge transfer were carried out on pyroelectric insulators (Harper, 1967; Kornfeld, 1974; Robins et al, 1975). It appears eventually that the contact electrification is influenced by the polarization of the pyroelectric material, but not by the presence of compensating ions.

The ion transfer mechanism when water is present on surface is also of particular interest, in addition to the transfers of ions attached to dry surfaces that have been discussed above. There is compelling evidence that contact charging of insulators may be varied by the presence of water. Harper (1967) has proposed that charge transfer might appear through a kind of *electrolytic proces*s. Such electrolytic charging is regarded as a process in which ions move in a superficial water layer. An extensive series of experiments, which suggest the electrolytic charging, has been described by several authors since early century. Knoblauch (1902) found a strong correlation between the sign of charging and acidic or basic properties (the presence of H^+ and $OH^{-)}$. Moreover, he proposed a mechanism to explain the charging of some totally insoluble materials, and concluded that the charging occurred as a result of the attraction of H^+ or OH^- ions present in a (probably contaminated) water layer to the material of greater dielectric constant. His findings were confirmed by Rudge (1914), who was unaware of the similar works he had carried out when compared with those of Knoblauch. Years later, Medley (1953) conducted his experiments on polar polymers. His work became more evident to electrolytic charging, with the result denoting that the polar polymers would acquire electrical conductivity in a humid atmosphere due to electrolytic dissociation in absorbed water. In summary, water may influence contact electrification in an indirect way, by increasing the conductivity of the insulator. Turning now to the concept of ion transfer which may be considered in the case of insulator-insulator

contacts rather than in the contact electrification of metal-insulator. Up to present, no comprehensive theory of ion transfer has been developed yet. But the redistribution of positive and negative ions between two surfaces, which have just been in contact, has been intensely contemplated by Henry (1957). Henry proposed an indicative theory in which the several different driving forces, which could transfer ions from the surface of one insulator to another, were pulled into observance. An expression was derived for the charge transfer involving all these effects. To make it rather more explicit, Lowell and Rose-Innes (1980) considered treating them separately, and their treatment should thus be followed.

As shown in Figure 4, the potential energy of an ion is given as a function of its position between two nearly separated parallel surfaces, and the vibrational levels are indicated. This potential includes that as a result of excess charge on the insulator surfaces. Basically, ions will concentrate near the minima adjacent to the two surfaces when in equilibrium. The number n_1 and n_2 of ions close to surface 1 and 2, respectively, will be assigned approximately by

$$n_1 / n_2 \sim exp\ (- \Delta U / kT), \qquad [4]$$

where ΔU is equal to $U_1 - U_2$ (Figure 4). ΔU is defined as an energy difference between the lowest vibrational levels in the two troughs at cut-off; simply put, it is the energy difference between the minima shown in the figure. The equilibrium may not be reached for a very long time if U_1 and U_2 are large compared to kT, but it will be disregarded at the moment. Furthermore, it is presumably for the time being that ions in the two minima remain attached to their individual surfaces after separation. If ΔU is considerably larger than kT, equation (4) will thus suggest that most of the ions would collect on one of the surfaces. However, if there are a lot of ions, ΔU will be modified by the electric field formed when those ions transfer. Obviously, all the ions will transfer to one surface if the total charge is less than σ_0, where

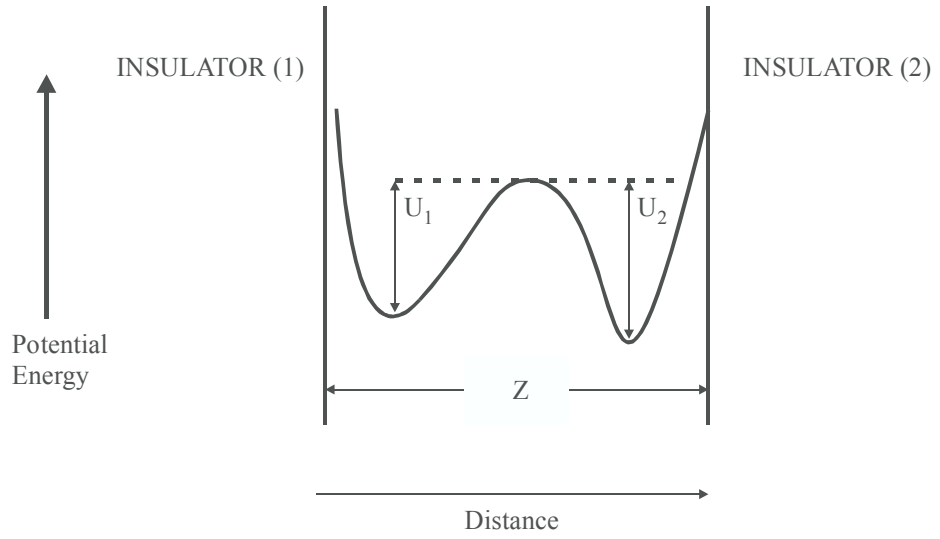

Figure 4 Dependence of the potential energy of an ion on its position between two plane parallel insulator surfaces.

$$(e\sigma_0 / \varepsilon_0)z \approx \Delta U \qquad [5]$$

It is assumed that the distance between the minima in Figure 4 is the order of the separation z of the surfaces. Correspondingly, if the ions on the two surfaces have total charge larger than σ_0, the charge transfer will proceed until the field is adequate to make the energies of the two minima equal. If ΔU is the initial energy difference between the minima, the charge transferred is given by

$$(e\sigma_z / \varepsilon_0) = \Delta U \qquad [6]$$

It is difficult to predict the charge density numerically with no information on ΔU or on the effective separation, z. However, a rough computation can be done by assuming z to be so small that ΔU is less than ~ 1 eV, so the thermionic emission of one surface to another while the two are in contact will not be very slow. It is noted that ΔU would be ≥ 1 eV in general if the binding energies of the ions to the surface are bigger than 1 eV, except that the surfaces are closer than ~ 0.3 nm so that the image forces reduce ΔU. Therefore, it is essential that z must be assumed

≤ 0.3 nm for contact electrification to happen. By substituting these numbers in equation (6), one can find $\sigma = 3 \times 10^{-2}$ C/m^2 as the condition for equation (5) to be satisfied. But the observed charge densities are nearly always smaller than this and equation (6) is, therefore, usually irrelevant.

If the binding energy of a given ion is supposedly different on dissimilar insulator surfaces, by the amount ~ 1 eV or more, the above mechanism will always be the dominant one. But once the two insulators are identical, the binding energy will spontaneously not differ, and make the small effects become important.

Results and Discussion

Particle Charge Measurement and Charger Design

Four parameters affecting triboelectrification mechanisms were investigated. These included: i) particle size, ii) temperature, iii) air velocity, and iv) feed rate. The charge measurements were conducted on coal, quartz and pyrite samples. The results show that charge density increases with:

- increasing air (or particle) velocity for all particle sizes studied,
- decreasing particle size,
- decreasing feed rate, and
- increasing temperature.

The particle charge measurement results showed that coal is positively charged, while both quartz and pyrite are negatively charged, which serves as the basis for the TES process. The results also showed that at a given experimental condition, pyrite is more negatively charged than quartz, suggesting that the former can be more readily separated than the latter by the TES process.

A statistical test matrix based on the composite Box-and-Behnken experimental design technique was developed to study the effects of operating parameters on particle charging mechanisms. The test matrix included four parameters that affect the charging mechanisms. These included: i) air velocity, ii) particle feed rate, iii) particle size, and iv) feed composition. The results are summarized as follows:

- the magnitude of the charge density increases with increasing air velocity at all particle sizes studied,

- charge density (given in units of coulombs per unit area) decreases with increasing ash content in feed regardless of feed rate,
- charge density decreases with increasing feed rate, and
- of the various parameters tested, particle size and air velocity are interacting with each other most significantly. The finer the particle size, the more significantly the air velocity affects the particle charge.

The effect of the work functions on particle charging using different materials was studied using: aluminum, chromium, copper, nickel, stainless steel, copper-nickel alloy, polyvinylchloride (PVC), and Teflon. The test results show that the quartz sample became negatively charged for the majority of materials examined.

Three different tribochargers were evaluated during the course of study. These chargers include 1) in-line static mixer made of copper, 2) Plexiglas pipe, and 3) turbocharger made of Plexiglas.

The general conclusion reached was that the turbocharger design fabricated with Plexiglas could achieve a minimum standard specific charge of 50uC/ kg and could provide the greatest separation efficiency. The improvement in separator performance can be attributed to the fact that the charger design maximizes particle-particle and particle-wall interaction.

Results and Conclusions of Bench-Scale Separator Tests

a) Drum-Type Bench-Scale TES Unit

The drum-type bench-scale TES unit was used to clean a Pittsburgh coal. The coal sample used for the tests was a clean coal product assaying 5.6% ash and 1.67% sulfur. The tests were conducted by varying the potential difference between the electrodes in the range of 20 to 70 kV at

a throughput of 4 kg/hr. The best separation results were obtained at 40 kV. According to the grade vs. recovery curve obtained at this potential, the ash content can be reduced to 3.7% at 80% Btu recovery and 4.3% at 90% Btu recovery. As for sulfur, the total sulfur content can be reduced to 1.2% at 80% Btu recovery and 1.25% at 90% Btu recovery.

The separator tests showed that the turbocharger gave significantly better results than those obtained with the straight pipe charger or in-line mixer that were used for particle charging. The TES unit equipped with the new charger gave more than 10% higher combustible recoveries than the straight pipe charger.

Based on the particle trajectory model developed for this test work, feeding a coal from off-center positions (bias feeding) should affect separation efficiency. However, based on the test results obtained with Pittsburgh coal, biasing the feeding point does not make a significant difference in separation efficiency.

A series of tests were conducted on the Sewell Seam clean coal sample using the drum-type bench-scale TES unit. Tests were conducted at a feed rate of 8.2 kg/hr, while varying the applied voltages at four different levels, i.e., +30, +40, +50, and +60 kV. The results show that the best separation efficiency of the TES unit on Sewell Seam coal was obtained at 40-50 kV. At an applied potential of 60 kV, the performance of the TES unit deteriorated. It is possible that in a strong electric field, the particle charge may be altered due to inductive charging mechanism, which is detrimental to the separation process.

The use of the turbocharger drastically improved the throughput capacity of the bench-scale TES unit with no loss in separation efficiency. Therefore, separator testing was conducted in order to obtain the information of maximum throughput capacity of the bench-scale TES unit incorporating the turbocharger. A series of separator tests have been conducted on the Pittsburgh No. 8 clean coal in order to obtain the information of the maximum throughput of the bench-

scale TES unit. It was found that reasonable separation efficiencies were obtained until the feed rate reached approximately 30 kg/hr. The separation efficiency deteriorated significantly above this limit. Thus, the throughput of the bench-scale TES unit can be further increased either by increasing the rpm of the rotor blade or by increasing the overall size of the turbo charger.

The bench-scale TES unit demonstrated that it is capable of achieving high degrees of ash and sulfur rejections, but at low Btu recoveries. In order to overcome this deficiency, it would be necessary to design a unit that has a built-in scavenger or scavengers.

b) Plate-Type Bench-Scale TES Unit

Two different bench-scale separators were tested on a low-sulfur Sewell Seam coal, namely

- a drum-type separator equipped with a turbocharger,
- a plate-type separator in a pie configuration, equipped with a turbocharger and a middlings recycle system.

Both separators produced reasonable separation efficiencies, but the plate-type separator produced better results with coarse particles, possibly because of the longer particle retention times and the provisions for middlings recycle. Despite the improvement achieved with the plate-type separator, there were difficulties in separating ultrafine particles. The test work conducted with a series of mono-sized particles showed that the plate-type separator is effective in separating particles in the range of 230 to 45 mesh. The particles outside this optimum range are more difficult to separate. The low separation efficiencies on both of the bench-scale units with fine particle size feed material may be attributed to the entrainment problem associated with fine particle separation which is possibly due to the drag force created by the turbulence at high air velocity.

c) Screen-Type Bench-Scale TES unit

A bench-scale TES unit was constructed and used to evaluate a wide range of electrode designs. The separator was constructed in a pie formation. Five different types of electrode systems were tested, i.e., horizontal rod, vertical rod, plate, drum and screen. A –14 mesh pulverizer reject sample (46.7% ash) from a local power plant was used in all tests.

Test results show that among the different electrode designs, the screen-type electrodes gave the best separator performance, while the drum-type electrodes gave the poorest. The screen-type unit was capable of reducing the ash content from 46.7% to 10% with a 60% combustible recovery (92% ash rejection) in a single stage operation. The test data also showed that the performance of the screen-type TES unit does not deteriorate significantly within the range of feed rates (6-44 kg/h) tested to date.

d) POC Electrostatic Separator Design

Data obtained from the separator test program was used to design an electrostatic separator suitable for incorporation into the 200-250 kg/hr POC test unit. The design incorporated a vertical feed of coal that has been pulverized in an impact mill and passed under pressure through a Triboelectrostatic charger. The separator consisting of screen electrodes set in a pie configuration. Clean coal and rejects were removed through an air-lock system, provision being made for the recirculation of by-pass material (middlings). The entire TES test circuit was designed to operate under a net positive pressure in a nitrogen atmosphere. Separator geometry was based on model predictions and data obtained from the bench-scale test work. Since the separator efficiency is also dependent on electrical field strength, the design allowed for a variable voltage up to 70 kV between the electrodes (up to 35 kV on each electrode). The design incorporated sufficient instrumentation

(i.e., flow meters, pressure gauges, etc.) to monitor the performance of the POC electrostatic separator.

The separator was built and supplied by Carpco, Inc.

A detailed test program was carried out to establish the performance capabilities of this process in terms of energy recovery, ash rejection, and throughput capacity.

Results and Conclusions of POC-Scale Separator Tests

Four different feed samples were used for the POC TES unit test program. These feed samples include: (i) Glen Lyn Raymond Mill Rejects (feed ash ≈ 42-45%), (ii) Moss 3 Raw Coal, (iii) Possum Point Raymond Mill Rejects and (iv) Shawville Raymond Mill Intermediate Products.

A series of tests were conducted to determine the influence of electrode position on combustible recovery and product ash content. The test results obtained from this series of tests were similar to the results obtained from the drum-type bench-scale TES unit under bias-feeding conditions. It was concluded that biasing the feeding point or relative electrode position does not make a significant difference in separation efficiency.

Relative humidity plays an important role in the particle charging process and triboelectrostatic separation. Combustible recovery and ash rejection remain relatively constant when the relative humidity is held below about 50%. On the other hand, the combustible recovery begins to deteriorate as the relative humidity increased to 60%. A further increase in relative humidity to 70% causes a sharp decrease in recovery with little change in the ash content of the clean coal product.

Initial test results showed that better separations could be made with the bench-scale unit than with the POC-scale unit under identical test conditions. By a process of elimination, it was concluded that the vertical recycle conveyor was grinding the feed material via attrition. This

resulted in dust coatings on both the coal and refuse particles that would not accept a differential charge at the turbocharger. In addition, the particle charging procedures used in the bench-scale TES unit is different from that of POC-scale TES unit. Therefore, 1) the recycle screw conveyor was replaced with bucket elevator, 2) turbo-charger was modified to install blades in two layers for the POC unit, and 3) screen electrode was installed to replace the original cylindrical electrodes.

A series of tests were conducted on the POC unit to evaluate the relative position of the electrodes and the splitter settings. The results show that as distance between the cathode and the splitter increased, the amount of the recycled material decreased, the ash content of this stream decreased (because more of the middlings reported to the clean coal product). However, the changes in recovery due to recycling were minimal. The results also suggest that there is no need to recycle the middlings stream for the sample tested in this series. This finding may indicate that the separation is as good as it can be on the first pass. The results also showed that the minus-35-mesh particles gave a higher recovery than the minus-28-mesh particles. A possible explanation may be that the coarse particles fall too fast to be attracted by the electrodes.

The effect of applied potential showed that coal recovery decreased with increasing electrode potential difference, which seemed surprising. A possible explanation could have been that the charge of the coal particles was substantially higher than that of the ash-forming minerals. At low potentials, highly charged coal particles could have been recovered in preference to the weakly charged ash-forming minerals, resulting in high recoveries. As the potential difference was increased, weakly charged ash particles and some of the middlings were then pulled toward the cathode, causing a decrease in recovery. Decreasing ash content observed with decreasing recovery can be attributed to the loss of middlings to the cathode.

Test results suggest that proper design of the charger is important for improving the combustible recovery and separation efficiency. Combustible recovery increased with increasing impeller speed, which suggests that the coal recovery increased with increasing charge of the coal particles.

Test results showed that the shielded electrodes, i.e., coated electrode surface or laminated electrode, provided a superior level of performance when compared to the unshielded electrodes. For the tests conducted with the rotary charger only, the shielded electrode test increased the reject ash content by approximately 3%, clean coal yield by 9-12%, recovery by 11-13%, and separation efficiency by 5-8%. The improved level of performance obtained with the coated electrodes is believed to be due to prevention of accidental charge reversal. The charge reversal occurs when selectively charged particles collide with uncoated electrodes fabricated from copper or steel wires. The plastic shielding insulates the electrodes and prevents the particles from making contact with the conducting surfaces, thereby preventing charge reversal. Therefore, the coated electrodes (i) allow higher field strengths to be tested without risk of arcing and (ii) minimize the likelihood of charge reversal caused by particles colliding with the uncoated electrode conductors.

Feed samples from several mill rejects in conjunction with different particle charging procedures were employed to evaluate the separation efficiency of the POC TES unit. The test results indicate that there is virtually no separation when no charger was employed. The average separation efficiency obtained with the pneumatic charger was slightly higher than that obtained with the rotary charger. It is also worth noting that the pneumatic charger provided a high recovery and poor clean coal ash, while the rotary charger provided a low recovery and good clean coal ash. Although the best separation efficiency was obtained by combining both the

pneumatic and rotary chargers in series, this two-stage configuration produced too low of a recovery (49%) and reject ash (43%) to be commercially viable.

Economic Evaluation

A technical and economic evaluation was carried out to assess the future commercialization of the TES technology. It was concluded that the TES cleaning of power plant pulverized coal and intermediate mill products would not be economically attractive. However when treating pulverized mill rejects, a TES installation would offer a reasonably attractive rate of return (25-75%) when compared to the alternative existing practice of discarding the reject material. The payback period on the capital investment would be relatively low (4-6 years). These margins would be expected to improve, as additional market premiums became available for lower ash and lower sulfur coal products. The introduction of new legislative restrictions associated with the emission of trace elements (particularly mercury) may also provide new incentives for utilizing this technology in the future.

Task 1 – Project Management

Sub-Task 1.1 Objectives

The objective of this task is the preparation of a project work plan and the performance of all aspects of project management. The contractor was required to prepare and submit to the DOE COR, within thirty (30) calendar days after contract award, a Draft Project Work Plan covering the entire period of performance of the contract. After approval of the Draft Project Work Plan, the contractor was required to submit a Final Project Work Plan to the DOE COR for review and approval. The Final Project Work Plan should be self-contained and present, in detail, all activities required for the successful completion of the work outlined in subsequent tasks of this Scope-of-Work

Sub-Task 1.2 Task Execution

A detailed Project Management Plan was prepared from the Center for Coal and Minerals Processing (CCMP) and was submitted to DOE's Contracting Officer's Representative (COR). Following minor revision the plan was approved by the DOE COR and the Office of Sponsored Programs (OSP) at Virginia Tech. The work plan included a description of all project activities and detailed the assignments of project responsibilities for each participant. No cost overruns were required to complete the proposed work.

Task 2 – Sample Acquisition

Sub-Task 2.1 Objectives

The objective of this task was to obtain suitable samples from U.S. coal preparation plants and power plants. Two of these coals will be obtained from the Pittsburgh No. 8 and Elkhorn No. 3 coal seams. The Pittsburgh No. 8 coal is well known for its large reserve base and relatively high pyritic sulfur content and the Elkhorn No. 3 coal for its applicability to production of superclean fuels

For each coal, all pertinent information will be documented, including geographic location, mine description, preparation plant description, sample description, sampling procedures, and gross sample weight. Final selection of coals will be made with DOE COR concurrence. The contractor will be responsible for the on-site sampling campaign, storage and safe transportation of the coal to its test facility.

Sub-Task 2.2 Execution

Although the prime contractor (CCMP) coordinated this activity, the industrial participants were largely responsible for most of the work related to the on-site sampling campaigns for the acquisition of samples from coal preparation plants. In the case of power plant samples, CCMP personnel organized the sampling campaign and collected the samples with the assistance of the power company personnel. Table 1 provides an overview of the samples used in the test program. In general, four different types of samples were used, namely: (i) clean coal products from the preparation plant, (ii) raw coal feed to a preparation plant, (iii) grinding mill reject from a power plant and (iv) grinding mill intermediate products from a power plant.

Sub-Task 2.3 Coal and Reject Samples Used in Test Program

Plant Name	Geographic Location	Coal Seam	Sample Description	Sample Weight
Not Disclosed	W V	Sewell	Clean Coal	50lb
Not Disclosed	PA	Pittsburgh No 8	Clean Coal	50lb
Moss 3	Dante, VA	Upper Banner	Raw Coal	300 lb
Glen Lyn	Glen Lyn, VA		Raymond Mill Rejects (Pyrite Trap)	500 lb
Possum Point	Possum Point, VA		Raymond Mill Rejects (Pyrite Trap)	500 lb
Possum Point	Possum Point, VA		Power Plant Feed	200 lb
Shawville	Shawville, PA	Kittanning	Raymond Mill Intermediate Products Sample Point # 1 Sample Point # 2 Sample Point # 3 Sample Point # 4	 500 lb 500 lb 250 lb 50 lb
Seward	Seward, PA	Kittanning	Raymond Mill Product	400 lb

Task 3 – Engineering Design

Objectives

The primary objective of this task is to complete the engineering design and testing of a 200-250 kg/hr proof-of-concept (POC) triboelectrostatic separator for upgrading fine coal. The engineering design will include the specification of all process equipment, completion of detailed material balance calculations and the preparation of all process flow diagrams, process and instrument drawings, electrical/mechanical drawings, bills of material, installation schematics and general equipment arrangement drawings. Prior to preparing the final engineering design, initial bench-scale test work will be conducted using a nominal 1 kg/hr test unit followed by testing of a larger bench-scale unit having a nominal capacity of 10-20 kg/hr. These tests will be carried out (i) to provide key scale-up criteria for the design of the 200-250 kg/hr POC test unit and (ii) to determine the maximum performance achievable by triboelectrostatic separation.

Sub-Task 3.1 – Tribocharger Design & Evaluation

3.1.1 Objectives

The separation efficiency of the triboelectrostatic separator (TES) is critically dependent upon the surface charges of the particles involved. An effective separation process needs to maximize the difference of the charges of the particles to be separated. The objectives of this subtask are to: (i) design an efficient charger for the triboelectric separator and (ii) carry out bench-scale tests to evaluate the efficiency of the charging system.

Variables to be examined include three physical characteristics of static mixers (i.e., construction material, geometry and element configuration) and three operational parameters (i.e., air velocity, solids concentration and particle size). The initial tribocharger tests will be conducted

using an apparatus designed with a nominal capacity rating of approximately 1 kg/hr. These tests will be followed by the design, construction and testing of a tribocharger system with a capacity of approximately 10-20 kg/hr. Operating parameters to be examined in the 10-20 kg/hr tests will include solids throughput, gas flow rate and particle size. The primary objective of the 1 kg/hr and 10-20 kg/hr test programs will be to (i) to evaluate the metallurgical performance of the TES process, (ii) to investigate effects of various operating parameters, and (iii) to characterize different designs of triboelectrostatic chargers and separators. Information obtained from the 1 kg/hr and 10-20 kg/hr test work will be used to develop scale-up and performance expressions for the POC test unit rated at a nominal capacity of 200-250 kg/hr.

A central-composite experimental design will be applied to develop a test matrix for the optimization of the 1 kg/hr tribocharger test work. The test matrix will include the operational parameters listed above (i.e., air velocity, solids concentration and particle size) and the L/D ratio of the static mixer (representative of its geometry). These parameters will be varied at three levels (low, intermediate, and high) representing a wide range of operating conditions. Specific settings for these levels will be established after completing several exploratory test runs with the experimental apparatus. These tests are necessary to investigate the effects of tribocharger material and configuration on the charging efficiency.

After completing the 1-kg/hr tests, a second series of tribocharger tests will be conducted at the 10-20 kg/hr scale in order to obtain scale-up data for the design of the POC charging system. An appropriate test matrix will be developed for investigating the performance of the 10-20 kg/hr charger. In order to minimize the number of tests required to identify the optimum design of the tribocharger, an additional four (4) tests will be conducted under optimum operating conditions with four tribochargers of different geometries and different element configurations for the Pittsburgh No. 8 and Sewell coals. The test matrix will be developed after completing the 1-kg/hr test work.

Since the impact of charger material is believed to be independent of mixer size, different types of construction materials will not be tested at a larger scale, i.e., the construction material used in the 1 kg/hr bench-scale testing will be used to construct larger tribocharger systems.

In all tribocharger tests, the charging efficiency will be determined in terms of charge per unit mass by measuring the electric current from the tribocharger to ground. This will be done with a Faraday cage/picoammeter connected to a data acquisition system that records and displays a plot of current from the tribocharger as a function of time. The charge can be obtained by integrating the area under the curve. Data obtained for static mixers of different geometries will be normalized by converting each of them to an equivalent open-pipe length and diameter. The normalization procedure assumes that the efficiency of particle contact is maintained so long as the equivalent L/D ratio and superficial gas velocity is maintained through the test units. This assumption will be validated from the test data or modified accordingly. The test data will also be used to develop expressions for pressure drop across the various tribocharger designs. This information will be useful for determining the air flow rate and power requirements necessary for triboelectric charging.

A minimum acceptable performance standard for the tribocharger will be determined by the contractor and approved by the COR. For planning purposes, a minimum standard specific charge of 50 μC/kg has been tentatively established for samples of pulverized coal (i.e., 200 mesh particles). The charge is expected to increase as the particle size decreases and gas velocity through the mixer increases. Implementation of the remainder of the project tasks is predicated on consistently achieving the minimum acceptable performance criteria.

3.1.2 Relevant Background Information

As particles flow through the charger in a gas stream they are subjected to particle-particle and particle-wall collisions. When two particles of different work functions collide with

one another, electrons move from the surface of the low work function material (coal) to the surface of the high work function material (mineral matter). Subsequently, the coal particles become positively charged, while the mineral matter becomes negatively charged. The charge density of the particles varies depending on the relative abundance of coal and mineral matter present in the feed stream. The particle-wall interaction also produces charges on the particle surface. Particles that possess a work function lower than those of the wall attain a positive charge and particles of higher work function become negatively charged.

The charger material employed must retain a work function that lies between that of the coal and the mineral matter. Copper is frequently employed because its work function lies between that of coal and mineral matter. In addition, applying a potential to the charger significantly affects the charge discrepancy. The applied potential is beneficial in regulating the work function of the charger material and the correct potential can ensure a maximum charge difference between the coal and the mineral matter.

3.1.3 Charge Measurement Apparatus

The difference in charge between coal and mineral matter plays a prominent role in determining separation efficiency. Therefore, a reliable and accurate charge measurement system is important. Two different techniques of charge measurement were considered for the TES.

The first method of charge measurement considered was the Mazumder technique. Employing this technique involves placing charged particles in magnetic fields. The trajectories of the particles are monitored. The data collected provides the necessary information to ascertain the charge of the particles. The Mazumder technique is the most accurate of the techniques considered. The method, however, requires sophisticated and costly equipment. In addition, this

technique is not applicable for particles possessing a length exceeding 60 μm. Given these restrictions, the decision was made to employ a Faraday cage for charge measurement.

The Faraday cage, depicted in Figure 5, consists of matched sets of inner and outer copper cylinders electrically isolated using nonconductive Teflon spacers. As shown in Figure 6, the cage is connected to a Keithley Model-642 electrometer and a data acquisition system. The inner copper cylinder is electrically connected to the electrometer through a coaxial cable; the outer cage is grounded to eliminate the influence of stray electric fields. Both cylinders possess copper lids to prevent the measurement being affected by possible ambient electric fields. The measurements were considered unreliable in the absence of the lids. This design differs from that generally reported in scientific literature as a result of the lid addition. Particles are delivered to the inner cage though small copper tubing which forms an extension of the inner cup. It was necessary to make the copper tubing a part of the inner cage in order to circumvent measurement error. Particles colliding with the inner wall of the copper tubing can acquire additional charges.

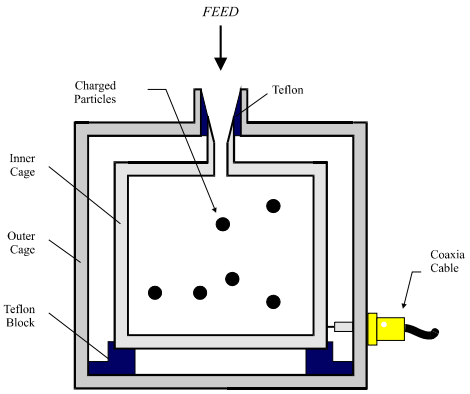

Figure 5 Schematic Representation of the Faraday cage used for the particle charge measurement.

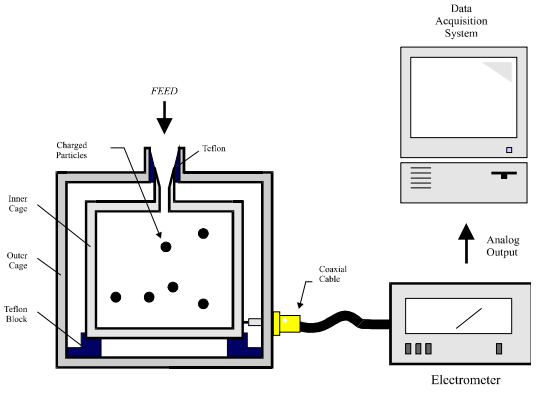

Figure 6 Instrumentation setup for the particle charge measurement using the Faraday cage

The mechanisms involved in the Faraday cage charge measurements are illustrated in Figure 7. Consider particles touching the walls of the inner cup Figure 7a. It is assumed that the particles are negatively charged thereby allowing electrons on the particle surface to transfer to the walls. The result is a flow of electric current from the Faraday cage to the electrometer. Referring to Figure 7b, consider negatively charged particles not in contact with the walls. These particles polarize the inner copper cup rendering the inner wall positively charged, while the outer wall attains the opposite charge. The free electrons establish an electric current by flowing from the negative charge sites of the inner wall to the electrometer. Thus, the net result is the same regardless of the scenario. The presence of negatively charged particles will result in a measurable current.

In order to facilitate an in-situ measurement, an on-line tribocharge analyzer has been developed as shown in Figure 8. This device consists of an in-line static mixer and an outer tube made of copper. The in-line static mixer is electrically connected to the electrometer by means of a coaxial cable, while the outer tube which served as a shield against surrounding electronic

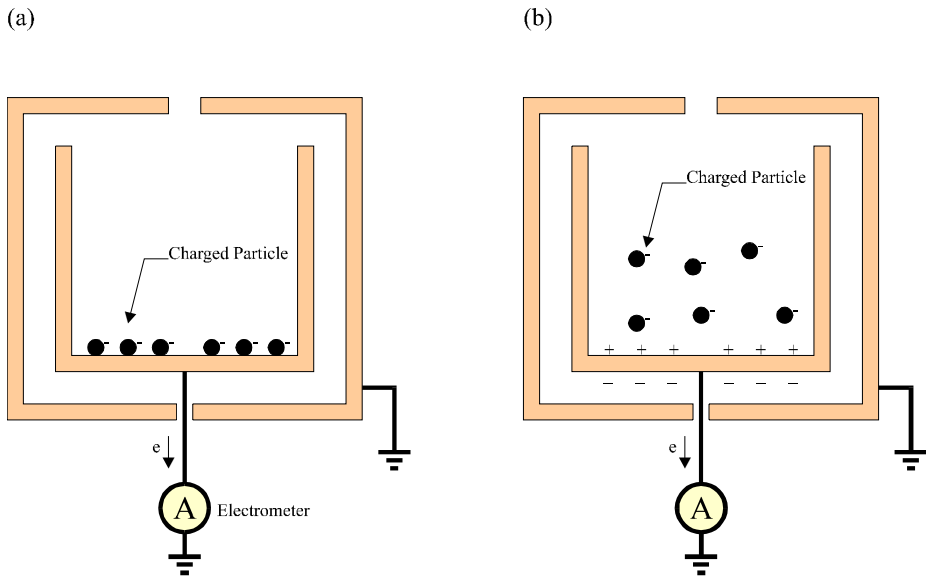

Figure 7 Schematic representation of the principles of charge measurement using the Faraday cage

Figure 8 Schematic representation of the on-line tribocharge analyzer

interference is connected to the ground. Figure 9 shows the entire on-line tribocharge analyzing system. It is capable of acquiring and digitizing the analog signal when particles pass through the tribocharger. The Fast Fourier Transformation (FFT) procedure has been applied to the digitized information for noise reduction.

This novel, on-line tribocharge analyzer possesses several distinct advantages. In-situ measurements can be executed for a large range of particle sizes. In addition, the on-line tribocharge analyzer is beneficial in studying charging mechanisms and separation efficiency of the TES. As shown later in this report, the charge measurement apparatus established that coal particles obtain a positive charge while mineral matter (represented by quartz) attains the opposite charge. This is the basis of the triboelectrostatic separation process.

The charger design changed as work progressed and is discussed later in this section. As the charger design progressed, the in-situ charge-measuring device gave rise to a modified on-line charge-measuring version. The device is capable of taking the product from a turbocharger and measuring the surface charges of the particles in the stream. Initial measurements were conducted on the particles coming out of a bench-scale turbocharger that had been specifically designed to vary the rpm of the impeller. The measurements were conducted by changing the feed rate, particle size in the feed streams, the rpm of the rotor blade and the material.

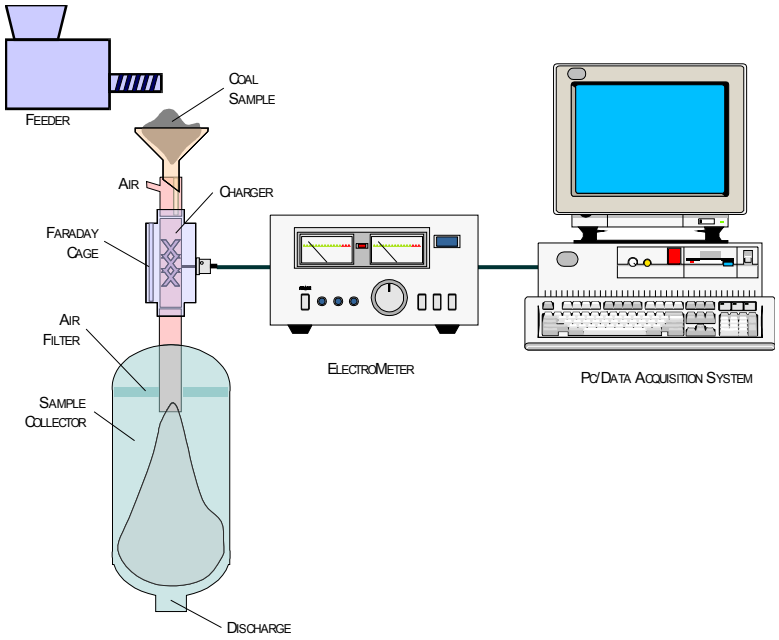

Figure 9 Schematic representation of the on-line particle charge measurement

3.1.4 Parameters That Effect Particle Charging

Several parameters are involved in determining the sign and magnitude of the charge. These parameters can include: particle size, coal rank, gas flow rate, feed rate, agitation intensity, agitation time, temperature, coal to particle ratio present in feed, and charger material. Preliminary studies were conducted examining the impact of aeration rate, particle feed rate, and particle size on charge density. The preliminary study was followed by a more detailed parametric study. Temperature is a very important parameter in the tribocharging mechanism. Therefore, the charge measuring system has a provision to maintain the temperature of the system at a desired level. In a given experiment, a sample is preheated in an oven at a desired temperature before being placed in the sample hopper. The sample is fed to the on-line charge analyzer by means of compressed air. The air is heated by using a heating tape before entering the system. The system temperature is monitored with a thermometer located between the air inlet and the charger.

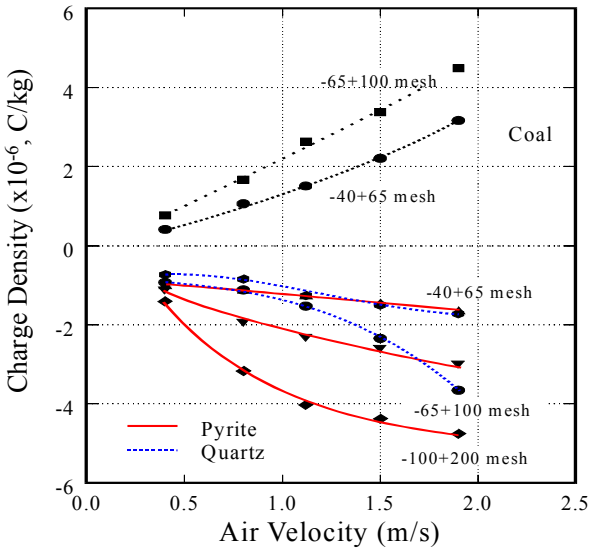

Figure 10 Effect of air velocity on the magnitude of the particle charge density.

Effect of Air Velocity

Figure 10 shows the effect of air velocity on the magnitude of the charge density of samples. The particle feed rate was maintained at 0.2 kg/min in average for all tests. As shown in the figure, an average charge per unit mass of all samples increases with an increasing of air velocity regardless of particle size. This can be described by the fact that an increase in the air velocity causes an increase in the impact velocity of the particles when they impinge on the copper walls and blades of the in-line static mixer charger, which, in turn, results in better particle-wall contact. This observation is consistent with what has been shown in the literature (Ban, et al., 1993). Apparently, the charge density of the coal samples is much higher than that of the quartz and pyrite samples. Also, the pyrite sample tends to be more negatively charged than quartz. This finding is in agreement with the previous work done by Finseth et al. (1993), which shows that the dry triboelectrostatic separation process can remove pyrite better than other ash-forming minerals. In addition, the results given in this figure show that the charge densities

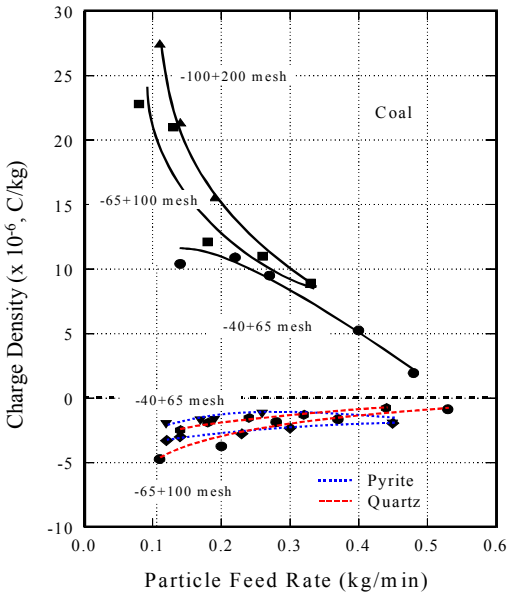

Figure 11 Effect of the particle feed rate on the magnitude of the particle charge density

of the particles increase with decreasing particle sizes. Such effect will be discussed later in this report.

Effect of Particle Feed Rate

The effect of the particle feed rate on the magnitude of the charge density is shown in Figure 11. The charge measurements were carried out at an air velocity of 1.9 m/sec. For all samples, an increase in the particle feed rate decreases the magnitude of charge density regardless of particle size. This is due to the fact that, at a given air velocity, the decrease in particle velocity often happens when the population of the particle in the charger is enlarged and the chance of particles hindering each other is elevated. As a result of that, the occurrence that the particles are obstructed in the charger is occasionally experienced at the high particle feed rate. At a given air velocity, the pyrite and quartz do not exhibit the large difference in their charge densities. It should be noted here that pyrite being a semi-conductor may lose its charge

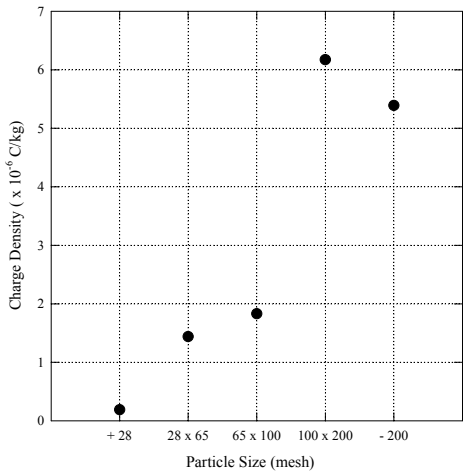

Figure 12 The effect of particle size on the magnitude of particle charging.

which may have contributed to low charge density of pyrite upon contact with another conductor (Rose-Innes, 1980). In addition, it is obvious that the clean coal sample acquires about 3-4 times higher charge density than both quartz and pyrite samples do. Such finding can also be seen in the effect of air velocity shown in Figure 10. This phenomenon may be explained by the fact that ash-forming minerals have higher mass-to-size ratio, when compared to coal, causing them to have lower particle velocities at a given particle size and air velocity.

Effect of Particle Size

The investigations were conducted using Pittsburgh No.8 coal sample (6.27% ash) with a particle feed rate of 0.08 Kg/min and an air velocity of 2.0 m/sec. The results are given in Figure 12. Note that the effect of particle size can be clearly seen also in Figure 10 and 11. Not surprisingly, a decrease in the charge density of the coal sample is observed with increasing mean particle diameter. This can simply be attributed to the higher surface area-to-mass ratio of the finer particles, creating larger contact area at a given mass.

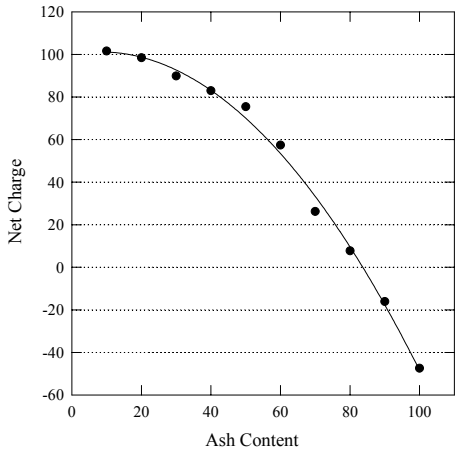

Figure 13 The effect of feed composition on particle surface charging.

Effect of Ash Content

Figure 13 shows the results of the charge measurements conducted on the Pittsburgh No.8 coal samples with approximately 6% and 20% ash contents. The results show that lower the ash content, the higher the charge density becomes. Consider that the data attained from the charge measurements are the net charge. It is presumed that the charge acquired on ash-forming minerals present in coal may offset the charge density of coal obtained while charging. However, the effect of ash content on the tribocharge density is still far from conclusive. No dependence of the charge density on the ash content can be established in this paper.

Effect of Temperature

Figure 14 illustrates the charge densities of the samples obtained from the experiments when the system temperature was varied. The charge measurements were conducted at an air velocity of 1.9 m/sec and at a particle feed rate of 0.2 Kg/min. The results show that the charge densities of clean coal and quartz samples increase with increasing temperature. It is well known

that humidity is one of the critical factors in electrostatic separation. Such water adsorbed onto the particle surface may increase the surface electrical conductivity. Accordingly, the charge on a particle that originated by contact electrification under humid environment, in most cases, will dissipate rapidly when touched by other particles due to the surface conductivity created by the surface moisture. It may thus be concluded that the increase in temperature in this case has an

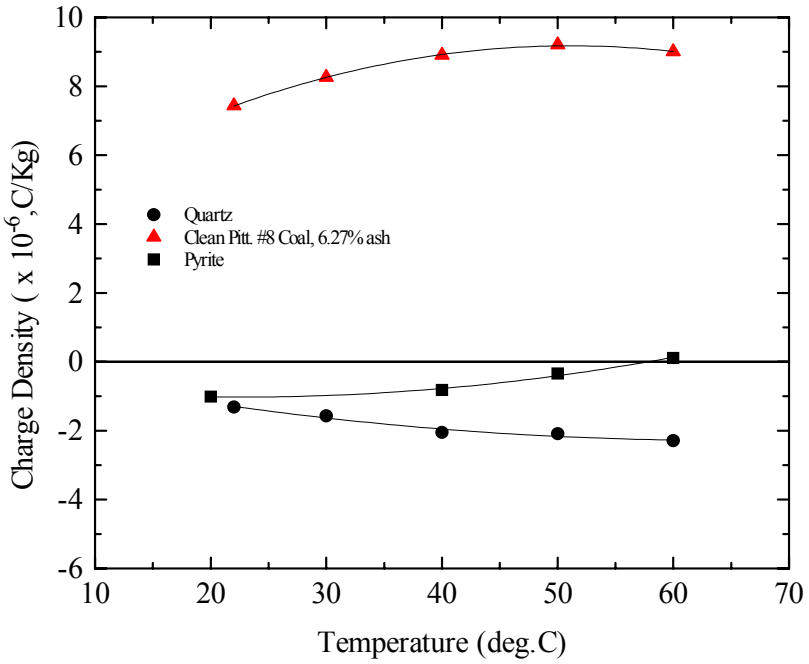

Figure 14. The effect of temperature on particle surface charging

effect on the charge density in such a way that the surface moisture of these insulator samples be dried away.

By contrast, the charge density of the pyrite sample decreases with increasing temperature. It is well established that pyrite possesses a conducting ability, maybe not as well as a pure metal but certainly not as bad as an insulator. In elementary solid state physics (Omar, 1993), it is stated that the conductivity depends on temperature. In this situation, the

conductivity is expressed in terms of the microscopic properties pertaining to the conduction electrons. One finds the following expression for the conductivity,

$$\sigma = Ne^2\tau / m^* \qquad [7]$$

where N is the concentration of the conduction electrons, τ is called the *relaxation time*, and m* is the *effective mass* of the electron. It has been seen that the conductivity increases as N increases, because there are more current carriers. From the result of statistical mechanics distribution, the concentration of conduction electrons is found increasing exponentially with temperature. Thus, as the temperature is raised, a greater number of electrons is excited and the conductivity increases accordingly. For this reason, the pyrite sample becomes more conducting with increasing temperature, resulting in a decrease in the charge density. As mentioned earlier, the conductivity allows the charge to leak away from the contact area when two conductors are touched with each other (Rose-Innes, 1980).

3.1.5 Parametric Study of Operating Parameters of Particle Charging

Test Matrix

A statistical test matrix based on the composite Box-and-Behnken experimental design technique was developed to study the effects of operating parameters on particle charging mechanisms. The test matrix included four parameters that affect the charging mechanisms: air velocity, particle feed rate, particle size, and feed composition. Each parameter was examined at three levels: high (+1), normal (0), and low (-1). Appendix A delineates the 4x27 test matrix; the table indicates the various combinations of parameters at different levels. In an attempt to minimize operational bias, all tests were performed in random order.

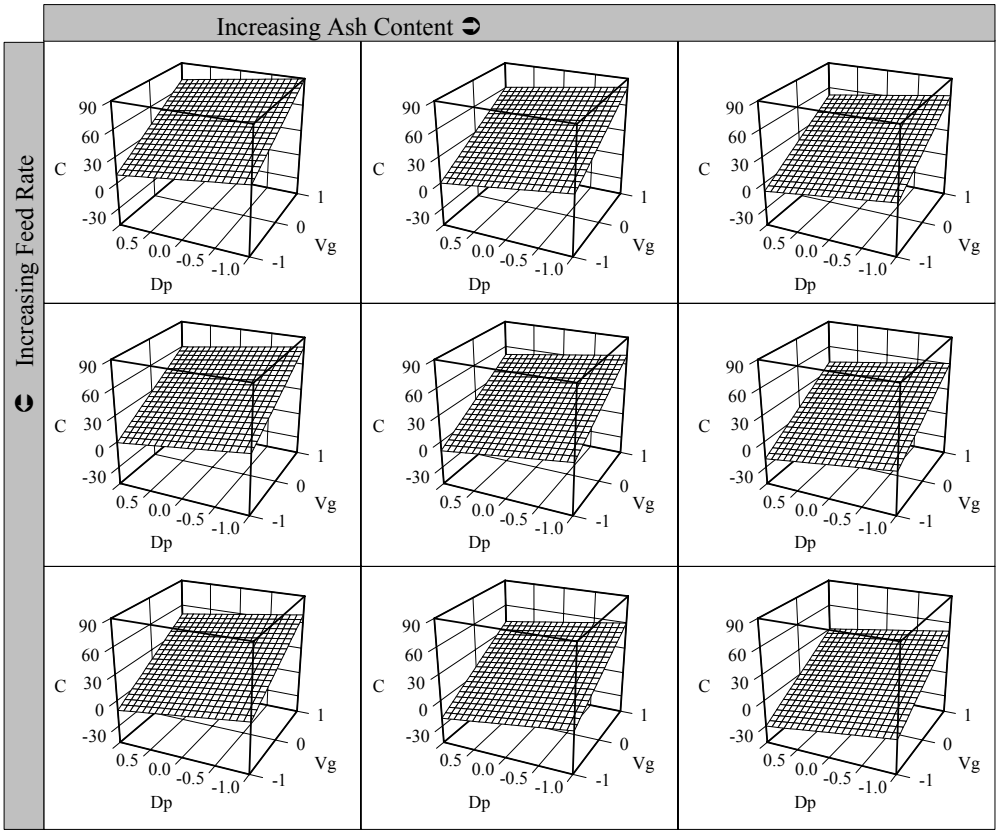

Figure 15 The effects of operating parameters on particle charging mechanisms. The study was based on the composite Box-and-Behnken experimental design technique. The test matrix included four parameters that affect the charging mechanisms: i) air velocity, ii) particle feed rate, iii) particle size, and iv) feed composition. (C: charge density, Dp: particle size and Vg: air velocity)

Effects of Air Velocity

Figure 15 shows the effects of operating parameters on the particle-charging behavior. The results are presented in such a way that the interactions between different parameters can be easily discerned. As shown, the magnitude of the charge density increases with increasing air velocity at all particle sizes studied. An increase in air velocity should increase the force with which a particle impinges on the copper walls and the blades of the in-line mixer charger

resulting in an increased charge density. This finding is consistent with reports submitted by numerous other investigators.

Effect of Particle Size

The results presented in Figure 15 further suggest that finer particles exhibit higher charge densities. This can simply be attributed to the high surface area-to-mass ratio associated with finer particles. Of the various parameters tested, particle size and air velocity interact significantly with one another. Air velocity exerts greater influence with finer particles. The velocity of the larger particles is not as significantly affected due to the greater inertia. The other parameters, feed rate and ash content, do not significantly interact with either particle size or air velocity. Figure 15 reveals that particle charge attains a maximum when particle size is small. Based on charge measurement it is concluded that better separation takes place with fine particles. However there appears to be a lower size limit beyond which the separation deteriorates.

Effects of Feed Composition

Figure 15 indicates that the charge density C (reported in Coulombs per unit area) decreases with increasing ash content in feed regardless of feed rate. The ash content in the feed was varied by mixing known amounts of coal (clean Pittsburgh coal assaying 6% ash) and quartz (representing ash-forming minerals in coal). The reason the charge density decreases with increasing ash content in the feed is because coal is positively charged while quartz is negatively charged. When a feed stream contains both positively charged coal and negatively charged quartz particles, the net charge registering on the charge-measuring device would be a weighted average of the two. The data were obtained at the feed rate of 0.3 kg/min with an air velocity of 1.9 m/s.

Effects of Feed Rate

The results of Figure 15 reveal that charge density decreases with increasing feed rate. This observation may be attributed to the decrease in particle velocity with increasing feed rate. At a given air velocity, particle velocity decreases with increasing feed rate.

3.1.6 Charge Measurements Using Tribochargers Made of Various Materials

The material that the charger is fabricated of impacts the charge magnitude of both the coal and the mineral matter; the particle-wall interactions produce charges on the surface of the particles. Thus, material selection for the in-line mixer is very important. Copper is frequently employed because it retains a work function that resides between that of coal and mineral matter. The effect work functions on particle charging using different materials was studied.

The materials studied were as follows: aluminum, chromium, copper, nickel, stainless steel, copper-nickel alloy, polyvinylchloride (PVC), and Teflon. Charge measurements were performed with the aforementioned novel device. A relatively pure sample of Pittsburgh No. 8 clean coal (5.29% ash) was employed in the charge measurement work. The sample was prepared by subjecting the lump coal to three stages of comminution; the coal was processed with a jaw crusher, roll mill, and hammer mill. The pulverized sample was dry-screened to procure a 65x100 mesh size fraction. In addition, charge measurements were executed with quartz (SiO_2) samples purchased from Fisher Scientific Company. The powdered sample was dry-screened to obtain the same size fraction as that of the coal. Quartz was selected since its charging behavior is representative of many ash-forming minerals typically present in coal.

The coal and the quartz samples were preheated in an oven to 118 degrees Celsius before being presented to the tribocharger. To avert possible oxidation complications, the coal sample was supplied to the tribocharger by means of compressed nitrogen gas. Charge measurements

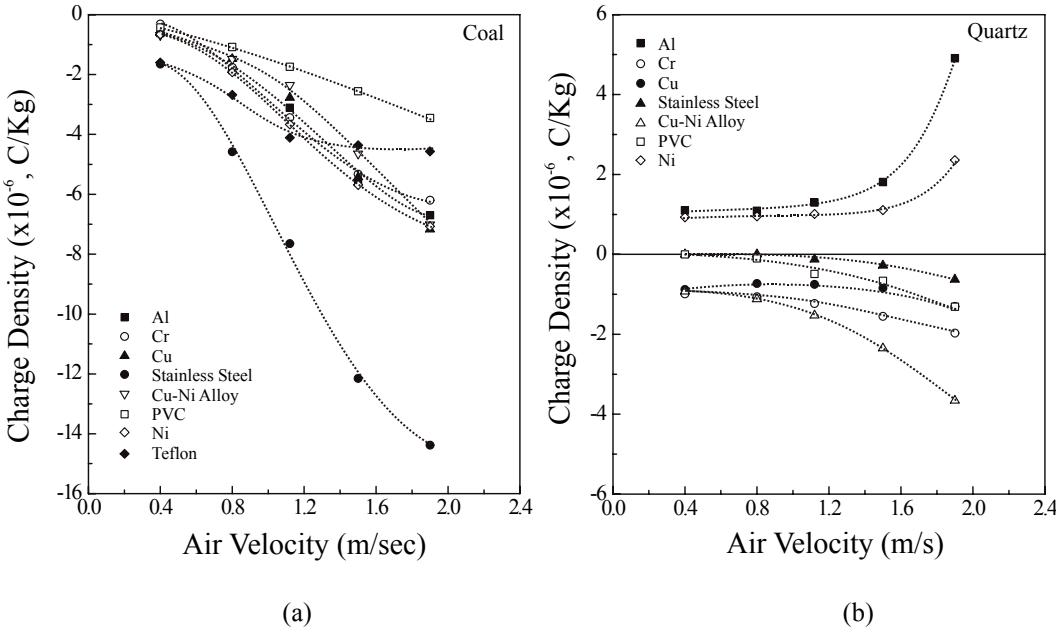

Figure 16 Results of particle charging mechanism study for coal and quartz as a function of the charging material work functions

were conducted at a pressure of 276 kPa (40 psig) with a particle feed rate of 0.2 kg/min. Measurements were performed a minimum of four times.

Figure 16a and 16b reveal the influence of material type on the charge densities of clean coal and quartz samples, respectively. The work functions of these materials are listed in Appendix B. In each set of experiments, the test results were obtained as a function of gas velocity. As expected, Figure 16b indicates that the quartz sample became negatively charged for the majority of materials examined. Such a finding is consistent with the charge measurement data reported by other investigators for typical ash forming minerals. The only exceptions to said finding occurred when either aluminum or nickel was employed as the charger material. In these two cases, positive charge densities were obtained over the range of the gas rates examined. This charge reversal may be explained by the relatively high work functions of nickel and aluminum (refer to Appendix B). Quartz particles obtain positive charges when

contacted with these metals since the work function for quartz (ϕ = 5.0 eV) is lower than that of aluminum (ϕ = 5.42 eV) or nickel (ϕ = 5.22 eV).

Conversely, coal should be positively charged when contacted with copper or a copper-nickel alloy. However, the results given in Figure 16a show that the coal particles tested in this analysis became negatively charged regardless of the type of material used to construct the tribocharger. These unexpected results may be attributed to i) alternation of coal feed or charger material work functions due to inadvertent surface oxidation or ii) the potential unusual chemical composition of the coal sample used in the present study. It is also possible that the Pittsburgh No. 8 coal sample used in this particular study has different chemical compositions than the sample used in the previous charge mechanism studies.

This work was repeated using a mill reject sample taken from a local utility site. This sample contained 42-43% ash and was sized and pre-cleaned in the laboratory-scale triboelectric separator to give a minus 42 mesh, 6.1% ash sample for use in this testwork. Figure 17 shows the particle charging data for coal and quartz as a function of the charging material work functions. In general, reasonable agreements have been found between particle charging behavior and the charger work function. As shown in Figure 17a, the charge density of a pre-cleaned utility reject sample (~6.1% ash) has an approximately linear variation with the work function of the charging materials. Similar results can be observed in Figure 17b for the case of quartz. It is worth noting that the work functions of both materials can be estimated by finding the eV value corresponding to a charge density of zero. For example, the work function of the pre-cleaned utility reject sample estimated from the results shown in Figure 17a is approximately 3.5-3.6 EV, whilst that for quartz estimated from the results shown in Figure 17b is 4.95 eV. These values are close to the work function values of 3.93 eV and 5.0 eV, respectively, that are commonly reported in scientific literature for coal and quartz.

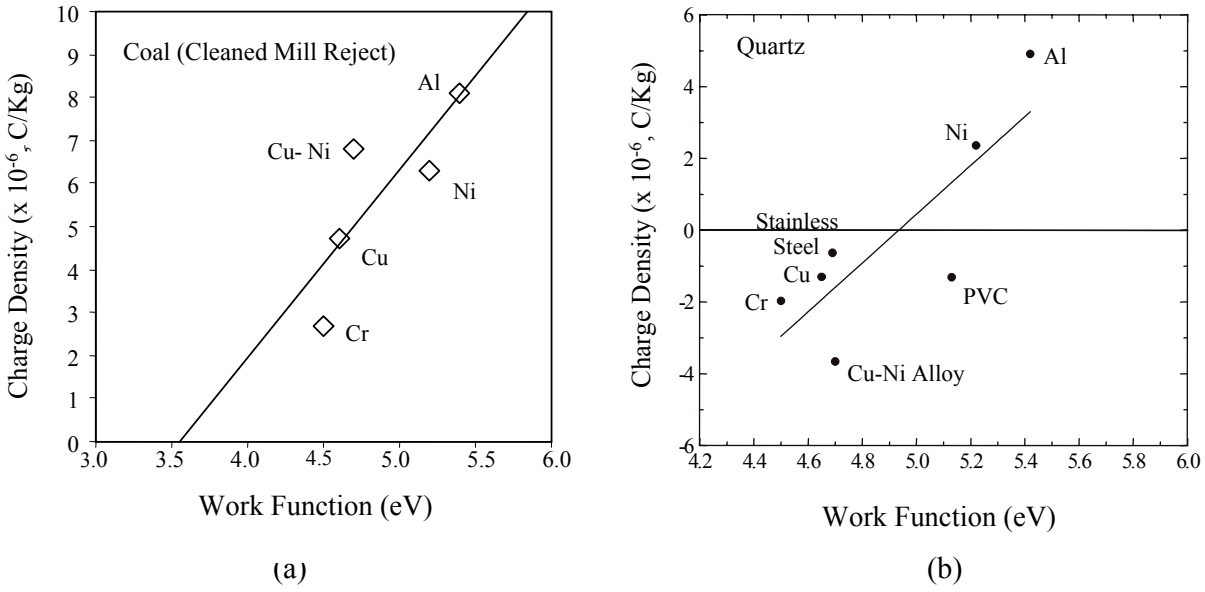

Figure 17 Results of particle charging mechanism study for coal and quartz as a function of the charging material work functions

3.1.7 Charger Design

An in-line mixer constructed of copper was utilized for the initial stage of engineering test work. The bench-scale tribocharger is depicted in Figure 18. The mixer possessed the following dimensions: 13 mm (½-inch) diameter coupled with a length of 152mm (6-inches). The Koflo mixer was equipped with four blades within the tubing. Testing at high feed rates revealed clogging and poor separation efficiencies. Such results suggested that the number of blades might have been excessive.

A tribocharger possessing straight Plexiglas tubing with no internal blades was installed to circumvent said problems. The employment of Plexiglas tubing eliminated clogging while increasing separation efficiency. Such results are not incongruous with NETL results where Nylon was determined to charge more efficiently than copper. This verifies that a charger made of Plexiglas yields higher ash and sulfur rejection than a copper charger without sacrificing yield and combustible recovery.

Figure 18 Bench-scale tribocharger made of Plexiglas used in conjunction with the drum-type bench-scale triboelectrostatic unit.

The Plexiglas charger was further modified and replaced by a newly designed feeder/charger system as shown in Figure 19. The engineering guidelines for the modification of the charger are based on the results obtained from the parametric studies. The new charger was designed to produce charged particles by mixing the feed by means of a specially designed impeller which was driven by an air motor. The charged particles are then directed to a feed distributor in the shape of a rectangular tube. A series of cylindrical blocks have been installed in a zigzag fashion to ensure an even flow of charged particles to the separator. In addition, the design maximizes particle-particle and particle-wall interactions. A notable characteristic of the design is that the particles in the feed stream are subjected to strong agitation by the impeller. Hence, the new charger is referred to as the turbocharger.

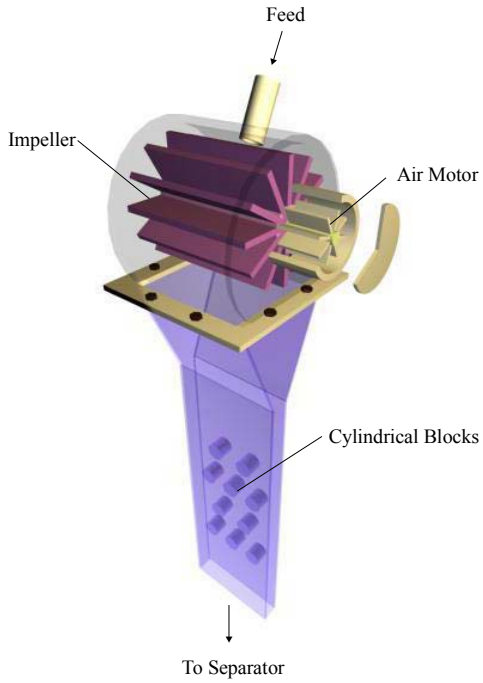

Figure 19 Schematic representation of the turbo charger used in the bench-scale TES unit separation study

The turbocharger was tested on the clean Pittsburgh No. 8 coal sample (-140+200 mesh fraction, 6.4% ash, and 1.68% sulfur). The results were contrasted with those obtained with the straight pipe. Figures 20 and 21 compare combustible recovery vs. ash and combustible recovery vs. total sulfur curves, respectively. The tests were conducted at a feed rate of 3 kg/hour with one electrode at +40 kV and the remaining electrode grounded. The tests indicate that the new charger is capable of producing significantly better results than the straight pipe charger. The new TES unit, equipped with the turbocharger, provided 10% higher combustible recoveries.

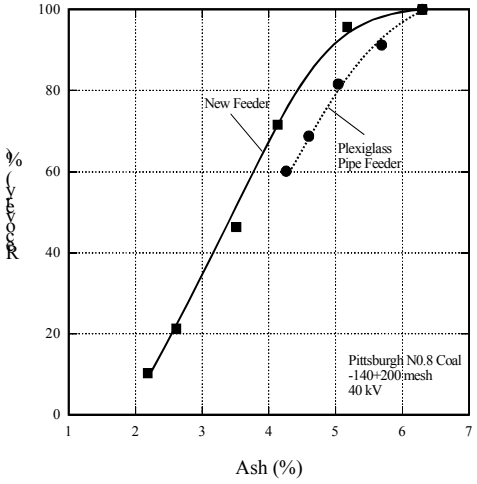

Figure 20 Comparison of separator performance (ash rejection) of the bench-scale TES unit using different turbochargers

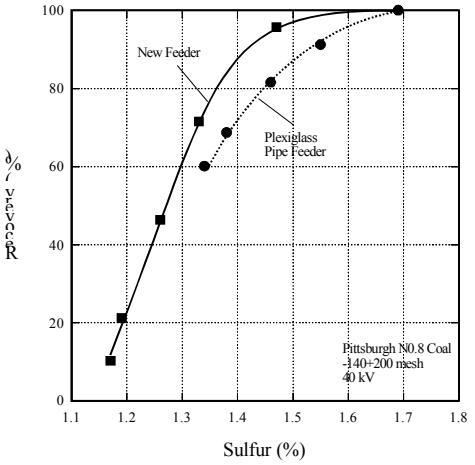

Figure 21 Comparison of separator performance (sulfur rejection) of a bench-scale TES unit using different turbochargers

3.1.8 Finalized Tribocharger Design for the POC Unit

Improvements in the charger designs that substantially improved charging and hence separation efficiency. The turbocharger design that was the last in the series of charger designs made a significant impact in the separation efficiency. The improvement in separator performance can be attributed to the charger that design maximizes particle-particle and particle-wall interactions.

3.1.9 Conclusion – Charge measurement and Tribocharger Design

Four parameters affecting triboelectrification mechanisms were investigated. These include: i) particle size, ii) temperature, iii) air velocity, and iv) feed rate. The charge

measurements were conducted on coal, quartz and pyrite samples. The results show that charge density increases with:

- increasing air (or particle) velocity for all particle sizes studied,
- decreasing particle size,
- decreasing feed rate, and
- increasing temperature.

The particle charge measurement results showed that coal is positively charged, while both quartz and pyrite are negatively charged. That coal is charged differently from both of these mineral matters serves as the basis for the TES process. The results also showed that at a given experimental condition, pyrite is more negatively charged than quartz, suggesting that the former can be more readily separated than the latter by the TES process.

A statistical test matrix based on the composite Box-and-Behnken experimental design technique was developed to study the effects of operating parameters on particle charging mechanisms. The test matrix included four parameters that affect the charging mechanisms, namely: i) air velocity, ii) particle feed rate, iii) particle size, and iv) feed composition. The results can be summarized as follows:

- the magnitude of the charge density (given in units of coulombs per unit area) increases with increasing air velocity at all particle sizes studied,
- charge density decreases with increasing feed rate,
- charge density increases with decreasing particle size, and
- charge density decreases with increasing ash content in feed regardless of feed rate,

- of the various parameters tested, particle size and air velocity are interacting with each other most significantly. The finer the particle size, the more significantly the air velocity affects the particle charge.

The effect of work functions on particle charging using different materials was studied. The materials studied were as follows: aluminum, chromium, copper, nickel, stainless steel, copper-nickel alloy, polyvinylchloride (PVC), and Teflon. The test results show that the quartz sample became negatively charged for the majority of materials examined. Quartz particles obtain positive charges when contacted with aluminum and nickel since the work function for quartz (ϕ = 5.0 eV) is lower than that of aluminum (ϕ = 5.42 eV) or nickel (ϕ = 5.22 eV).

Three different tribochargers have been evaluated during the course of study. These chargers include 1) in-line static mixer made of copper, 2) Plexiglas pipe, and 3) Turbocharger made of Plexiglas. The turbocharger design that was the last in the series of charger designs made a significant impact in the separation efficiency. The improvement in separator performance can be attributed to the charger design that maximizes particle-particle and particle-wall interaction.

Subtask 3.2 – Separator Development Tests

3.2.1 Objectives

The primary objectives of this task were i) to evaluate different bench-scale designs for the triboelectrostatic separator, and ii) to investigate the effect of various operating parameters on separator performance. The information obtained from this task was then subsequently used for obtaining engineering guidelines for the design, manufacture, operation and optimization of the 200-250 Kg/hr POC unit.

A statistical design of experiments (central-composite) will be used to develop a test plan for evaluating the performance of 1 kg/hr bench-scale electrostatic separator. Operating variables that have previously been determined to influence the efficiency of the triboelectrostatic separation process will be included in the statistical design along with several of the primary machine design variables. These include particle size, feed solids concentration, feed flow rate, path length and electrode potential. At least three different levels for each operating and design parameter will be tested. The feed size will vary in the range of 50 to 100 μm top-size and the maximum potential difference between two electrodes will be 100 kV. The experimental design will result in thirty-two (32) tests for each of Pittsburgh No. 8 and Sewell coal samples. For each coal, the resultant test data will be statistically evaluated using the response surface methodology (RSM) technique to clearly establish the significance of each variable and the degree to which it influences the performance of the triboelectrostatic separation of coal. Implementation of the remainder of the project task is predicated on consistently achieving the minimum acceptable performance previously determined by the contractor and accepted by the DOE COR.

The performance data obtained from the 1 kg/hr test unit will be validated using a second bench-scale separator having a nominal capacity of approximately 10-20 kg/hr. Data collected from this system will be very useful for the establishment of accurate scale-up criteria and the achievement of the desired performance of the TES process at the POC scale. The entire prototype-scale TES circuit will be thoroughly examined under various operating conditions using samples from the Pittsburgh No. 8 and Sewell Seams. Operating parameters to be tested under this task include solids throughput, gas flow rate, particle size, and electrode potential. At least three different levels for each parameter will be employed. Particle sizes up to 100 μm and differential potentials between the two electrodes up to 100 kV will be examined in this series of tests. A central-composite statistical design of experiments requiring thirty (30) tests will be employed for

each coal sample. The system will be designed to operate continuously and its performance will be evaluated only after reaching steady-state operation. The design of 10-20 kg/hr system will start immediately after the 1 kg/hr bench-scale tests are completed and test data analyzed. The configuration of 10-20 kg/hr separator will be essentially identical to the POC system constructed, tested and evaluated later within the project.

All of the bench-scale tests will be conducted by forcing pulverized coal under pressure through a static mixer tribocharger system. After passing through the static mixer, most particles will be charged and attracted toward either the positive or the negative electrode in the electrostatic separation zone. The ultimate destination of particles depends on the sign and magnitude of their surface charge which is determined by the surface characteristics of particles. Particles with a high negative charge will be deflected toward the positive electrode and discharged from the separator as reject, while those with a high positive charge will be attracted toward the negative electrode and discharged as the clean coal product. However, some particles may not be charged effectively by the static mixer and pass through the electrostatic field in the separator without undergoing electrostatic separation. Therefore, the bench-scale separators will be designed so that the "by-pass" material can be re-introduced with the feed and recycled through the system until it becomes charged and separated.

The technical performance of the bench-scale systems will be evaluated in terms of energy recovery, ash and sulfur rejection, throughput capacity, and power consumption. Data collected from experiments in this phase of work will be statistically analyzed and the significance of each operating parameter to the performance of the TES process obtained. The optimum operating conditions will be established for the POC system after completing the analysis of the bench-scale test data.

Scale-up and performance expressions will be developed during the bench-scale test programs. It is anticipated that the scale-up of the 200-250 kg/hr POC triboelectrostatic separator from the bench-scale units will be primarily a function of the separator width, i.e., mass rate of feed per unit of roller width in kg/cm. On the other hand, separation efficiency will depend on electric field strength and the path length for a particle within the separation zone. The initial design value for the separator length will be based on modeling predictions obtained from bench-scale test work. To assist in the scale-up effort, a first-order mathematical model will be developed to describe the performance of the bench-scale test units. This model will be used in conjunction with the experimental test data to provide engineering criteria for the design and development of the 200-250 kg/hr POC separator.

A minimum acceptable performance standard for the electrostatic separator will be determined by the contractor and approved by the COR. For planning purposes, the performance standard will be the rejection of at least half the feed coal mineral matter while maintaining a combustible recovery of at least 80% by weight. This performance criteria is expected to be highly dependent on coal type and grind size.

3.2.2 Separator Testing Program

The bench-scale tests were conducted using several separators of different design having nominal capacities in the range of 1 kg/hr and 10-40 kg/hr. The performance data obtained from these units were used to develop scale-up criteria for POC unit. The separators were designed for the application of separating fine coal particles from high mineral (ash) content material. The principal differences in the designs were the configuration of the electrodes generating the electric field through which the feed material passes. All the separators were of the entrained-flow type as opposed to the surface-based type. The following type separators were designed, constructed and tested.

1. Rotating drum electrodes with no middlings recirculation
2. Pie configuration plate electrodes with middlings recirculation
3. Pie configuration electrode housings with the facility to interchange the following electrode types – Horizontal Rod, Vertical Rod, Plate, Drum and Screen.

The development and testing of the charger units took place in conjunction with the testing of the above separators. Tests were carried out on a number of fine coal feeds varying in size range, ash and sulfur.

Rotating Drum Electrode Separator

The separator consisted of two parallel horizontally mounted rotating cylindrical electrodes. The unit produces a non-uniform electrostatic field (open gradient) because of the cylindrical electrode design, which in turn induces an additional force on the particles that varies from the top to bottom of the electrodes. As turbulence can result in poor separation, a collimator (flow straightener) was incorporated into the design to provide laminar air flow within the separator. The cylindrical electrodes were constructed of brass which was chosen for its charging behavior, wear resistance and ease in using thin sheets for construction. Teflon was selected as the most appropriate material for holding the electrodes in position because of the low electrical conductivity, high strength and excellent heat resistance. A vacuum was applied to the base of the unit to draw air through and control the flow. Figure 22 shows a schematic representation of the separator. Figure 23 shows the photograph of the equipment.

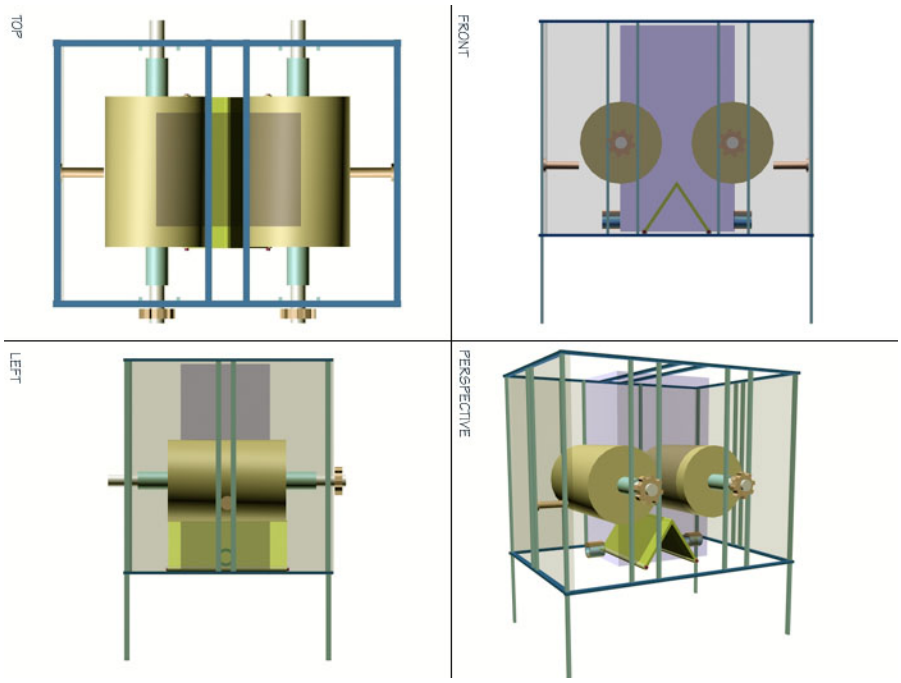

Figure 22 Schematic representation of the drum-type bench-scale TES unit.

Figure 23 Photograph of the drum-type bench-scale TES unit

The separator was initially operated in conjunction with an in-line mixer type charger, which imparted a positive charge to the coal and a negative charge to the mineral matter. The charged particles passed through the collimator and then through the uneven electric field created between the two rotating cylindrical electrodes. The coal particles were directed toward the negative electrode, while the mineral matter was directed toward the positive electrode. The splitter between the two electrodes could be located in different positions to achieve control of grade and recovery. The main advantage of the open-gradient separator concept is that the throughput is essentially proportional to the volume of the entrained flow. In addition, the rotating cylindrical electrodes are self-cleaning.

The separator was powered by a power pack which was capable of attaining a maximum applied voltage of 100 kV across the electrodes, i.e., +50 kV to the positive electrode and -50 kV to the negative electrode. Shakedown testing of the unit established the following.

1. Without the installation of the collimator the disturbance of air flow within the separator resulted in a poor separation. Poor separation was also experienced when there was no downward air flow
2. All of the tests were conducted by applying a potential to one of the electrodes and the other one grounded. It was observed that the grounded electrode did not attract significant amount of the ash-forming mineral matter or pyrite.
3. Tests showed that low ambient temperatures and high humidity resulted in poor separations.
4. Heating the feed material prior to testing improved the separation.

Following the shakedown testing a detailed test program was carried out to ascertain the separating efficiency of the unit. The effects of the following parameters were investigated.

- Bias Feeding
- Feed Rate

- Electrode Potential

Bias Feeding

The drum separator has two 305 mm (12-inch) diameter electrodes separated by 102 mm (4-inches) at the nearest point from each other. The standard method of feeding the unit was at the mid-point between the two electrodes, commonly referred to as 'feeding without bias'. However according to the simulation model feeding from off-center positions ('feeding with bias') should affect separation efficiency.

A series of tests were carried out by feeding the coal samples with and without bias. The tests were conducted on the Pittsburgh No. 8 ROM coal (-140+200 mesh) using the turbo charger. The results are presented in Figures 24 and 25. It was concluded that biasing the feeding point does not make a significant difference in separation efficiency.

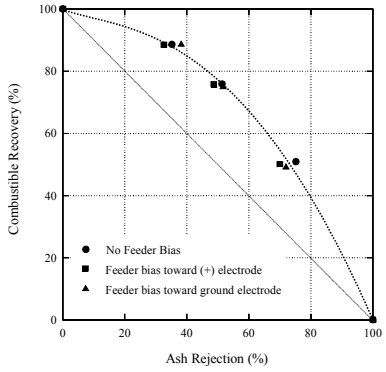

Figure 24 Effect of charger/feeder position on ash rejection of rotating drum separator using 140x200 mesh Pittsburgh No.8 coal sample

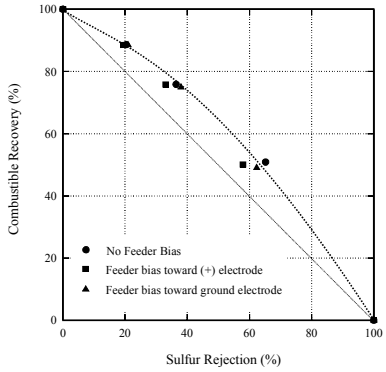

Figure 25 Effect of charger/feeder position on sulfur rejection of rotating drum separator using 140x200 mesh Pittsburgh No.8 coal sample

Optimum Feed Rate

A series of tests were carried out to establish the maximum throughput capacity of the bench-scale separator unit incorporating the turbo charger. The test coal used was Pittsburgh No. 8

clean coal (140+200 mesh), at 6.4% ash and 1.68% sulfur. Tests were conducted with the positive electrode at 50 kV, while varying the feed rate in the range of 3.6-40.0 kg/hr. At a given feed rate, the coal sample was cleaned in multiple stages to establish grade vs. recovery curves (see Appendix C for flowsheet). The samples used in this series of tests ranged between 4.9-6.3% ash and 1.5-1.75% sulfur and the product grade was therefore normalized with respect to the feed.

The test results showed that the performance of the bench-scale TES unit improves with increasing feed rate (Figures 26 and 27). This finding may be attributed to the possibility that at higher feed rates particles acquire higher charges. It is possible that the higher the feed rate to the turbo charger, the higher the probability of inter-particle collision will become, which should in turn give rise to higher surface charge on the particles. However, at a feed rate of 31.8 kg/hr, the separation efficiency begins to deteriorate, which may be attributed to the likelihood that the energy input per unit weight of feed decreased to the minimum required for efficient charging. In addition, the choke feeding results in a decrease in the particle-wall charging mechanism, which may play an important role in the triboelectrification mechanism.

From the combustible recovery vs. ash and sulfur rejection curves given in Figures 26 and 27, the maximum separation efficiencies were obtained and plotted in Figure 28 as a function of the feed rate. As shown, the separation efficiency was low at 3.6 kg/hr, which may be attributed to the difficulty in charging particles at a low feed rate. However, at feed rates above approximately 8.4 kg/hr, the separation efficiency remained more or less constant until the feed rate reached approximately 30 kg/hr. The separation efficiency deteriorated significantly above this limit. Thus, the maximum throughput of the bench-scale TES unit is approximately 30 kg/hr with the specific charger used.

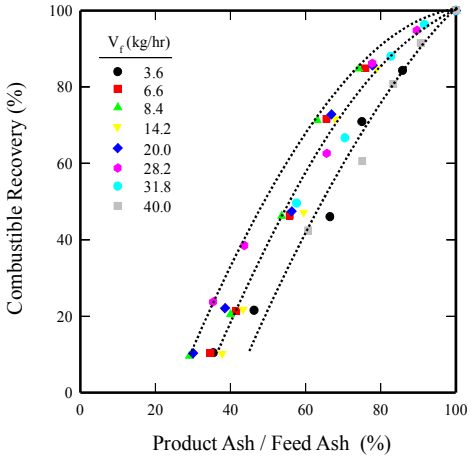

Figure 26 The effect of feed rate on the separation efficiency of the bench-scale TES unit. The normalized ash vs. recovery curves were obtained on a Pittsburgh No. 8 clean coal sample with a feed rate in the range of 3.6 – 40.0 kg/hr.

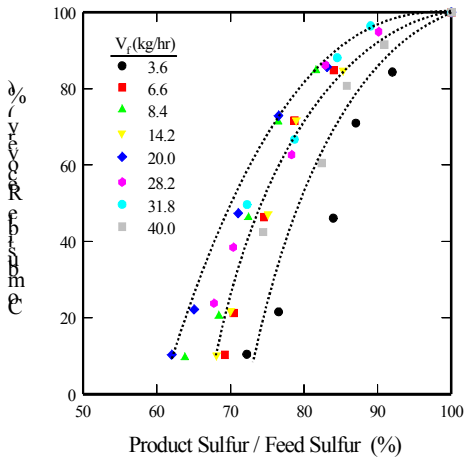

Figure 27 The effect of feed rate on the separation efficiency of the bench-scale TES unit. The normalized sulfur vs. recovery curves were obtained on a Pittsburgh No. 8 clean coal sample with a feed rate in the range of 3.6 – 40.0 kg/hr.

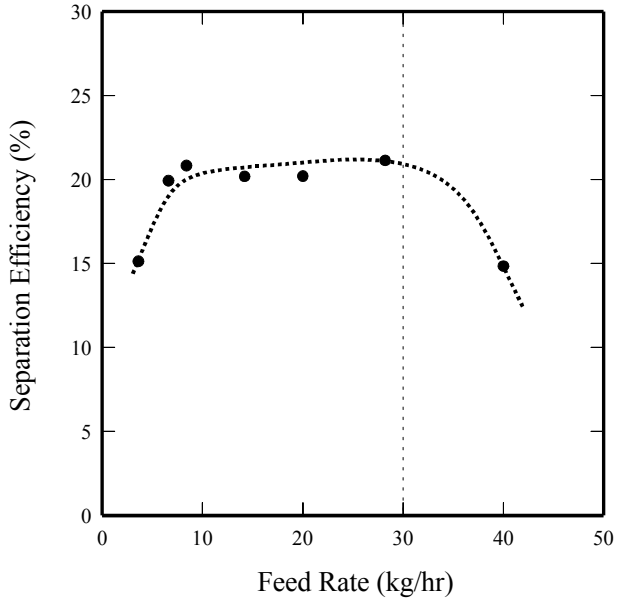

Figure 28 Separation efficiency as a function of feed rate. The maximum throughput of the bench-scale TES unit was found to be approximately 30 kg/hr.

It is possible to extend the throughput of the separator beyond 30 kg/hr by increasing the energy dissipation. The energy dissipation is the rate of energy input to a system, and is usually given in units of ergs per unit weight of feed per unit time. The throughput of the unit could be further increased either by increasing the rpm of the rotor blade or by increasing the overall size of the turbo charger.

Electrode Potential

A series of tests were carried out on both Sewell and Pittsburgh No 8 coals, where the electrode potential was varied at a given feed rate and a series of grade vs. recovery curves were prepared.

a) Sewell Coal Tests

The tests were conducted on a Sewell Seam clean coal sample using the -140+200 mesh fraction. The ash and sulfur contents were 6.7% and 0.97% respectively. The drum separator was operated in conjunction with a turbocharger. Tests were conducted at a feed rate of 8.2 kg/hr, while varying the applied voltages at four different levels, i.e., +30, +40, +50, and +60 kV. At a given test condition, the coal sample was cleaned in multiple stages to establish grade vs. recovery curves. Figures 29 and 30 show the combustible recovery vs. ash and the combustible recovery vs. sulfur curves, respectively.

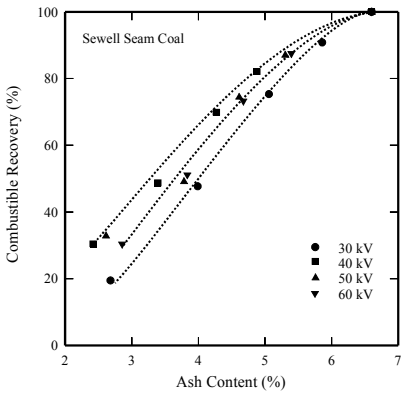

Figure 29 Effect of the electrical field strength on the separation efficiency of the bench-scale TES unit. The grade vs. recovery curves (ash) were obtained on a Sewell Seam clean coal sample with different voltage intensities.

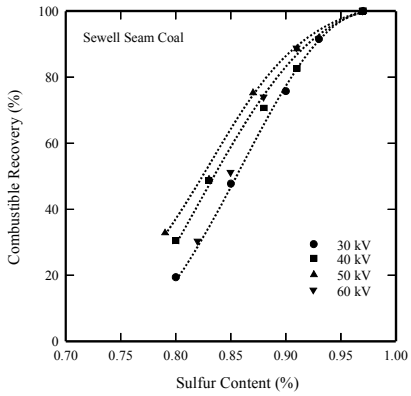

Figure 30 Effect of the electrical field strength on the separation efficiency of the bench-scale TES unit. The grade vs. recovery curves (sulfur) were obtained on a Sewell Seam clean coal sample with different voltage intensities.

The results show that the grade vs. recovery curves shift considerably depending on the potential applied to the electrodes. The best separation efficiencies were obtained at 40-50 kV. It appears that an electrode potential of 30 kV is not strong enough to pull the charged particles toward the electrodes. The slightly inferior results obtained at 60 kV can be attributed to entrainment (due to rapid particle movement at high electrode potentials) and/or particle charge alteration (due to inductive charging in the stronger electric fields).

Combustible recovery vs. ash and sulfur rejection curves have also been constructed, and are presented in Figures 31 and 32. The results show that the ash rejection was better than the total sulfur rejection with the Sewell coal tested under the conditions employed in the present work. The low sulfur rejection on this particular coal can be attributed to its low inherent sulfur content.

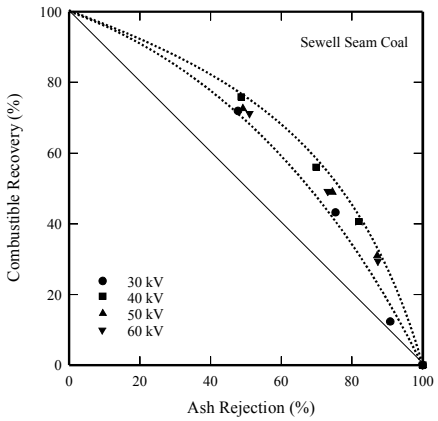

Figure 31 Ash rejection as a function of combustible recovery. The results were obtained on a Sewell Seam coal sample in the bench-scale TES Unit study.

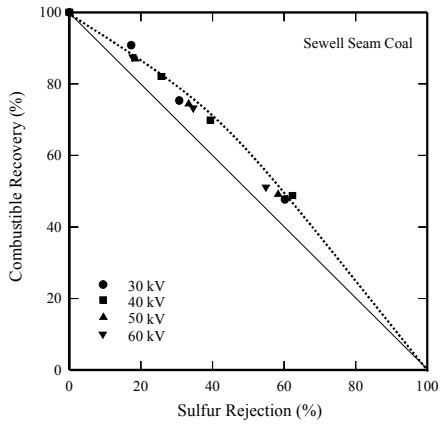

Figure 32 Sulfur rejection as a function of combustible recovery. The results were obtained on a Sewell Seam coal sample in the bench-scale TES Unit study.

b) Pittsburgh No. 8 Coal Tests

A series of tests were conducted on the Pittsburgh clean coal using the drum separator. Electrode potentials were varied while using a constant feed rate 4 kg/hr. A minus 200 mesh fraction was used in the majority of the tests, with one set of tests being conducted on the -140+200 mesh fraction to see the effect of particle size.

It has been noted that the drum separator is capable of producing very clean products in a single pass but at relatively low combustible recoveries. The solution to this problem would be to either to improve the design of the separator, and increase the recovery while maintaining the product quality or secondly increase the recovery by feeding the reject stream containing unrecovered coal to a second separator. At this stage the reject stream was collected, and reprocessed using the same separator.

A test was also carried out in recleaning the clean coal product obtained from the first stage to further improve the product quality. The test results have been plotted in Figures 33 and 34 in the form of recovery vs. grade curves for ash and sulfur, respectively. The results show that the grade vs. recovery curves shift considerably depending on the potential applied to the electrodes. Again, the best results were obtained at intermediate potentials (40 kV), with markedly poorer performance at 20 kV and slightly inferior results at 70 kV.

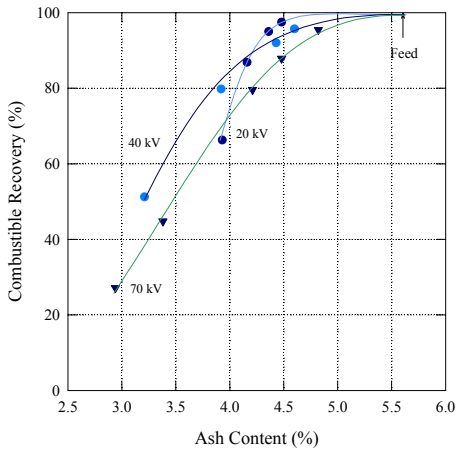

Figure 33 Grade-recovery curve (ash content) of the test results obtained with the drum-type bench-scale TES unit at various potential settings.

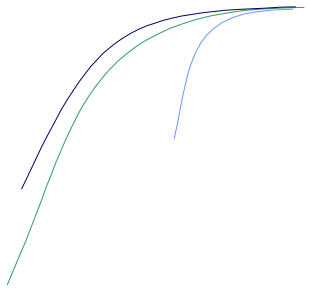

Figure 34 Grade-recovery curve (sulfur content) of the test results obtained with the drum-type bench-scale TES unit at various potential settings.

3.2.4 Comparison Between Drum Separator and NETL Plate Separator

The drum electrode separator is based on the entrained flow (or open-gradient) concept, which differs from the original NETL (surface-based) plate electrode separator. In the latter, positively and negatively charged particles are collected on negatively and positively charged electrodes, respectively. There are several problems associated with a surface-based design, which include:

- difficulty in removing the particles collected on electrodes,
- throughput being limited to the surface area of the electrodes,
- loss of particles in the bypass stream (i.e., the particles not collected on the electrodes).

In theory, the entrained-flow type separator can overcome all of these deficiencies. However, it has one drawback in that the quality of the clean coal product will not be as good as those obtained using the plate separator, simply because there is no bypass stream. Although the drum separator is an entrained-flow type, it has been found that considerable amounts of particles adhere on the surfaces of the drum electrodes. It was decided to use this phenomenon to test the surface-based separator concept. In order to compare the two types of separators the drum separator was operated in a) its normal rotating mode and b) as a surfaced based with the drum kept stationary. In the stationary mode the feed was introduced for 20 to 30 minutes and the materials remaining on the drum surface were scraped off, weighed, and assayed.

A series of comparative grade recovery tests were carried out between the rotating drum separator (entrained-flow type) and the stationary separator (surfaced-based type). The test was conducted with the positive electrode at 70 kV and with the other electrode grounded. The feed coal was a Pittsburgh No. 8 clean coal sample assaying 5.86% ash and 1.63% S. The results are shown in Figures 35 and 36 for ash and sulfur, respectively. These data show that the stationary separator gave significantly better results than the entrained-flow separator.

A review of the drum separator operations concluded that it was not a suitable design on which to base the POC separator. It was concluded that the drum separator had several problems:

- The separation efficiency is less than desirable;

- Short retention time for the particles in the electric field;
- The drum type electrodes make the equipment bulky and calculations showed that a very large POC unit would have to be built to accommodate the designated throughput; of 200-250 kg/hr.
- There are no provisions for recycling the middling fraction which is mainly responsible for the low separation efficiency.

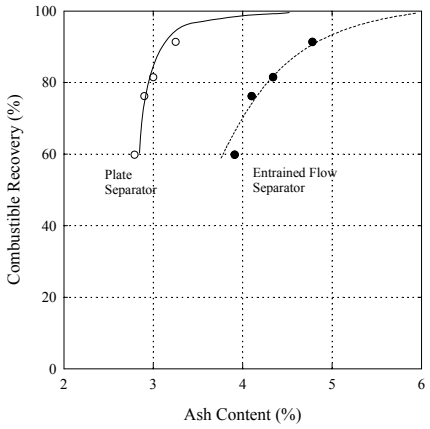

Figure 35 Product ash content as a function of combustible recovery for plate (surface-based) and drum (entrained-flow) type separators.

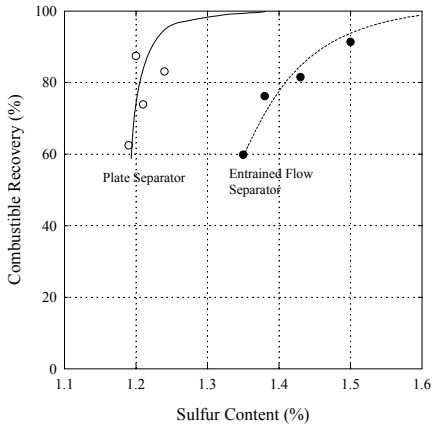

Figure 36 Product sulfur content as a function of combustible recovery for plate (surface-based) and drum (entrained-flow) type separators.

It is considered that this is not a problem specific to this particular entrained-flow unit, but is a generic problem associated with all of the triboelectrostatic separators tested to date by various investigators. It was decided therefore to design and build a new TES bench-scale unit that can provide both a high throughput capacity per unit volume of the separator and a high separation efficiency. Therefore, the new TES unit should have provisions for recycling a middling streams in order to achieve high separation efficiencies.

A theoretical model was developed and used to simulate the separator tests conducted using the bench-scale TES unit with drum-type electrodes. The model allows calculation of the particle trajectory in a non-uniform electric field created between two drum-type electrodes. The model predicts the trajectories as functions of particle size, particle charge density (in μC/kg), feed velocity, feed point, etc

3.2.5 Prediction of the Particle Trajectory

The particle trajectory is an important feature in determining the effect of field on the motion of the particle. Ideally, the particle (charged positive or negative) should follow a trajectory that is just enough to move it away from the similarly charged electrode, towards the oppositely charged electrode. The parameters that come into play while establishing the path followed by a particle include charge induced on the particle in the tribocharger, particle size and position of the feeder. The ability of a particle to move towards the correct electrode helps in establishing the good grade-recovery curves. The force balance equations developed in the population balance model (described earlier) define the nature of forces acting on the particles due to the effect of the varying electric field (open-gradient separator) and gravity. In the actual separator used in the project work, one was a positively charged electrode and the other connected to ground. Therefore, a negatively charged particle is just subjected to attractive forces (from the positive electrode) while the positively charged particle is under the influence of repulsive forces (again from the positive electrode). The electrode connected to ground provides neither an attractive force nor a repulsive force. It provides a surface for the positively charged particles to collect. As a part of the exercise of predicting the path taken by a particle, the force equations mentioned earlier are used. This model was aimed to develop the paths taken for four

different sizes of particles, four different charges induced on a particular size and four different feed positions.

Model Description:

Figure 37 describes the motion of the particle based on their relative charges with the electrodes. The same convention of axes was used for the following equations of forces. A negatively charged particle was considered while describing the forces acting on the particles. If a positively charged particle were to be considered, the electrostatic forces would be repulsive, instead of being attractive. The process was described in very small time intervals 'δt' and in this interval the initial velocity is 'u' and the final velocity, 'v'. In this infinitesimally small segment, the electrostatic force was assumed to be a constant.

The force acting on the negatively charged particle in the z-direction is:

$$ma_z = F_e \sin\theta \qquad [7]$$

where, 'a_z' is the resultant acceleration of the particle in the z-direction, m is the mass of the particle, 'F_e' is the force due to electrostatic attraction and θ is the angle described in the Figure 37. It should be noted that the force due to gravity was considered in determining the initial velocity of the particle entering the field (described later). Considering the size range of the particle, the only force influencing the particle in the electrostatic field is the force due to electrostatic attraction.

Since $F = E.q$,

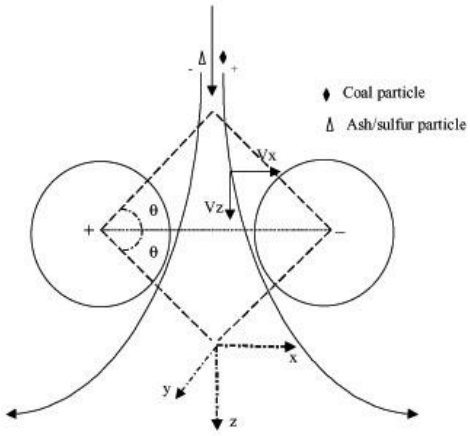

Figure 37 Experimental model for particle trajectory analysis

$$ma_z = Eq\sin\theta \qquad [8]$$

Substituting for E and q in the above equation gives:

$$a_z = \frac{q_e(mq_d)}{4\pi\varepsilon\varepsilon_0 r^2 m}\sin\theta \qquad [9]$$

and since $q_e = V \cdot 4\pi\varepsilon\varepsilon_0 l_d$

we get

$$a_z = \frac{Vl_d q_d}{r^2}\sin\theta \qquad [10]$$

where 'E' is the electric field intensity, 'q' is the charge on the particle, 'q_e' is the charge per electron, 'q_d' is the charge per unit mass of the particle, 'ε' is the permittivity of air, 'ε$_0$' is the permittivity of free space, 'V' is the voltage applied to the electrodes, 'l_d' is the distance between the electrodes, 'ρ$_p$' is the density of the particle, and 'r' is the distance of the particle from the center of the electrode.

$$z = u_z t + \frac{1}{2}a_z t^2 \qquad [11]$$

$$v_z = u_z + a_z t \qquad [12]$$

Here 'z' is the distance traveled by the particle in the vertical direction under the influence of the acceleration in the z-direction. The initial velocity of the particle (entering the electrostatic field)

in the z direction was taken to be the terminal velocity which was attained by using Stokes' law described below.

$$F_g = 6\pi\eta r_p u \qquad [13]$$

$$u = \frac{mg}{6\pi\eta r_p} \qquad [14]$$

where, 'u' is the terminal velocity of the particle, 'η' is the co-efficient of viscosity of the medium (air), 'r_p' is the radius of the particle being considered, 'm' is the mass of the particle described earlier and 'g' is the acceleration due to gravity. At the end of each segment, the acceleration is computed due to a change in the electrostatic force and all the subsequent steps are repeated. After each set of computations, 'v' of the earlier step becomes the 'u' of the next step and the new 'z' is the sum of the old 'z' and the incremented component. In the x-direction, only the electrostatic force caused a movement in the particle in that direction, which results in

$$ma_x = F_e \cos\theta \qquad [15]$$

Here, 'a_x' is the resultant acceleration of the particle in the x-direction (horizontal direction).

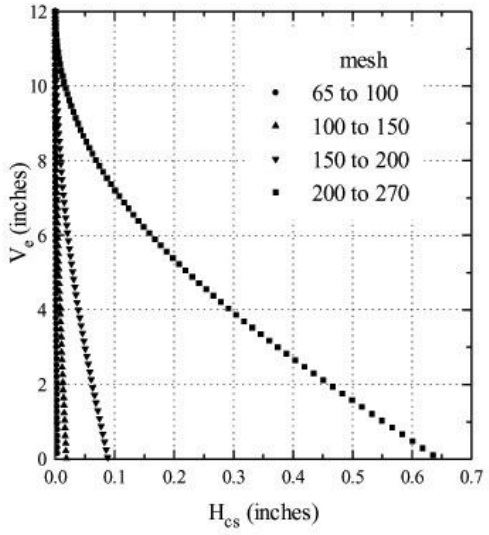

Figure 38 Trajectory of different size particle on being charged in a regular method

$$a_x = \frac{Eq}{m}\cos\theta \qquad [16]$$

Substituting the values of E and q in the above equation,

$$a_x = \frac{Vl_d q_d}{r^2}\cos\theta \qquad [17]$$

Taking equations of motion in x-direction,

$$x = u_x t + \frac{1}{2}a_x t^2 \qquad [18]$$

And,

$$v_x = u_x + a_x t \qquad [19]$$

A procedure similar to the one used in the computation of 'z' is also done for 'x'.

Following each set of computations, 'r' was calculated again using the equation given below.

$$r = \sqrt{z^2 + x^2} \qquad [20]$$

Figure 38 shows the results obtained with different sizes of coal at a particle charge density of 300 μC/kg. As shown, the smaller particles deflected less toward the electrode due to

the smaller coulombic force. This finding might be considered to provide an explanation for the difficulty in separating fine particles. However, the simulations were carried out under the assumption that the particles of different sizes have the same charge density, which is not realistic. As indicated earlier in this report, the charge density increases with decreasing particle size.

3.2.6 Development of Pie –Shaped Separator

A conceptual design of a commercial separator was prepared which would overcome some of the problems of the conventional entrained flow separators. Figure 39 represents a conceptual design of a new separator. It is based on the concept of non-parallel electrodes in a

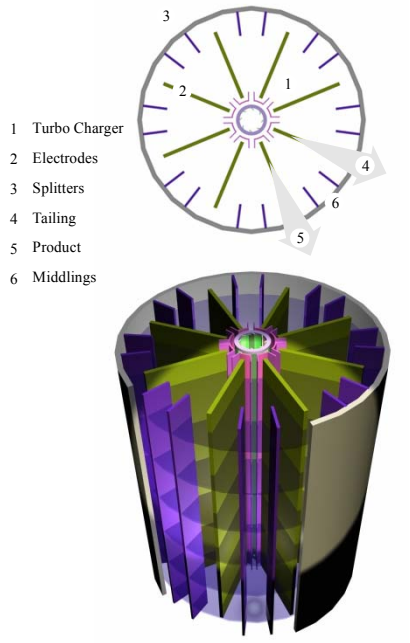

Figure 39 Schematic representation of the conceptual design of the pie-shaped TES separator.

circular arrangement with the circular units stacked in a column. It represents a full-size unit, which is designed to have a very high throughput per unit volume of the separator.

Some of the main design features are listed as follows:

- The turbocharger is located at the core of the unit, so that charged particles can be fed radially to the multiple units of pie-shaped separators.
- In each of the pie-shaped separator, there are two plate electrodes. These are designed to provide a long retention time for the particles and to provide laminar flow conditions.
- Each electrode is shared by two neighboring pie-shaped separators, so that savings in space and materials can be realized.
- Multiple units, each unit comprising 8 individual pie-shaped separators, can be stacked on the top of each other, so that the throughput per volume of the separator can be maximized.
- The compact design minimizes the requirement for materials and electrical wiring network.
- The new separator is designed to recycle the bypass materials back to the feed line, so that they can be recharged in the turbocharger before being given another chance to be separated.

In order to test the concept of the pie-shaped separator it was decided to construct a single section consisting of two non–parallel plates. Figure 40 shows the newly designed and constructed bench-scale TES separator incorporating the new design features. It represents a single pie-shaped separator, which is a part of the full-size unit shown in Figure 39.

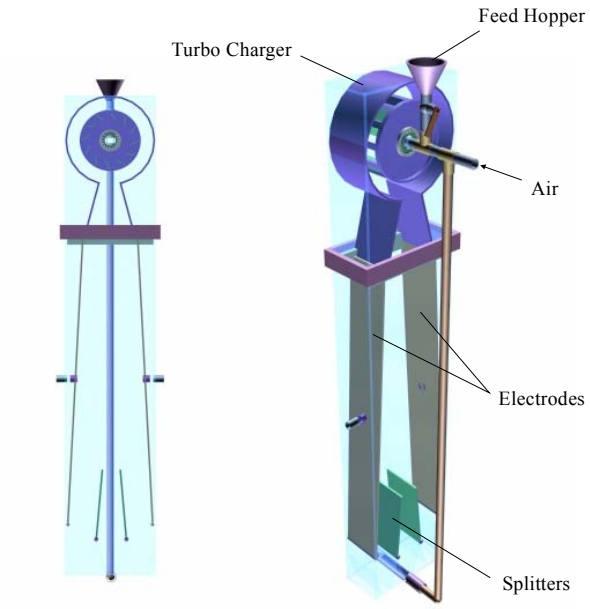

Figure 40 Schematic representation of the plate type bench-scale TES separator incorporating the turbocharger design.

The bench-scale unit consists of a turbo charger, two plate electrodes, a high-voltage power supply, and a recirculation conduit. Each electrode has dimensions of 102mmx508mm (4x20-inches) and its thickness is 3.175mm (1/8-inch). The distance between the electrode is 76mm (3-inches) at the top and 127mm (5-inches) at the bottom. The electrodes are connected to a high-voltage power supply (Hipotronics), which provides a constant potential difference of 30 kV between the two electrodes. During the operation pulverized coal is pneumatically fed to the turbo charger by means of compressed air. Particles discharged from the turbocharger flow through the electric field created between the two electrodes and are separated into two final product streams and a middling stream. The middling stream is pneumatically recycled back to the feed inlet. The electrode plates can be mechanically rapped to discharge any particles that adhere.

3.2.7 Comparison of the Bench-Scale TES Units in Terms of Separation Efficiency

The bench-scale TES tests were conducted using a clean-coal sample from the Sewell Seam provided by the A.T. Massey Coal Company. The original plan was to use ROM coals for the bench-scale testing. However, a decision was made to test clean coals. The reason behind this decision was that the most likely commercial application of this technology would be to upgrade the clean coals being burned at utilities. Sewell Seam coal was believed to be a good candidate for producing superclean coal fuels using the TES process, because of the low inherent ash.

Sample preparation was done one day before each test program to minimize possible surface oxidation. As-received Sewell coal samples were first crushed to minus 42 mesh, then pulverized in a hammer mill to minus 150 mesh and dry-screened to obtain four different size fractions, namely: 42x65, 65x100, 100x150 and minus 150 mesh. These samples were kept in an oven at 112^{o}C overnight to remove moisture from the surface of the coal particles..

Separator Test Results

Several series of tests were conducted on the Sewell Seam clean-coal sample using both the drum-type and plate-type bench-scale TES units incorporating the turbo charger developed in the present work. Separator tests were conducted with an electrode potential at 30 kV and a feed rate of 12.5 kg/hr. At a given feed rate, the coal sample was cleaned in multiple stages to establish grade vs. recovery curves (see Appendix C for flowsheet).

Three different configurations of the electrostatic separator were evaluated in the test program:

i) drum-type,

ii) plate-type without recycling, and

iii) plate-type with recycling.

All tests were conducted using feeds of different particle size fractions. These fractions differed considerably in feed assay, varying from 5.25-8.25% ash and 0.95-1.04% sulfur, and separator performance was therefore compared on the basis of the ratios of product ash to feed ash and product sulfur to feed.

Figure 41 shows the test results obtained on the bench-scale TES units with drum-type and plate-type electrodes. All tests were conducted with a 42 mesh x 0 Sewell Seam coal. The results show that the ash rejection was better than the (total) sulfur rejection under the conditions employed in the present work. It should be pointed out, however, that the low sulfur rejection is largely due to the low pyritic sulfur content of the coal sample tested. With this unsized (or by-zero) coal sample, there are no significant differences among the results obtained using the three different separators. The most likely reason for this is that the ultrafine particles present in the feed is creating difficulties in achieving high degrees of separation efficiencies. In other words, the advantage of using a superior separator is masked by the difficulty in treating a by-zero coal sample.

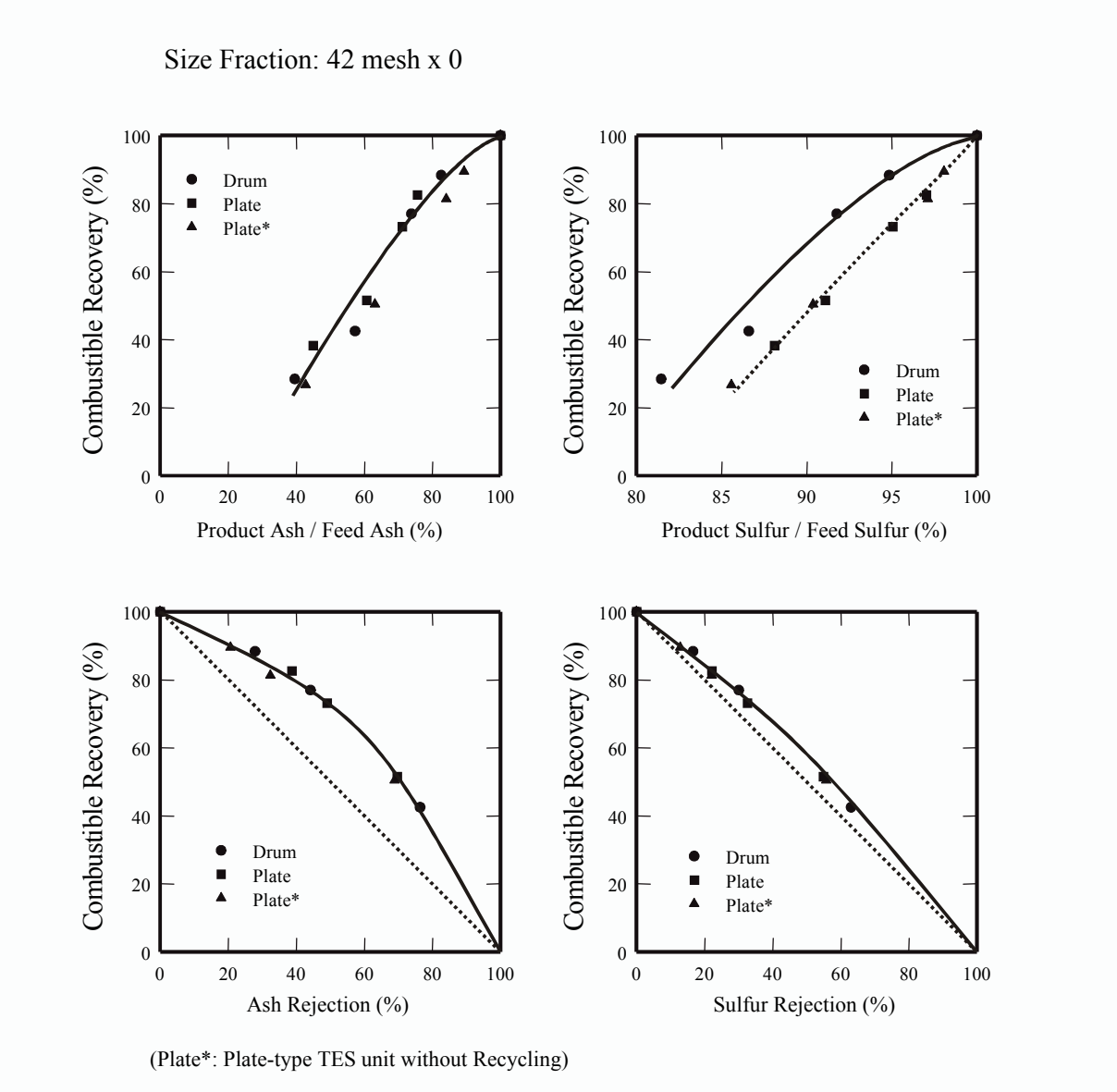

Figure 41 Comparison of the separation performance of the drum-type, plate-type without recycling (*plate**) and plate-type with recycling bench-scale TES units. The separator test results were obtained on a Sewell Seam minus-42-mesh clean-coal sample.

Figures 42 - 44 show the test results obtained with the feed coal samples from which ultrafine particles were removed. Three different feed coal samples were prepared; including monosized samples of 42x65, 65x100 and 100x150 mesh fractions. Figure 45 shows the test results obtained with the –150x0 mesh fraction of the same sample. The tests were conducted using the three different bench-scale TES units. In general, the plate-type TES unit with

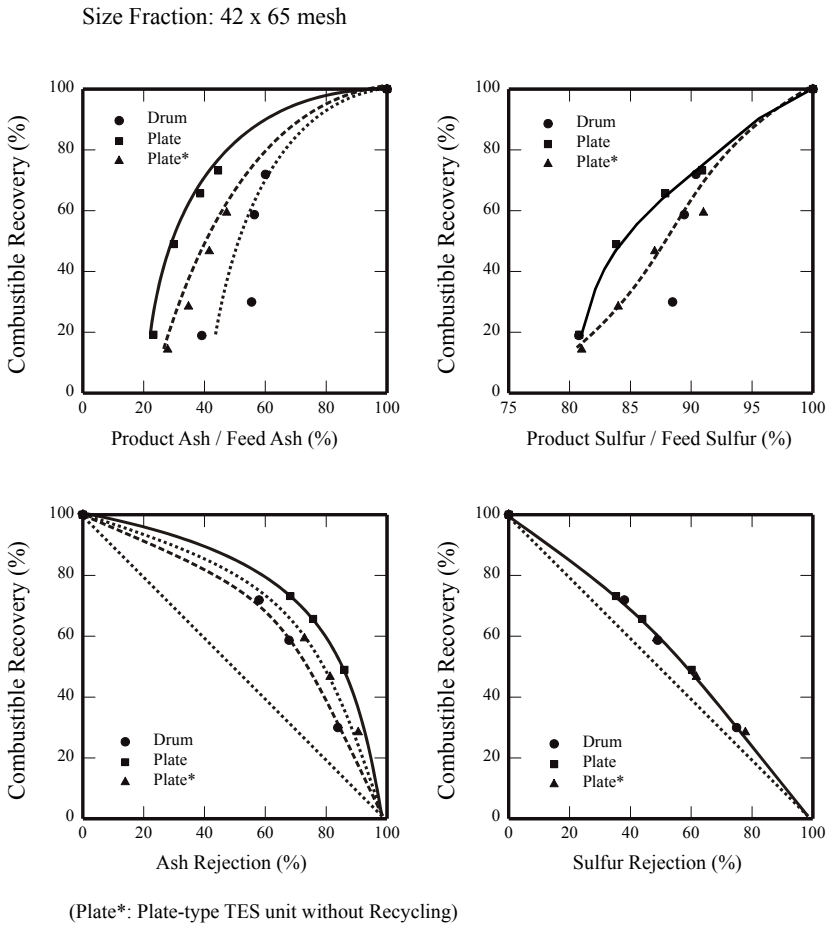

Figure 42 Comparison of the separation performance on the drum-type, plate-type without recycling (*plate**) and plate-type with recycling bench-scale TES units. The separator test results were obtained on a Sewell Seam 42x65-mesh clean-coal sample.

recycling provisions gave the best performance, while the drum-type unit without recycling provisions provided the poorest. The plate-type TES unit without recycling provisions achieved a level of performance intermediate to that of the other two configurations. The higher separation efficiencies obtained on the plate-type TES unit may be attributed to i) recycling of the middling particles, and ii) the longer retention times for the particles in the electric field.

In general, the separation efficiencies obtained with the monosized feeds were substantially higher than those obtained with the coal samples containing ultrafine particles (see

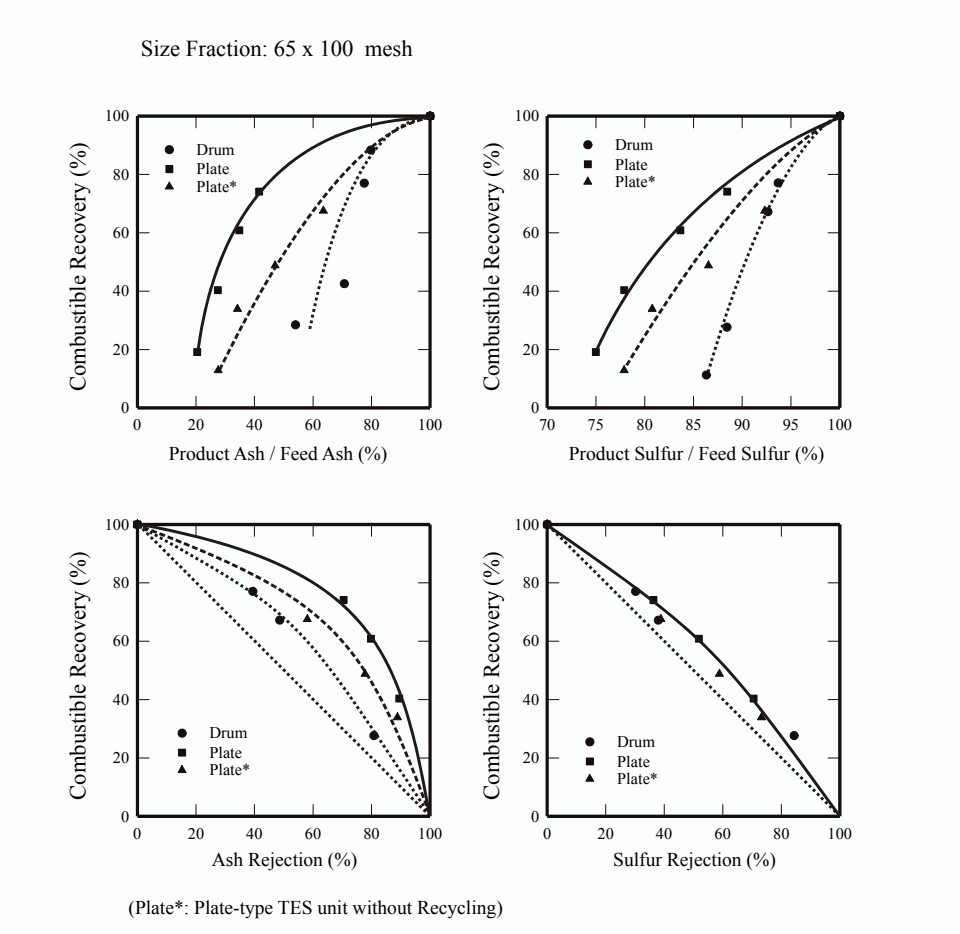

Figure 43 Comparison of the separation performance on the drum-type, plate-type without recycling (*plate**) and plate-type with recycling bench-scale TES units. The separator test results were obtained on a Sewell Seam 65x100-mesh clean-coal sample.

Figure 41). The difficulty in cleaning feeds containing ultrafine particles can also be seen with the test results obtained with a 150 mesh x 0 Sewell Seam coal (see Figure 45).

In Figure 46, the separation efficiencies of the test results given in Figures 41-45 are plotted. It shows the following:

1. The plate-type TES units with provisions for middlings recycle gave the highest separation efficiencies.

2. The separation efficiency deteriorates with decreasing particle size.

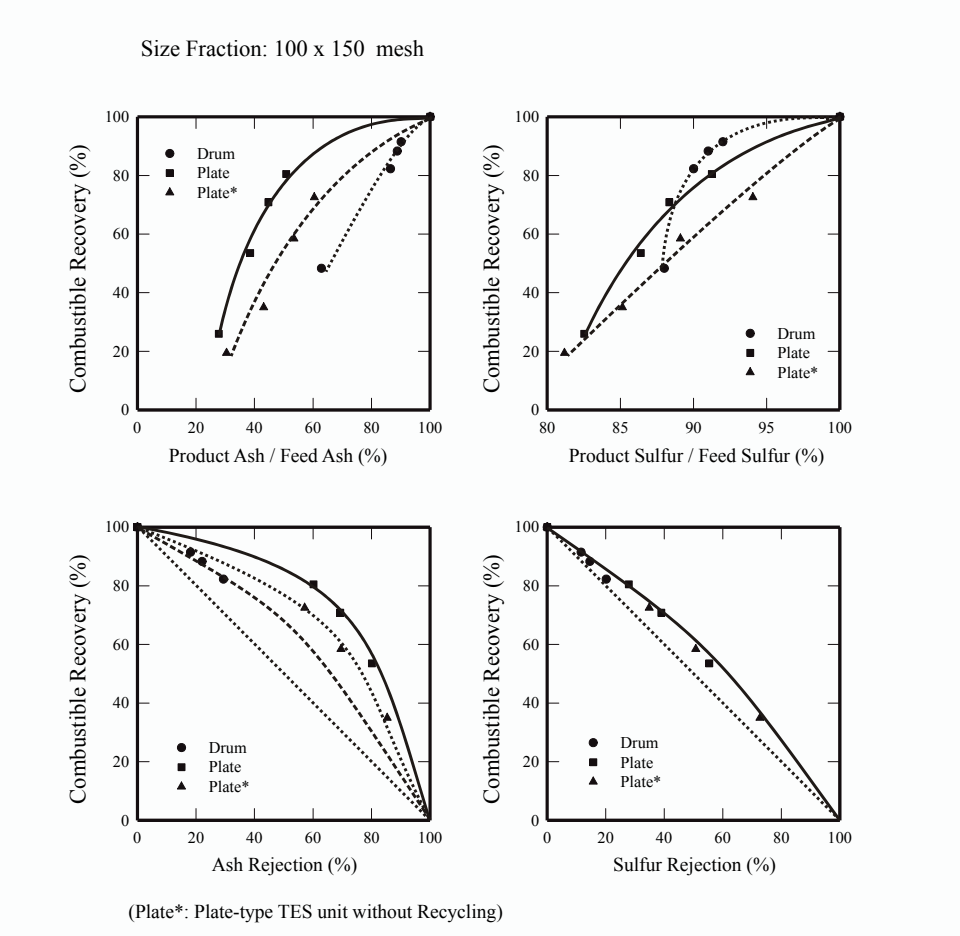

Figure 44 Comparison of the separation performance on the drum-type, plate-type without recycling (*plate**) and plate-type with recycling bench-scale TES units. The separator test results were obtained on a Sewell Seam 100x150-mesh clean-coal sample.

One should note, however, that the differences in separation efficiencies obtained with the monosized samples are not substantial. This finding suggest that high separation efficiencies can be obtained as long as the feed coal does not contain ultrafine particles. When using plate-type TES units, the separation efficiency deteriorates only when the feed coal contains ultrafine particles.

The difficulty in cleaning coals containing ultrafine particles (i.e., by-zero coals) may be explained as follows. The finer particles show higher surface charge densities, given in units of μCoulombs per gram of sample. Furthermore, the difference in charge densities of coal and

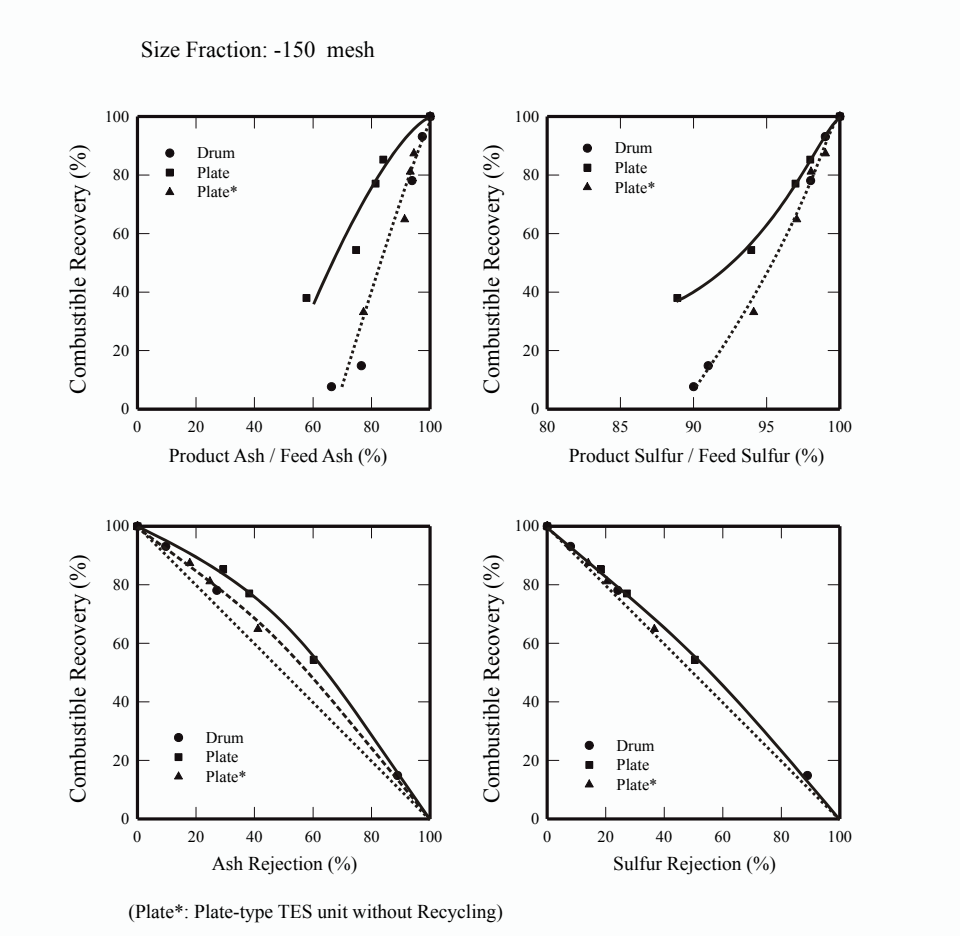

Figure 45 Comparison of the separation performance on the drum-type, plate-type without recycling (*plate**) and plate-type with recycling bench-scale TES units. The separator test results were obtained on a Sewell Seam minus 150-mesh clean-coal sample.

mineral matter increases with decreasing particle size. According to these results, the separation efficiency of the TES process should increase with decreasing particle size. However, the results obtained with the by-zero coals (see Figures 41 and 45) show the contrary. The reason may be that the ultrafine particles of coal and minerals are attracted to each other, due to the large differences in surface charge relative to the mass (or inertia) of particles. This phenomenon may be referred to as heterocoagulation. It would be difficult to separate the particles from each other once the particles are heterocoagulated. If this explanation holds true of what actually happens, the problem could be solved by three possible ways. First, the heterocoagulation phenomenon

should be prevented by applying some form of mechanical forces, e.g., ultrasonic vibration. Second, the ultrafine fraction may be treated separately, as has been done with the monosized samples (see Figures 42-44). Finally, the ultrafine fraction may be subjected to a less vigorous charging mechanism, so that the coal and mineral particles are not attracted to each other.

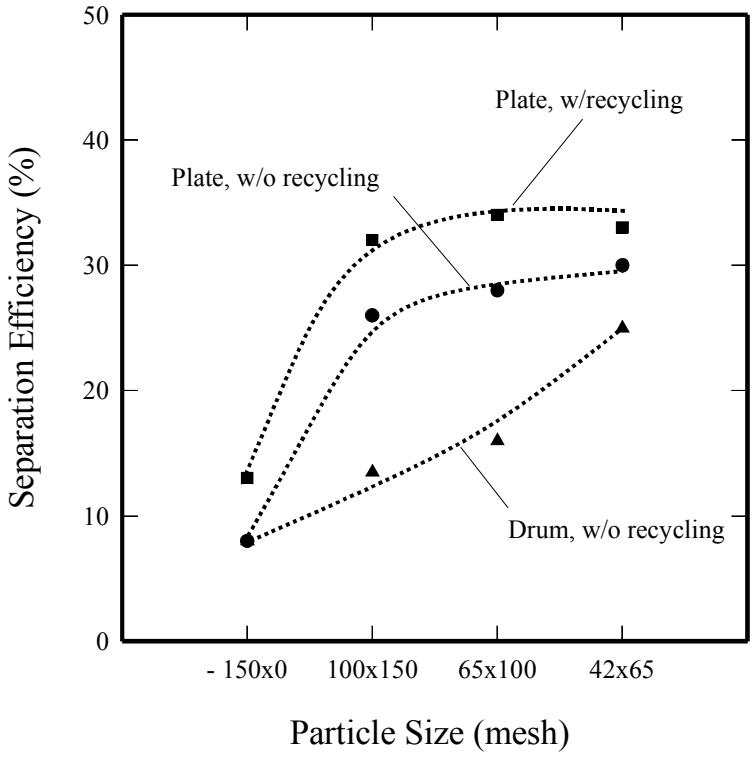

Figure 46 Comparison of the bench-scale TES units used in the present study in terms of the separation efficiency based on a variety of feed particle sizes.

Other possible reasons for the difficulties in separating the coals containing ultrafine particles may include i) entrainment and ii) inductive charging mechanisms.

Separator test results suggest that the separation efficiency deteriorated when feed samples contained significant amounts of ultrafine particles. It was, therefore, decided to determine the lower particle size limit for the new bench-scale TES unit with plate-type electrodes.

3.2.8 Determination of Lower Particle Size Limit For Single Unit Pie Shaped Separator

The bench-scale TES tests were conducted using a clean-coal sample from the Sewell Seam provided by the A.T. Massey Coal Company. The sample was crushed first in a roller crusher, and then pulverized in a hammer mill to minus 270 mesh. The mill product was dry-screened to obtain eight different size fractions, namely: +42, 42x65, 65x100, 100x150, 150x200, 200x230, 230x270 and minus 270 mesh. The standard procedure for drying and minimizing surface oxidation was applied.

Separator Test Results

A series of bench-scale tests were conducted on the Sewell Seam coal samples at the size fractions described above using the TES unit with the pie-shaped plate-type electrode separator. The particles in a feed stream were charged by the turbo charger, and the charged particles were fed into the electric field created between the plate electrodes. In all tests, the potential difference between the electrodes was set at 30 kV, and the feed rate was fixed at 12.5 kg/hr. The middlings fraction was pneumatically fed back to the feed stream. A given feed coal sample was cleaned in multiple stages to establish grade vs. recovery curves.

Table 1. Ash contents of the different size fractions of the Sewell Seam clean-coal sample

Particle Size (mesh)	Ash Content (%)
+42	7.20
42 x 65	4.95
65 x 100	4.93
100 x 150	5.36
150 x 200	6.43
200 x 230	8.03
230 x 270	9.67
-270 x 0	11.25

Each of the different size fractions of the coal sample used in the bench-scale test work had considerably different feed assays. The feed assays varied from 4.93 to 11.25% as shown in Table 1. Therefore, it was necessary to normalize the grade of each product with respect to the feed grade, so that the results obtained with various size fractions can be compared with each other. The clean coal and refuse products were not analyzed for sulfur, as the feed coal contained very little pyritic sulfur.

Figure 47 shows the results obtained with the eight different size fractions. Seven of them were narrowly sized (mono-sized) samples, and one was a by-zero (270 mesh x 0) coal sample. The three intermediate size fractions (i.e., 100x150, 150x200, and 200x270 mesh) gave more or less the same combustible recovery vs. grade curve. The results improved as the particle size increased to 65x100 and then to 42x65 mesh. As the particle size was further increased to +42 mesh, however, the recovery dropped substantially. The recovery decreased also with

decreasing particle size. The slope of the recovery vs. grade curve was rather steep at 230x270 mesh. With the 270x0 mesh coal sample, the results deteriorated further.

Based on the data shown in Figure 47, a set of combustible recovery vs. ash-rejection curves have been constructed and given in Figure 48. In Figure 48, the diagonal line drawn between the top left-hand corner (100% combustible recovery) and the lower right-hand corner (100% rejection) represents the zero separation efficiency. The farther a recovery vs. rejection curve is from this diagonal line, the higher the separation efficiency. As shown, the results obtained with the five intermediate size fractions (i.e., 200x230, 150x200, 100x150, 65x100, and

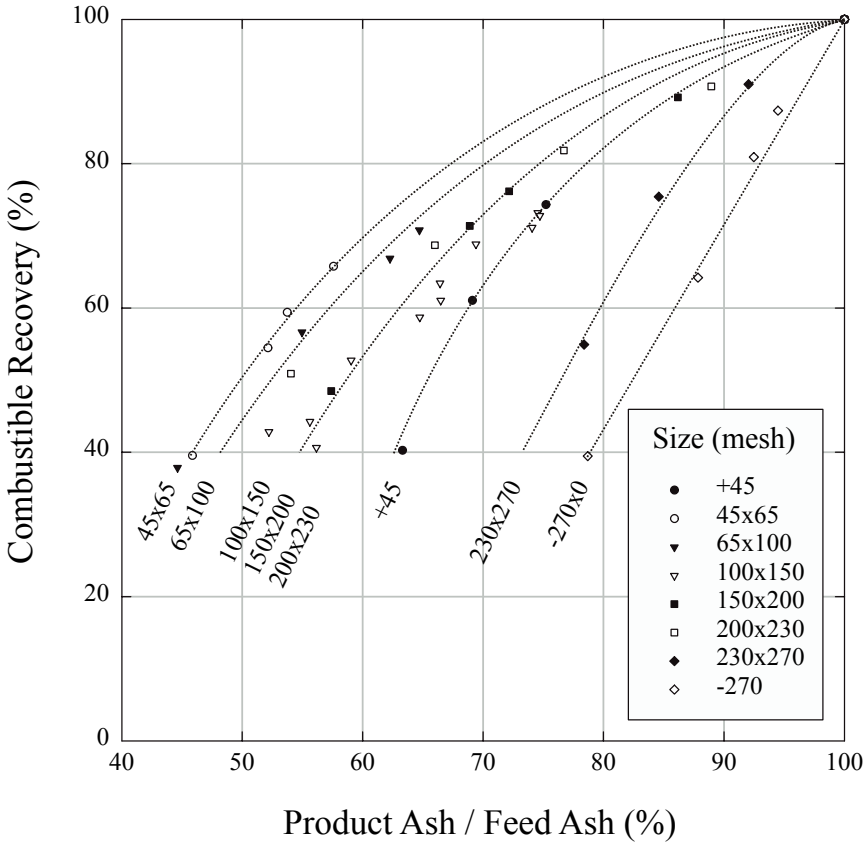

Figure 47 Combustible recovery as a function of normalized product ash content. The test results were obtained on the plate-type bench-scale TES unit with different size fractions of the Sewell Seam clean-coal sample.

42x65 mesh) fall on a single recovery vs. rejection curve, which represents the best results. As the particle size moves up or down from these optimum size range, i.e., 230 to 45 mesh, the separation efficiencies deteriorated significantly.

In Figure 49, the separation efficiencies of all of the test results given in Figures 47 and 48 are plotted versus particle sizes in mesh. The separation efficiencies vary relatively little within the optimum size range. The smallest particle size that can be effectively treated by the new TES separator with plate-type electrodes is 230 mesh (62 μm), while the largest particle size that can be treated is 45 mesh (350 μm). The 270 mesh x 0 coal gave the worst results, possibly

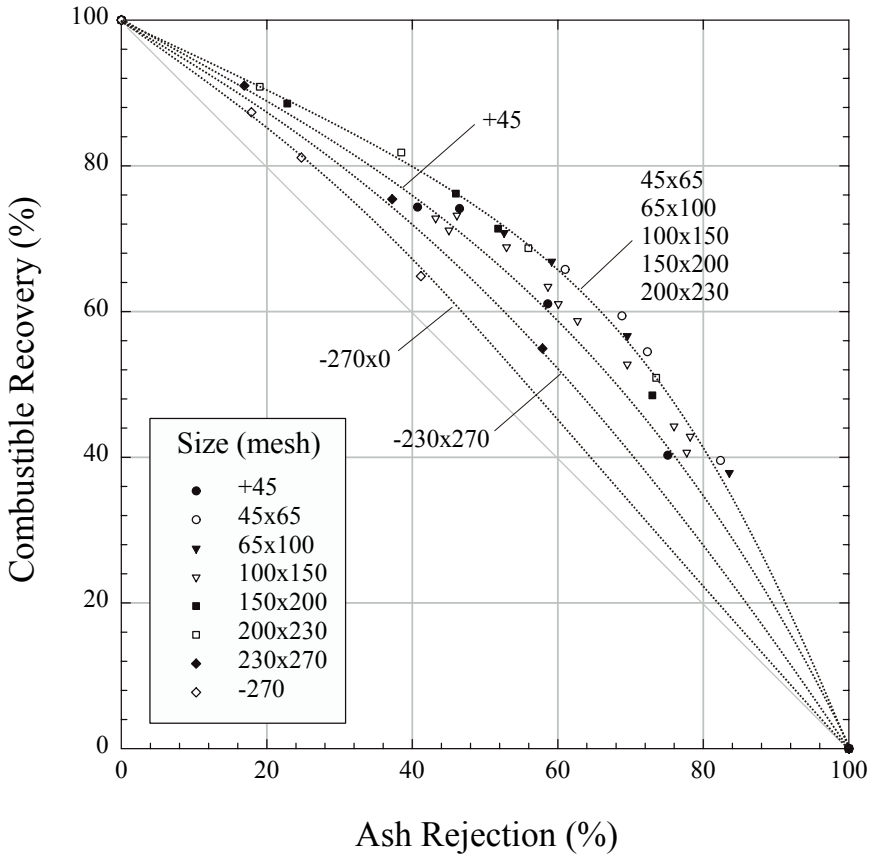

Figure 48 Combustible recovery as a function of ash rejection. The test results were obtained on the plate-type bench-scale TES unit with different size fractions of the Sewell Seam clean-coal sample.

due to the large proportion of ultrafine (-10 μm) particles present in the sample.

The difficulty in separating material containing ultra fines is caused by the fact that the finer particles show higher surface charge densities, given in units of μ Coulombs per gram of sample. Also, the difference in charge densities of coal and mineral matter increases with decreasing particle size. According to these results, the separation efficiency of the TES process should increase with decreasing particle size. However, the results obtained with the ultrafine coals show the contrary. The reason may be that the ultrafine particles of coal and minerals are

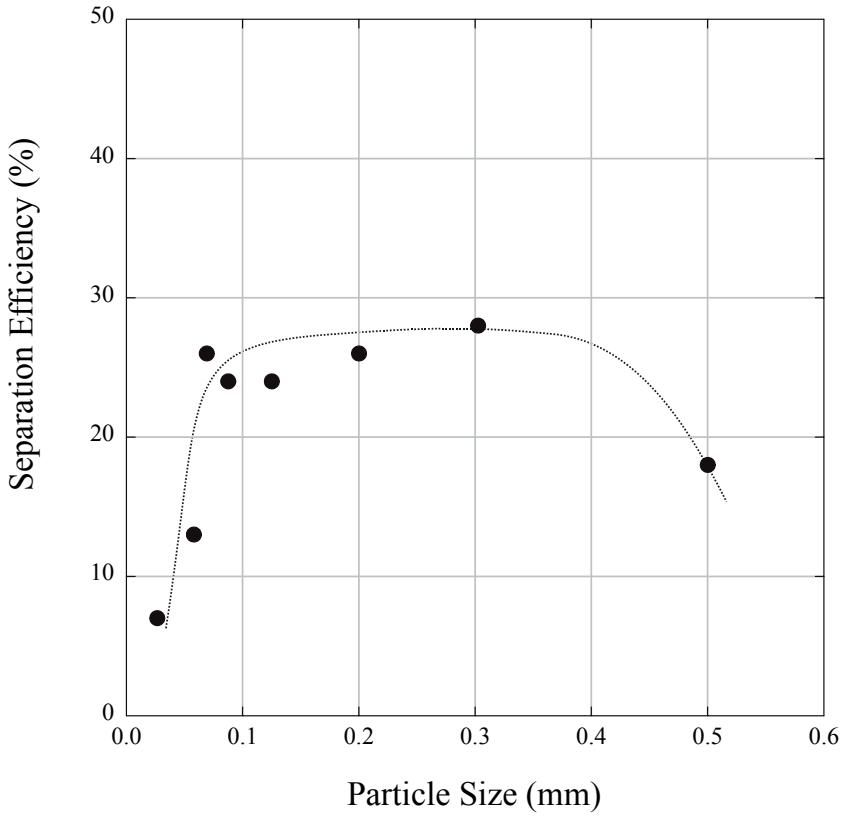

Figure 49 Separation efficiency as a function of feed particle size. The test results were obtained on the plate-type bench-scale TES unit with different size fractions of the Sewell Seam clean-coal sample.

attracted to each other, due to the large differences in surface charge relative to the mass (or inertia) of particles.

3.2.9 Evaluation of Electrode Design

Two different types of bench-scale TES units have been tested. One is equipped with drum-type electrodes without provisions for middlings recycle, and the other one is equipped with plate-type electrodes with the recycling provisions. In general, the latter produced better results than the former. It is not certain, however, whether the improvement is due to the recycling provisions, or due to the longer retention times of the particles in the electric field. Furthermore, the plate-type electrodes still have problems with the fine particles.

In order to determine whether additional improvements could be made in the performance of the electrostatic separator, a final bench-scale test unit was constructed as shown in Figure 50. The new unit was designed with two interchangeable electrodes that could be easily installed without further modifications. The electrodes are connected to a high-voltage power supply capable of creating a potential difference of 30 kV. The unit is also equipped with a circulation conduit capable of recycling middlings particles back to the feed inlet.

Five different electrode systems were fabricated for this unit, i.e., horizontal rods, vertical rods, drum, plate and screen. Each of these electrode designs is shown in Figure 51. For obvious reasons, the drum- and rod-type electrodes produce non-uniform electric fields. It was originally believed that a non-uniform field might be useful for separating finer particles. The advantage of using a series of small diameter 9.525mm (3/8-inch) rods as electrodes in place of the drum is that this approach permits a longer residence time to be achieved by simply adding more rods. In addition, the rod-type design allows deflected particles to exit the electrostatic field as soon as possible. This minimizes problems associated with particles being collected at the electrode surface, becoming recharged and jumping to the other electrode. This phenomenon

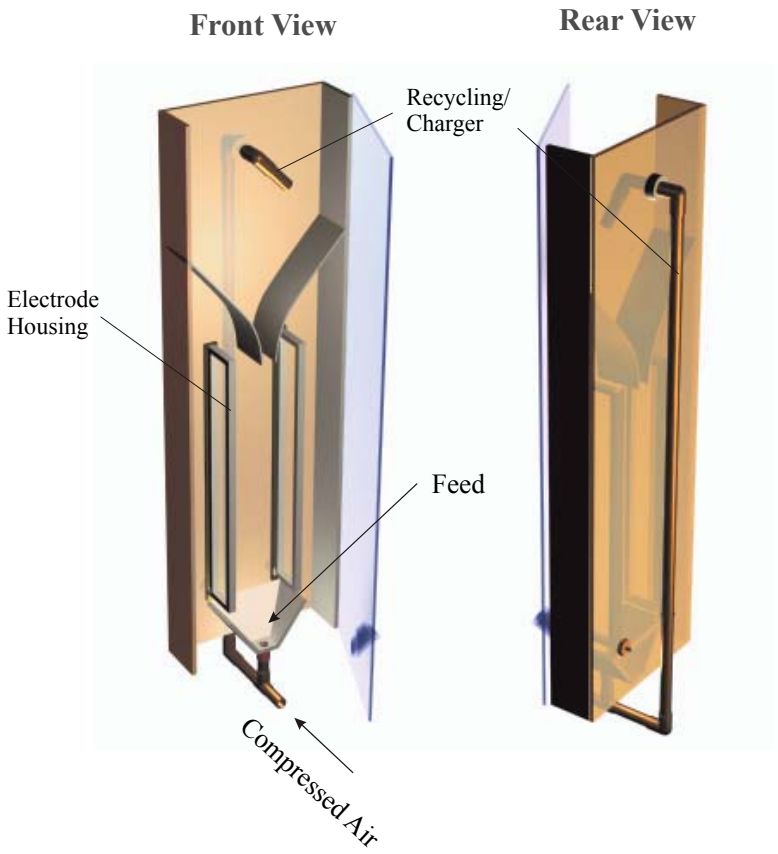

Figure 50 Schematic representation of the generic bench-scale TES unit. The unit was designed with two interchangeable electrodes that could be easily installed without further modifications of the TES unit.

was recognized in a high-speed photographic studies conducted at NETL. Also, like the drum-type design, the individual rods rotated to remove particles that may accumulate on the electrode surfaces during operation.

Initial tests were carried out on the horizontal rod system that consists of two grill-type electrodes, a high-voltage power supply, and a circulation conduit for recycling middling particles. Each grill-type electrode consisted of twelve 9.525mm (3/8 inch) diameter cylindrical stainless steel rods separated from each other by-1 inch. The distance between the two grill-type electrodes, which were aligned parallel with each other, was 102mm (4-inches). The electrodes were connected to a high-voltage power supply capable of creating a potential difference of 30 kV between the two electrodes.

A coal sample is fed continuously to the hopper at the bottom, which collects the

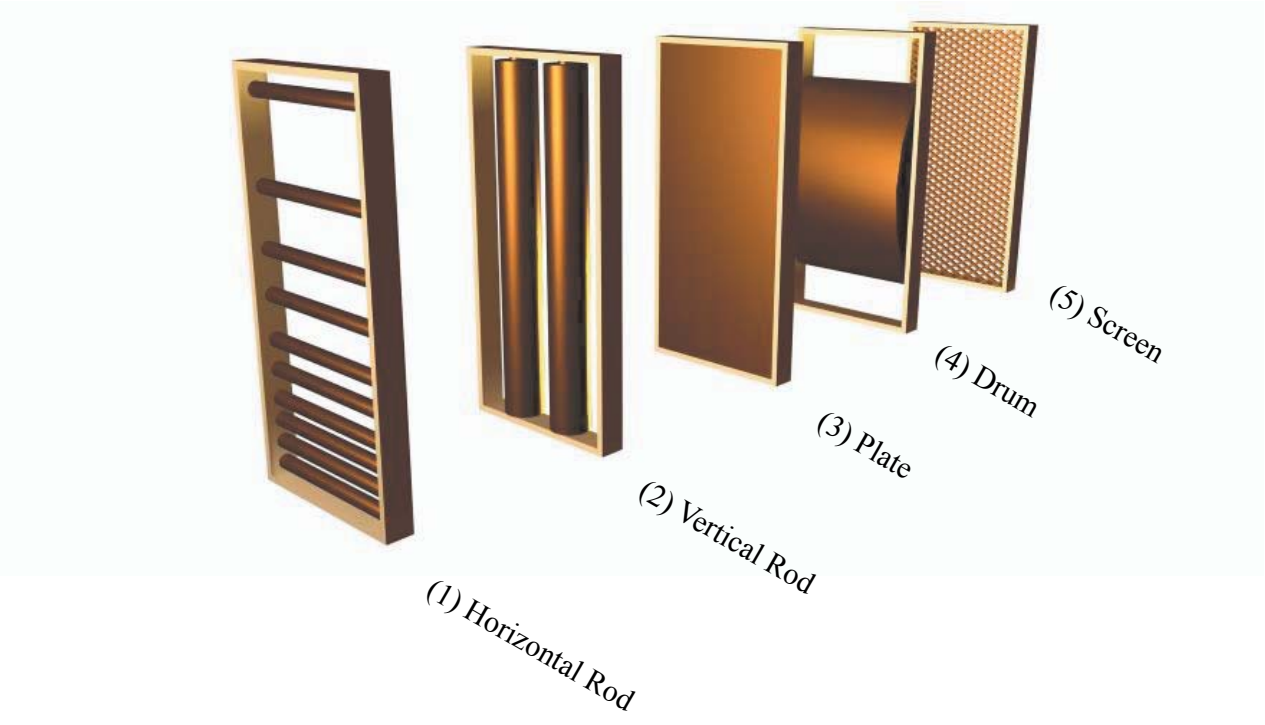

Figure 51 Schematic representation of the five different electrode systems used in the bench-scale TES unit study. These electrode systems include horizontal rods, vertical rods, plate, drum and screen.

middling particles. The mixture of the feed and the middlings is drawn into the recycle pipe by means of compressed air. The recycle pipe is made of either copper or PVC tubing, which is used as a charging device. The charged particles are discharged from the top of the separator, and fall into the electric field created between the two grill-type electrodes. The particles are then separated into three product streams, i.e., clean coal, reject, and middling streams. The clean-coal and refuse products are collected outside the electrodes, while the middlings are collected in between the electrodes and recycled as has already been described.

The horizontal rod separator was designed to combine the advantages of the drum-type and the plate-type separators. The advantage of using the drum-type electrodes is that the non-uniform electric field created between the electrodes may be useful for separating finer particles. The series of small diameter (9.525 mm) electrodes should provide multiples of non-uniform electric fields. The new electrode system are also designed to provide a long retention times, which may be useful for separating finer particles. An important aspect of the new electrode design is that the particles deflected in the electric field exit the field as soon as possible, which will prevent the probability for some of particles being recharged at one electrode and jump toward the other electrode. This phenomenon was recognized in high-speed photographic studies conducted at NETL. In addition, the individual electrodes can be rotated to remove the particles collecting on the electrode surface.

Experimental

Bench-scale TES tests were conducted on all five electrode systems using reject sample from the pulverizers of two local power plants. Upon receipt, the coal samples were dry-screened to obtain two size fractions, i.e. +14 mesh and –14 mesh. The –14 mesh size fraction contained about 47% ash and was used for this series of test. Figure 52 shows the size

distribution of the –14 mesh size fraction for both samples. The samples were kept in an oven at 112°C overnight to remove the moisture from the surface of the coal particles before being subjected to each test program.

Tests were conducted by continuously feeding the pulverized sample into the hopper used to collect the middlings particles at the bottom of the separator. The mixture of the feed and middlings particles was drawn into the recycle pipe by means of compressed air. The recycle pipe was constructed of either copper or PVC tubing and was used as the charging device. The charged particles were discharged from the top of the separator and directed into the electric field created between the two electrodes. The electric field separated the particles into three products, i.e., clean coal, reject, and middling stream. The clean coal and refuse products were collected outside the electrodes, while the middlings particles passed between the electrodes without being collected and were recycled as previously described.

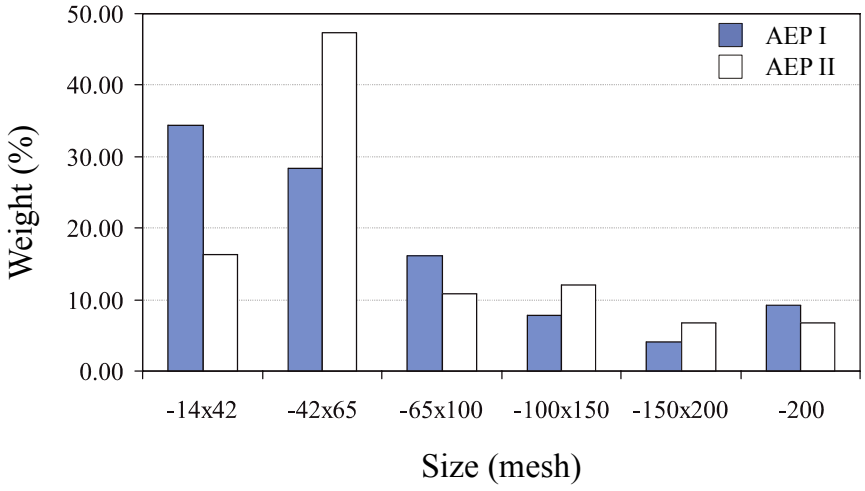

Figure 52 Particle size distribution of the –14 mesh size fraction for the pulverizer reject samples used in the present separator study.

Separator Test Results

Figure 53 shows the separator test results obtained with the bench-scale TES unit incorporating the five different types of electrode systems. As shown, the electrode configurations that provided the most uniform fields (i.e., screen and plate) gave the best overall separation curves. For this particular sample, the bench-scale TES unit incorporating the screen-type electrode reduced the ash content from 46.7% to 10% with a 60% combustible recovery in a one-stage operation. This corresponds to an ash rejection of approximately 92%. The plate-type electrode TES unit also shows significant improvement in separation efficiency, although the results were not as good as those obtained with the screen-type design. The results obtained using the plate-type electrode show that the ash content can be reduced from 46.7% to 15% at a 62%

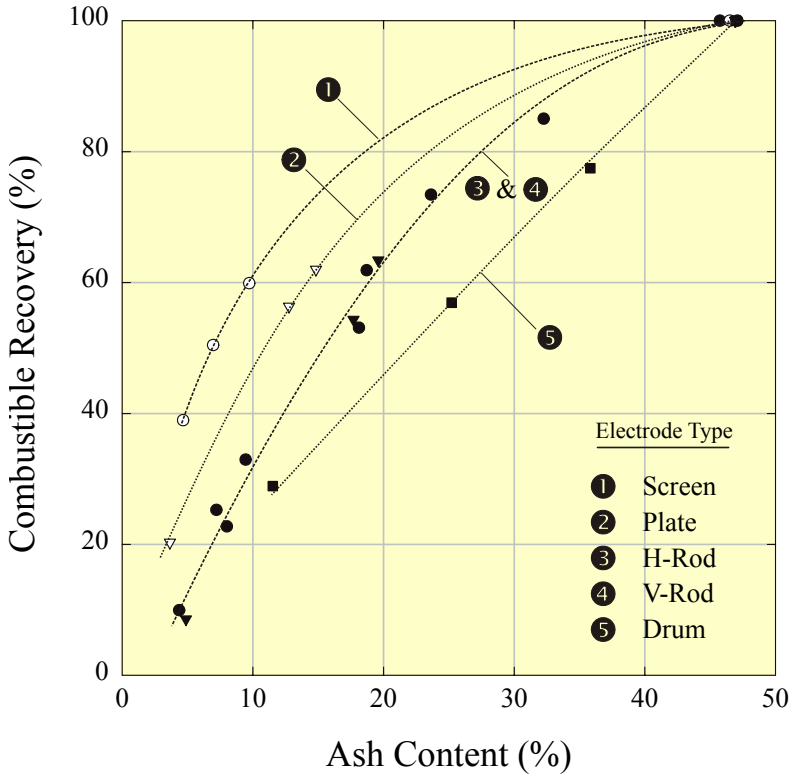

Figure 53 Separator test results obtained with the bench-scale TES unit incorporating the five different types of electrode systems.

combustible recovery. The separation performance achieved using the electrode systems constructed from both the horizontal and vertical rods was inferior to those achieved using the screen-type and plate-type designs. In fact, the bench-scale TES unit incorporating the vertical cylinder-type electrode that is similar to the Carpco's VSTAT design gives more or less the same combustible recovery vs. grade curve as the horizontal electrode configuration. The drum-type separator gave the worst grade-recovery curve among the different electrode designs compared in this series of tests.

Based on the data shown in Figure 53, a set of combustible recovery vs. ash-rejection curves was constructed and is given in Figure 54. In this diagram, the diagonal line drawn between the top left-hand corner (100% combustible recovery) and the lower right-hand corner (100% ash rejection) represents the line of zero separation efficiency. The farther a recovery vs. rejection

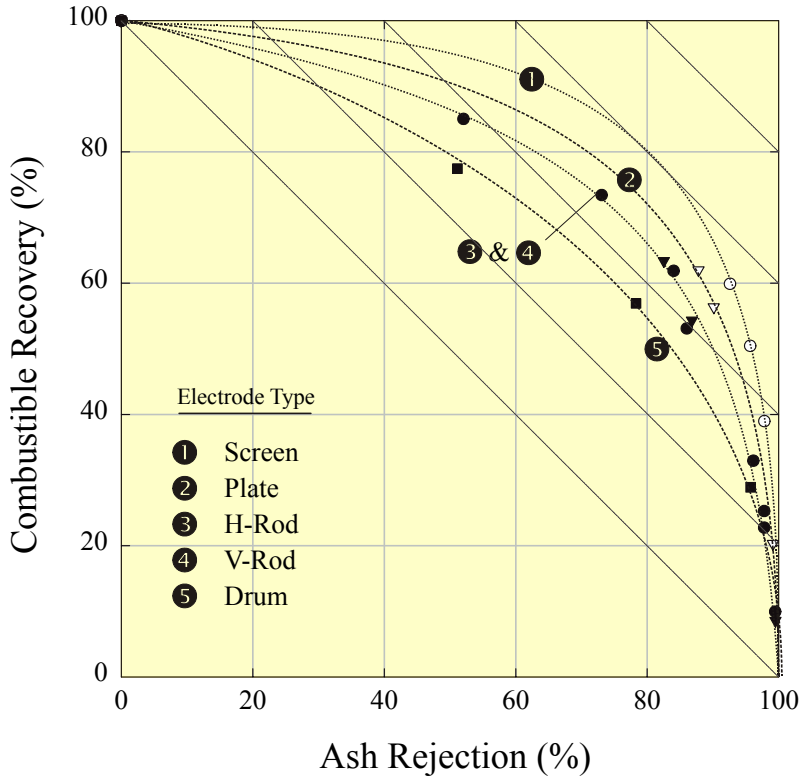

Figure 54 Combustible recovery vs. ash rejection curves for the separator test results obtained with the bench-scale TES unit incorporating the five different types of electrode systems.

curve is from this diagonal line, the higher the separation efficiency. As shown, the results obtained with the screen-type electrode TES unit gave the best separation efficiency (60%), while the drum-type TES unit had the worst separation efficiency (32%). It is interesting to note that electrode systems that produced the most uniform electric fields (i.e., screen-type and plate-type) gave better separator performance than the electrode systems that produced a non-uniform electric field (i.e., drum-type and rod-type).

Evaluation of Throughput Capacity

One of the important considerations in the design of the POC-scale TES unit will be throughput capacity. Therefore, it was decided to conduct further separator tests in order to obtain the information related to the maximum throughput capacity of the bench-scale TES unit. These tests were conducted using the screen-type electrode system since this configuration provided the best overall separation performance. The evaluations were conducted using the –14 mesh pulverizer reject sample (46.7% ash) described previously. The tests were conducted with an applied potential at 30 kV, while varying the feed rate in the range of 6-44 kg/hr. At a given feed rate, the coal sample was cleaned in multiple stages to establish grade vs. recovery curves. Figure 55 shows the grade vs. recovery curves obtained from this series of tests. The results show that the performance of the bench-scale TES unit incorporating the screen-type electrode deteriorated only slightly as the feed rate was increased. At a feed rate in the range of 6-18 kg/hr, the TES unit was able to reduce the ash content from 47% to 10% with a 50% combustible recovery in a single-stage separation. However, at a feed rate in the range of 30-44 kg/hr, the ash content was reduced from 47% to 16% with a 60% combustible recovery for a single stage separation. For comparison, Figure 56 shows the combustible recovery vs. ash rejection curves that were constructed from the test data. As shown, the bench-scale TES unit incorporating the

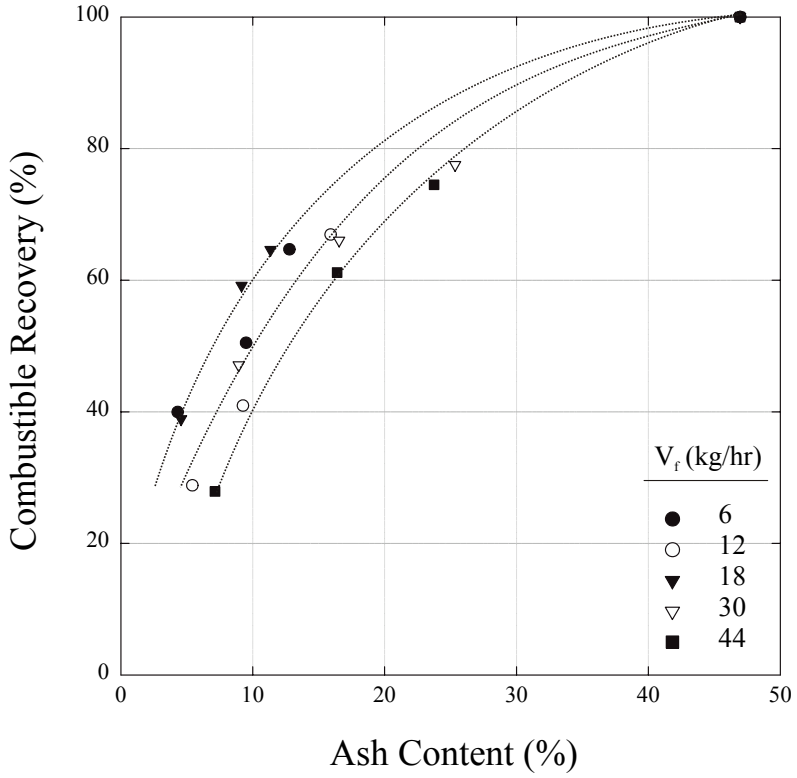

Figure 55 Grade vs. recovery curves of the throughput capacity study using the bench-scale TES unit incorporating the screen-type electrode system.

screen-type electrode achieved a 50-60% separation efficiency with the pulverizer reject sample. These data are replotted in Figure 57 as a function of feed solids rate. As shown, the separation efficiency remained more or less constant for the test conditions employed in the present work. In fact, the slightly poorer performance at high feed rates may be attributed to the likelihood that the energy input per unit weight of feed decreased to the minimum required for efficient charging. In addition, the choke feeding may result in a decrease in the particle-wall charging mechanism, which may play an important role in the triboelectrification of the coal particles.

According to the data obtained to date, a TES unit incorporating a screen-type electrode system and a middlings recycle stream offers the best overall performance in terms of separation efficiency and throughput capacity. Several possible explanations for the significant improvement in performance include:

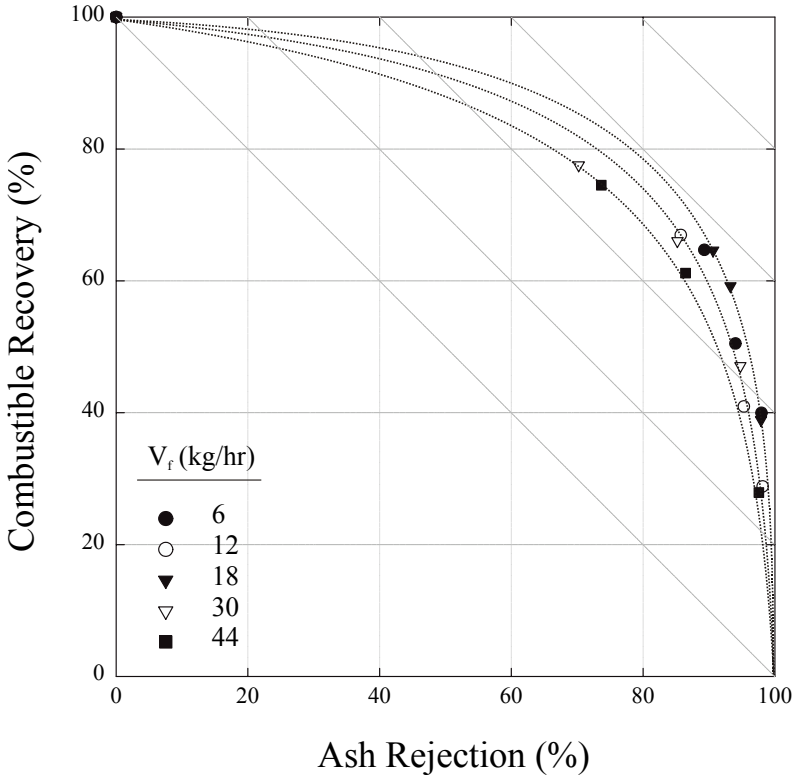

Figure 56 Combustible recovery as a function of ash rejection. Test results were obtained using the screen-type bench-scale TES unit in the throughput capacity study.

i) the bench-scale TES unit has provisions to recycle the middling stream, which gives the bypass materials another chance to be recharged and separated,

ii) the electrode system is designed to provide a long retention time, which may be useful for separating finer particles,

iii) the flow-through screen allows particles deflected in the electric field to exit the as soon as possible, which increases capacity and reduces the problem of particles becoming recharged or being dropped back into the middling stream.

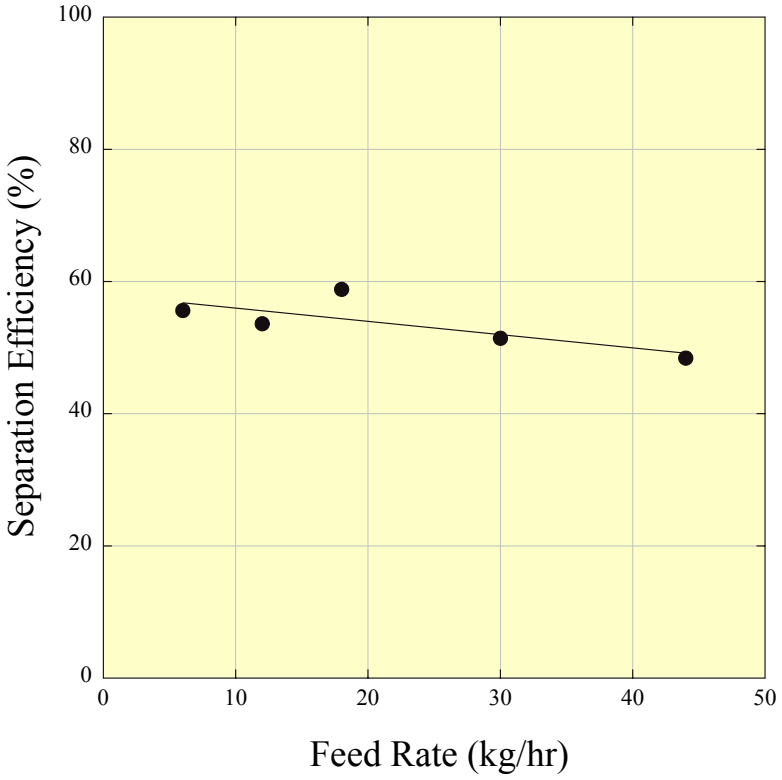

Figure 57 Separation efficiency as a function of solid feed rates. Test results were obtained using the screen-type bench-scale TES unit employed in the present work.

3.2.10 Summary of the Bench-Scale Separator Test

a) Drum-Type Bench-Scale TES Unit

The drum-type bench-scale TES unit was used to clean a Pittsburgh coal. The coal sample used for the tests was a clean-coal product assaying 5.6% ash and 1.67% sulfur. The tests were conducted by varying the potential difference between the electrodes in the range of 20 to 70 kV at a throughput of 4 kg/hr. The best separation results were obtained at 40 kV. According to the grade vs. recovery curve obtained at this potential, the ash content can be reduced to 3.7% at 80% Btu recovery and 4.3% at 90% Btu recovery. As for sulfur, the total sulfur content can be reduced to 1.2% at 80% Btu recovery and 1.25% at 90% Btu recovery.

The use of a 4-stage inline mixer made of copper created clogging problems at high feed rates, and the separation efficiencies were poor. A charger made of Plexiglas tubing with dimensions of 25 mm (1-inch) diameter and 406 mm (16-inches) in length was used in conjunction with the drum- type bench scale TES unit. The in-house researchers at NETL also found that it is not necessary to use inline mixers to create charges, and that non-metals may be better suited for making tribochargers.

A new charger, tentatively named 'turbo charger', has been developed and tested with the drum-type bench-scale TES unit. This new design is intended to provide i) maximum wall-particle and particle-particle charging mechanisms, and ii) even distribution of particles in the feed stream. The separator tests showed that the turbo charger gave significantly better results than those obtained with the straight-pipe charger or in-line mixer that were used for particle charging. The TES unit equipped with the new charger gave more than 10% higher combustible recoveries than the straight-pipe charger.

Based on the particle trajectory model developed for this test work, feeding a coal from off-center positions (bias feeding) should affect separation efficiency. However, based on the test results obtained with Pittsburgh coal, biasing the feeding point does not make a significant difference in separation efficiency.

A series of tests were conducted on the Sewell Seam clean-coal sample using the drum-type bench-scale TES unit. Tests were conducted at a feed rate of 8.2 kg/hr, while varying the applied voltages at four different levels, i.e., +30, +40, +50, and +60 kV. The results show that the best separation efficiency of the TES unit on Sewell Seam coal was obtained at 40-50 kV. At an applied potential of 60 kV, the performance of the TES unit deteriorated. It is possible that in a strong electric field, the particle charge may be altered due to inductive charging mechanism, which is detrimental to the separation process.

The use of the turbocharger has drastically improved the throughput capacity of the bench-scale TES unit with no loss in separation efficiency. Therefore, separator testing was conducted in order to obtain the information of maximum throughput capacity of the bench-scale TES unit incorporating the turbo charger. A series of separator tests have been conducted on the Pittsburgh No. 8 clean coal in order to obtain the information of the maximum throughput of the bench-scale TES unit. It was found that reasonable separation efficiencies were obtained until the feed rate reached approximately 30 kg/hr. The separation efficiency deteriorated significantly above this limit. It is possible, however, to extend the throughput beyond 30 kg/hr by increasing the energy dissipation. The energy dissipation is the rate of energy input to a system, and is usually given in units of ergs/unit weight of feed/unit time. Thus, the throughput of the bench-scale TES unit can be further increased either by increasing the rpm of the rotor blade or by increasing the overall size of the turbo charger.

The bench-scale TES unit demonstrated that it is capable of achieving high degrees of ash and sulfur rejections, but at low Btu recoveries. In order to overcome this deficiency, it would be necessary to design a unit that has a built-in scavenger or scavengers.

b) Plate-Type Bench-Scale TES Unit

Two different bench-scale separators have been tested on a low-sulfur Sewell Seam coal. These include a drum-type separator equipped with a turbocharger, and a plate-type separator with a turbocharger. The latter was tested with a middlings recycle system, while the former was tested without the recycling. Both separators produced reasonable separation efficiencies, but the plate-type separator produced better results with coarse particles, possibly because of the longer particle retention times and the provisions for middlings recycle. Despite the improvement achieved with the plate-type separator, there are difficulties in separating ultrafine particles. The

tests work conducted with a series of mono-sized particles showed that the plate-type separator is effective in separating particles in the range of 230 to 45 mesh. The particles outside this optimum range are more difficult to separate. The low separation efficiencies on both of the bench-scale units with fine particle size feed material may be attributed to the entrainment problem associated with fine particle separation which is possibly due to the drag force created by the turbulence at high air velocity.

c) Screen-Type Bench-Scale TES unit

A bench-scale TES unit was constructed and used to evaluate a wide range of electrode designs. Five different types of electrode systems were tested, i.e., horizontal rod, vertical rod, plate, drum and screen. A –14 mesh pulverizer reject sample (46.7% ash) from a local power plant was used in all tests. Test results show that among the different electrode designs, the screen-type electrodes gave the best separator performance, while the drum-type electrodes gave the worst. The screen-type unit was capable of reducing the ash content from 46.7% to 10% with a 60% combustible recovery (92% ash rejection) in a single stage operation. The test data also showed that the performance of the screen-type TES unit does not deteriorate significantly within the range of feed rates (6-44 kg/h) tested to date.

Task 3.3 Final POC Design

3.3.1 Objectives

The primary objectives to be completed under this task include:

- Determination of the optimum tribocharger and electrostatic separator and the maximum performance achievable by TES based on the data obtained from bench- and prototype-scale testing. A minimum acceptable performance standard will be demonstrated by the contractor and approved by the DOE COR prior to the implementation of further tasks.
- Preparation of a detailed listing of required equipment including equipment type, unit size, throughput capacity, power requirements, air/water requirements, and operating limitations.
- Development of a flowsheet that illustrates the physical arrangement of all unit operations, connecting streams, valves, pumps, sampling points, process control instrumentation, etc. Complete material balances will be determined for the entire circuit for each of the three coals to be tested. The flowsheet will specify expected flow rates, solid contents, mean particle sizes, assays, etc., for all streams.
- Preparation of engineering drawings that detail the construction, fabrication and installation of all components required to operate and evaluate the proposed TES circuit. These drawings will unambiguously specify the spatial layout of equipment, location of electrical wiring, arrangement of piping and plumbing, and other pertinent electrical/mechanical requirements. These documents are to be of sufficient detail and quality to be utilized by the mechanical/electrical subcontractor for the construction and assembly of the proposed circuitry.

The proposed flowsheet, detailed engineering drawings, equipment specifications, plant layout, test plan, etc., will be approved by the DOE COR before any additional work elements are initiated. The design of the POC test circuit will be in accordance with all national, state and local

codes applicable to electrical and mechanical equipment operating within atmospheres that may contain explosive dust.

A detailed evaluation of the design of the POC-scale test circuit was carried out using the engineering guidelines developed in Subtasks 3.1 and 3.2. The circuitry was designed to be totally self-contained and to incorporate all unit operations for materials handling, selective tribocharging, particle-particle separation and particle-gas separation on a continuous basis. Descriptions of these various systems are provided in the following sections.

Tribocharger Design

Data from Subtask 3.1 (Tribocharger Tests) will be used to design a tribocharger suitable for incorporation into the 200-250 kg/hr POC test unit system. Scale-up and performance expressions developed from the 1 kg/hr and 10-20 kg/hr test work will be used to specify the mixer geometry, construction materials and preferred operating conditions (i.e., feed rate, air velocity, solids concentration, etc.) for the POC tribocharger system. If deemed necessary by the scale-up criteria, a distribution manifold will be designed to permit the use of multiple static-mixer tribochargers across the top of the electrostatic separation chamber. The design will incorporate sufficient instrumentation (i.e., flow meters, pressure gauges, etc.) to monitor the performance of the POC tribocharger.

Electrostatic Separator Design

Data obtained from Subtask 3.2 (Separator Tests) will be used to design an electrostatic separator suitable for incorporation into the 200-250 kg/hr POC test unit. The design will consider a vertical feed of coal that has been pulverized in an inert-gas swept impact mill and passed under pressure through a static mixer tribocharger. The design will allow for removal of clean coal and rejects through an air-lock system, and secondary discharge of fines through a dust collection

system. Provisions will be made for removal of by-pass material and reintroduction of fines at a low-pressure point upstream of the pulverizer. The entire TES test circuit will be designed to operate under a net positive pressure with recirculation of inerting gas. Separator geometry will be based on model predictions and data obtained from the bench-scale test work described in Subtask 3.2 (Separator Tests) so as to optimize throughput capacity and separation efficiency. Since the separator efficiency is also dependent on electrical field strength, the design will allow for a variable voltage up to 100 kV between the electrodes (up to 50 kV on each electrode). The design will incorporate sufficient instrumentation (i.e., flow meters, pressure gauges, etc.) to monitor the performance of the POC electrostatic separator.

Ancillary Equipment

In the proposed POC circuit, raw coal will be brought into the coal receiving area by truck. All of the equipment required to produce the 50-100 μm top size feed coal for the TES POC-scale unit is already available at the contractor's facilities. These facilities will be augmented by additional equipment for the conveying, charging, separating, and metering of coal feed and product streams. The entire TES POC-scale unit will be operated in an inert atmosphere. The ancillary equipment will be selected on the basis of vendor performance specifications and standard selection criteria developed in the particulate industries.

POC Test Plan

Three of the most important operating parameters identified in the bench-scale experiments will be examined during the POC test program. These parameters are anticipated to be feed throughput, and electrode potential and setting. However, the specific selection of parameters to be examined in the POC test work may be subject to change. All POC tests will be conducted in accordance with all national, state and local codes.

3.3.2 Engineering of the POC Separator

It was decided to purchase a custom designed POC–scale test unit from Carpco. Discussions were conducted between CCMP and Carpco concerning the key issues related to the design, scale-up, construction of the unit. Design specifications based on bench-scale performance data were prepared for the POC separator.

The design consisted of pulverized coal being fed to a rotary turbocharger mounted atop the electrostatic separation chamber by means of a screw feeder. Details of the turbo charger design are shown in Figure 58. The charged particles that exit through the bottom of the turbocharger pass into the top of the separation chamber and through the electrostatic field. Depending on the particular mode of operation selected, the particles either "free-fall" through the electrostatic field or are "entrained" in a carefully controlled laminar flow of gas. In either

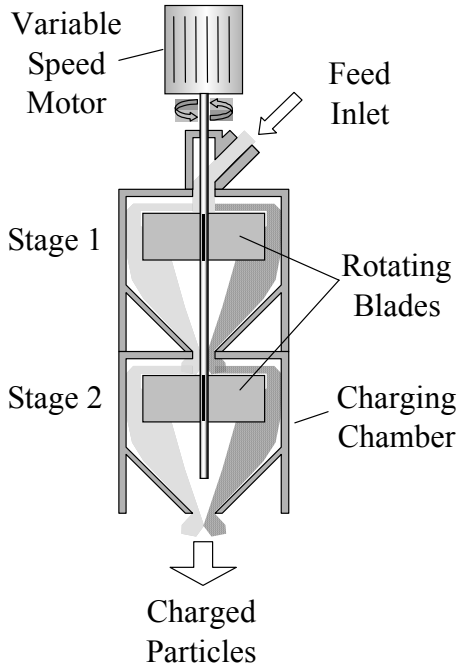

Figure 58 Turbocharger used in conjunction with the POC-scale TES unit.

operating mode, baffles near the entrance of the separation chamber minimize the turbulence created by the feed stream.

The charged particles pass through the electrostatic separation chamber where positively charged particles of carbonaceous matter are attracted to the negative electrode and the negatively charged particles of mineral matter attracted to the positive electrode. The electrodes are interchangeable so that different electrode configurations could be tested (i.e., screen and vertical rod). The electrode support frame was designed so that the angle of electrode inclination could also be changed. The unit has been configured so that the electrode voltage can be varied over a range of 0-120,000 volts. After being deflected by the electrodes, the products (clean coal, middlings and reject) are discharged from the bottom of the separator through discharge ports into collection bins.

3.3.3 Engineering of the POC Test Circuit

Typical preliminary copies of the POC flowsheets and material balances are provided in Appendix I. Three separate flowsheets have been prepared for the processing of two pre-cleaned coal samples (i.e., Sewell and Pittsburgh No. 8) and a reject coal sample from a utility pulverizer. The material balances show the expected solid flow rates, gas flow rates, solid concentrations and assays (ash content) for each stream in the POC circuit. The flowsheets have been provided in both metric and English units. For reference, an overview of the baseline data used to develop

Table 2. Baseline data used for the preliminary design of the POC flowsheet.

Coal Sample	Feed Ash	Clean Ash	Reject Ash	Mass Yield	Combust. Recovery	Ash Rejection
Sewell	7.2%	4.5%	8.9%	38.6%	39.8%	75.9%
Pittsburgh	8.5%	4.1%	17.5%	67.2%	70.4%	67.6%
Mill Reject	45.0%	12.0%	65.0%	37.7%	60.4%	89.9%

the POC flowsheets is provided in Table 2.

The entire POC test circuit was installed in the recently renovated high bay area of the Coal Preparation Test Facility at Virginia Tech. The conceptual layout of the various POC unit operations is shown in Figure 59. The triboelectrostatic test module occupied most of the available high bay area on the left side of the test facility.

The triboelectrostatic separator was located on the top floor, while the fine coal pulverizer and dust collector are located on the bottom floor. The supply system for the pressurized nitrogen gas has been placed adjacent to the separator. Modular design concepts were employed to speed the installation of the required circuitry. Where possible, each module was pre-tested without coal prior to being shipped.

Raw (or pre-cleaned) coal shipments will be brought into the coal receiving area by truck. The raw coal is fed to a Jeffery hammer mill for primary size reduction to approximately 3 mm. A secondary hammer mill (Holmes 451) which will further pulverize the feed particles to the required top size. The product from the secondary hammer mill is fed to a vibrating feed storage. Material from the feed storage bin will be introduced at the desired production rate into the top of the POC turbocharger. Initially a calibrated screw feeder was used to control the solids feed rate. The discharge arm from the screw feeder was sealed into the side of the turbocharger to create a barrier that will act as a seal to prevent inert gas from escaping from the pressurized test circuit.

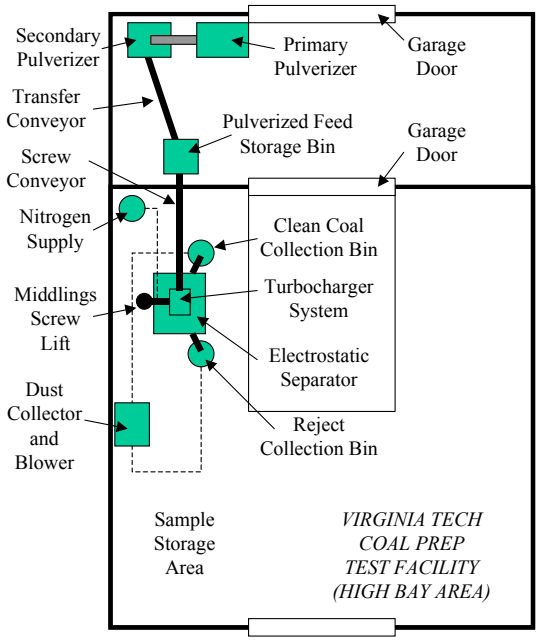

Figure 59 The entire POC test circuit installed in the recently renovated high bay area of the Coal Preparation Test Facility at Virginia Tech.

After passing through the turbocharger and electrostatic separator, the charged particles are deflected into different collection bins located below the POC separator. In addition, middlings particles that pass through the electrostatic field without being separated are recycled via a screw conveyor back to the feed hopper where they join fresh feed and are then re-introduced into the tribocharging system and recycled through the system until the particles become charged and/or separated.

The entire POC test circuit is operated under an inert gas (nitrogen) atmosphere. Fresh nitrogen gas is added directly to the separator as make-up for gas that bleeds from the system. Pressure relief valves have been provided as required to protect the equipment from over or under pressure situations. In addition, the electrostatic separation chamber was equipped with an oxygen monitor that automatically disconnect the electrodes from the applied potential in the case of excessive oxygen levels occur.

Task 4: Procurement and Fabrication

Sub-Task 4.1 Objectives

The objectives of this task are to complete the following work elements described below. The procurement and fabrication of all key components of the proposed TES process will begin immediately upon approval of engineering drawings and specifications. Appropriate venders will be selected on the basis of the competitive bidding process, which includes specification preparation and approval, bidding and bid evaluation, recommendation for purchase, and final award in accordance with provisions for Subcontract Consent. The work elements to be undertaken in the bidding process include:

- preparation and solicitation of competitive bid packages for major purchases of equipment, materials, fabricated components, and services necessary to complete the installation of the proposed TES circuitry, and
- review of bid packages and selection of appropriate venders based on quoted cost, availability and suitability.

After the competitive bidding process is completed, the following work elements will be initiated by CCMP:

- request to the DOE COR for the approval of purchase of equipment, supplies and contractual services,
- preparation and submission of all required purchase orders and requests for services,
- procurement and shipping of major equipment, fabricated components, materials, supplies, etc., to the test facility, and inspection of all purchased equipment, materials, and fabricated components to ensure that they are of suitable workmanship, and are structurally, mechanically and/or electrically operational.

Fabrication milestones and delivery schedules will be established for each item procured, and each procurement will be tracked and reported in conjunction with the Monthly Cost Management Report. The quality control and inspection procedures delineated in the approved QA/QC Plan will be implemented.

Sub-Task 4.2 Execution

The TES unit was purchased from Carpco and the associated helical screw conveyors purchased from Automated Flexible Conveyors, Inc. Motor controllers were also supplied by AFC. Nitrogen for the purge system is supplied locally. All the various chargers used in conjunction with the unit were designed and fabricated by CCMP personnel. All equipment was delivered on time.

Task 5 – Installation and Shakedown

Sub-Task 5.1 Objectives

The objectives of this task are to install the POC module in a safe manner as designated in the flowsheet and layout drawing, and to carry out the shakedown procedures as described below.

5.1.1 - Installation

Upon completion of fabrication, the various components of the POC module will be shipped to the contractor's test facility. When the module components arrive at the site, they will be placed directly into the appropriate location in the test circuit as designated in the flowsheet developed in Subtask 3.3. All necessary construction permits will be obtained prior to initiating the installation. Pertinent local, state and federal regulations on safety and health will be followed during the installation of the test circuit. Electrical power will be obtained from a central distribution panel at the test facility. All electrical control panels and starters will be co-located as a group. The existing

fire protection system will be upgraded to satisfy the additional capacity requirement. Explosion doors and oxygen sensors will be installed on the TES POC unit.

5.1.2 - Shakedown

Upon completion of circuit installation and individual component tests, all elements of the POC circuit will be assembled and individually tested without coal with air. Any operating problems will be identified and corrected as required to avoid unnecessary delays during shakedown testing of the integrated module. Following this initial shakedown period, the integrated circuit will then be tested without coal with inerting gas to:

- establish the electrical and mechanical readiness of the circuit for detailed testing and evaluation of the triboelectrostatic separation process with coal,
- economically validate the design capacities for the various gas-handling components required by the POC circuitry,
- demonstrate that the additional duct network and electrical service are suitable at minimum load, and
- establish that explosive atmosphere monitoring, fire protection, and equipment control systems are compatible, and properly working, alarmed, and interlocked.

Upon satisfactory completion of shakedown tests without coal, the integrated system will be operated with coal and under inerting gas, but with all potential ignition sources (i.e., tribocharger and electrostatic separator electrodes) de-energized to:

- establish that the ancillary equipment, including grinding mills, compressors, storage bins, feeders, pulverizers, dust collectors, conveyors, etc., are adequate,
- validate the design capacities for the various unit operations included in the test circuit,
- train operators and gain confidence in circuit operation, and
- verify the proper operation of the explosive atmosphere monitoring and control system.

Sub-Task 5.2 Execution

5.2.1 Installation

The TES unit is shown in Figure 60. All ancillary equipment such as screw conveyors, motor controllers, instrumentation and electrical services were installed by Virginia Tech personnel.

During operation of the pilot-scale TES circuit, pulverized feed is manually dumped into the feed bin and transferred via an inclined feed screw into a sealed surge bin. Once in the surge bin, the fresh feed is blended with the middlings product from the electrostatic separation chamber as shown in Figure 61. A vertical screw conveyor is then used to carry the blended material to the second floor of the pilot-plant facility where it is discharged into a transfer chute that directs the material into the top of the tribocharger (Figure 62). Two chargers were initially tested, namely, a stationary tribocharger equipped with fixed copper rods and a two-stage vertical turbocharger equipped with high-speed rotating vanes.

Figure 60 POC-scale TES unit supplied by Carpco.

Figure 61 Feed arrangement of the POC-scale TES unit test setup.

Figure 62:POC Scale tribocharger made of copper used for the preliminary separator study.

After passing through the tribocharger system, the charged particles were directed through an insulated (glass) feed inlet box located just above the electrodes (Figure 63). The feed inlet box passes through a perforated plate that serves to straighten/distribute gas in a laminar pattern down through the separation chamber. This arrangement directs the feed particles between oppositely charged sets of four-roll electrodes (Figure 64). The electrodes are constantly cleaned by means of two sets of twin brushes located behind each set of electrodes. When desired, maintenance and/or replacement of the electrodes is performed through removable panels located on each side of the TES unit .

Figure 63 Feed introducer made of tempered glass was used to direct the feed material into the separator chamber.

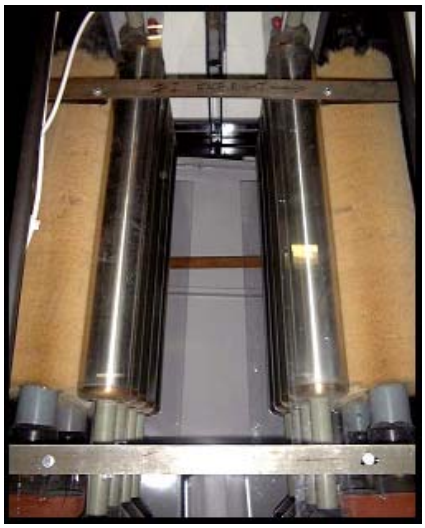

Figure 64 Self-cleaning rotary electrodes supplied by Carpco.

The bottom of the separation chamber is equipped with clean-coal (left) and refuse (right) splitters that can be adjusted during operation to achieve a given product quality (Figure 65). Particles that are misplaced or poorly charged pass between the splitters and form a middlings product. The three different products are collected in partitioned product bins built into the bottom of the TES unit. The products are continuously removed by means of three different variable-speed screws, i.e., reject screw, middlings screw and clean-coal screw (Figure 66). As indicated previously, the product from the middlings screw conveyor is blended back with fresh feed in the surge bin and recycled back through the charger and separator. The reject product is discharged into a barrel on the left side of the TES unit while the clean-coal product is discharged into a barrel on the right side of the unit. Particulate material that accumulates in each screw prevents inert (nitrogen) gas that is constantly injected into the separation chamber from escaping.

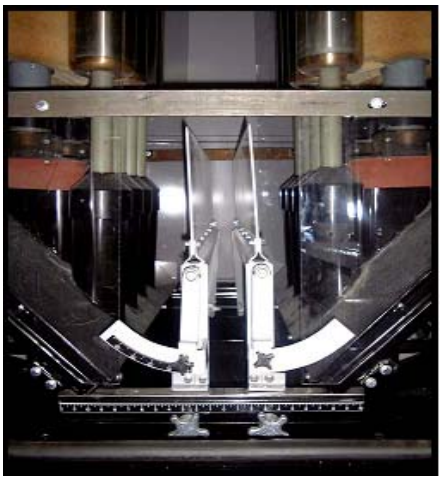

Figure 65 Splitter arrangement of the POC TES unit.

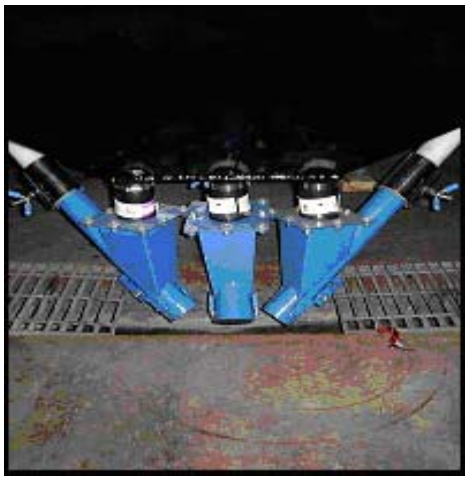

Figure 66 Flexible screw conveyors used to remove material from the TES units.

The control and monitoring panel for the TES unit is mounted on the front of the TES unit for easy access. The unit is equipped with a complete instrumentation package that allows the on-line monitoring of humidity, oxygen and internal pressure (Figure 67). To improve safety, the unit is equipped with a backup oxygen sensor to ensure that faulty readings

Figure 67 Pressure and oxygen sensors were used to monitoring the chamber pressure and oxygen concentration in the separation chamber.

from the primary system do not allow operation under potentially explosive conditions. The speed of the inclined and vertical screws can also be adjusted to any set value using digital controllers mounted on the back wall of the pilot-plant facility. The installation was inspected by the Virginia Tech Environmental Health and Safety Services.

5.2.2 Shakedown

Shakedown testing was carried out using AEP Glen Lyn mill rejects crushed to pass 2 mm. In general, most of the installed circuitry was found to perform well within the design specifications. However, during some of the preliminary test runs, some initial operational problems have been encountered. For example, the vertical screw conveyor was found to have a lower capacity than that specified by the manufacturer. Follow-up tests performed by the manufacturer indicated that the discharge chute from the surge bin was improperly designed. This problem was rectified by the manufacturer at no cost to the project.

Another technical problem that occurred during shakedown testing was the relatively poor performance of the tribocharging system. The preliminary tests were performed using a stationary tribocharger system equipped with several series of stacked layers of copper pipes. Data collected using the stationary charging system suggests that this approach does not provide the necessary degree of particle contacting for good charging. To correct this problem, a high-intensity turbocharger was installed. This system uses high-speed rotating blades to create efficient contacting between particles and the rotating vanes and charger wall. The installed turbocharger operates as a two-stage system to ensure that good contacting and charging is achieved.

Several series of shakedown tests were successfully completed using samples of pulverizer mill rejects from the Glen Lyn power plant. These tests were conducted to determine whether the fundamental design of the TES circuit was adequate. Components evaluated in the

shakedown tests included systems for materials handling, gas inerting, particle charging, electrostatic field generation and instrumentation/control.

5.2.3 Materials Handling

The inclined screw conveyors were found to be very effective for introducing feed solids into the TES and for discharging the clean/reject products from the TES. These conveyors also provided an effective and inexpensive means for sealing the unit from outside air so that the inert atmosphere could be maintained within the separation chamber. However, a problem occurred with the vertical recycle screw in that it was creating a large amount of dust via attrition of the coal and mineral particles. The mixture of coal and mineral dust appears to adhere non-selectively to the surfaces of larger particles and adversely impacts their charging characteristics. To solve this problem the vertical screw conveyor was replaced by an enclosed bucket elevator.

5.2.4 Particle Charging System

The shakedown test data indicate the static charger equipped with fixed copper rods cannot provide the level of charging necessary to obtain good separations. On the other hand, the two-stage rotary turbocharger equipped with high-speed rotating vanes proved to be effective for selectively charging the feed particles.

5.2.5 Electrode System

No major problems were noted regarding the design of the interchangeable electrode systems. No arcing was observed between the electrodes except when the adjustable power supplies are set to extreme potentials. The only design shortcoming of the unit appeared to be the amount of time and effort required to switch from the rotating cylindrical electrodes to the screen electrodes. To minimize this turn-around time, a special set of flat screen electrodes were

fabricated. The new design allowed the screens to be mounted over the cylindrical electrodes without requiring their removal.

5.2.6 Inerting System

The nitrogen flushing system used to maintain an inert atmosphere within the TES unit performed as designed. The inert gas eliminates the possibility of coal dust explosions and has the added benefit of reducing the relative humidity within the separation chamber. The only disadvantage of the current design is that the expanded gas from the liquid nitrogen tank was significantly reducing the temperature within the TES unit. Since electrostatic separations are generally more effective at higher temperatures.

5.2.7 Instrumentation

The design of the instrumentation package has proven to be very effective in providing on-line information for controlling and monitoring the performance of the TES unit. All of the system interlocks were thoroughly tested and found to work in accordance with all safety protocols. In particular, the twin oxygen sensors were been found to effectively provide redundant data that ensure that the unit is not operated under a condition that may be unsafe. The humidity sensor appeared to be adequately robust to withstand the dusty conditions within the separation chamber.

Task 6 – Detailed POC Testing

Sub-Task 6.1 Objectives

The primary objective of this task is to ascertain the optimum operating conditions of the POC unit on a variety of feed samples and reproduce the best results of the bench-scale tests. With the triboelectrostatic test circuit fully commissioned, the DOE approved POC-scale test plan will be implemented. Tests will also allow the optimum operating conditions to be established for the separation of coal and mineral matter by the TES process. The results obtained on POC-scale will be compared with those generated on bench-scale units and used to validate the performance expressions developed at the bench-scale. Modifications to the design expressions will be made as deemed appropriate after examining the POC-scale test data.

Sub-Task 6.2 Detailed Testing

After completing the preliminary shakedown tests, several series of detailed tests were initiated to evaluate the separation capabilities of the current design. A series of confirmatory bench-scale tests was also carried out in parallel to the POC–scale testing, to further quantify the effects of several important operating variables on separation performance.

The POC test program and the accompanying bench–scale program were carried out on pulverized samples of the following materials: (i) Glen Lyn Raymond Mill Rejects (feed ash ≈ 42-45%), (ii) Moss 3 Raw Coal, (iii) Possum Point Raymond Mill Rejects and (iv) Shawville Raymond Mill Intermediate Products.

Initially a series of preliminary bench–scale tests were carried out on Glen Lyn Raymond Mill Rejects. The tests examined the effect on the separation of the electrode position, humidity and particle size.

6.2.1 *Effect of Electrode Position*

Figure 68 shows the results of tests performed to determine the influence of electrode position on combustible recovery and product ash content. In these tests, the position the negative electrode was moved between five different positions (0, 1.5, 3.0, 4.5 and 6.0 cm), while the position of the positive electrode was held fixed at three different values (i.e., 0, 3.0 and 6.0 cm). The first experiment was performed with the positive electrode held in the closest position (0-cm) to the feed inlet. Under this condition, the combustible recovery increased from 58% to 68% as the negative electrode was moved outward by a distance of 6 cm. The increased recovery was obtained with very little increase in product ash content. Similar results were also obtained for the other two positive electrode positions of 3 and 6 cm. However, the increase in recovery was somewhat less pronounced (i.e., 57% to 62%) at the larger electrode spacing.

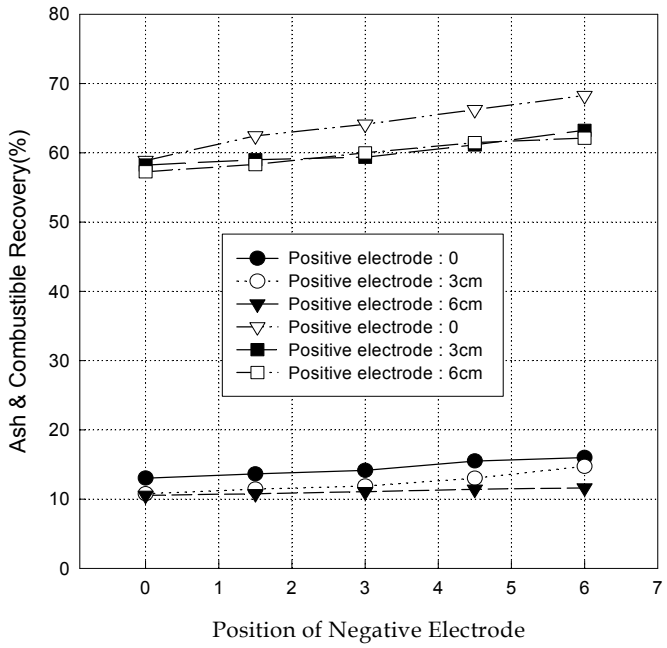

Figure 68 Effects of electrode position on the separation performance of the bench-scale TES unit.

6.2.2 *Effect of Humidity*

Figure 69 shows the effect of relative humidity on combustible recovery and clean-coal ash content. As shown, the combustible recovery and ash contents remain relatively constant at approximately 66-68% and 15-16%, respectively, when the relative humidity is held below about 50%. On the other hand, the combustible recovery begins to drop from 68% to 62% as the relative humidity increased to 60%. A further increase in relative humidity to 70% causes a sharp decrease in recovery to 54% with little change in the ash content of the clean-coal product. These results suggest that humidity is an important parameter in the particle charging process and will need to be monitored to ensure that good recoveries are maintained.

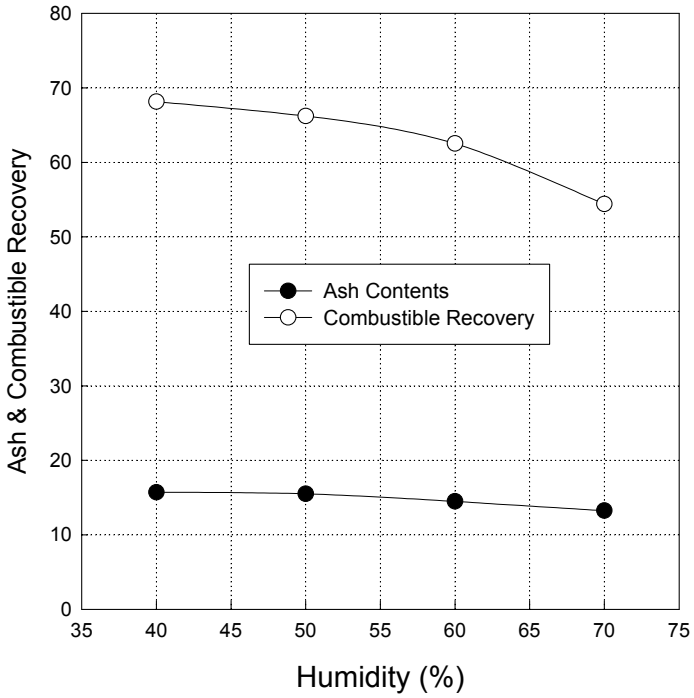

Figure 69 Effects of relative humidity on the separation performance of the bench-scale TES unit.

6.2.3 *Effect of Particle Size*

Figure 70 shows the separation curves (combustible recovery versus ash content) obtained for coal pulverized to three different topsizes (i.e., 20, 30 and 65 mesh). As shown, the coarsest grind size (20 mesh x 0) produced the worst recovery-ash curve, while the finer grind sizes (minus 30 and 65 mesh) were upgraded more efficiently. It is unknown whether the poorer results were due to incomplete liberation, inadequate charging or inefficient collection. The results suggest that the optimum top size for upgrading this particular coal is approximately 30 mesh.

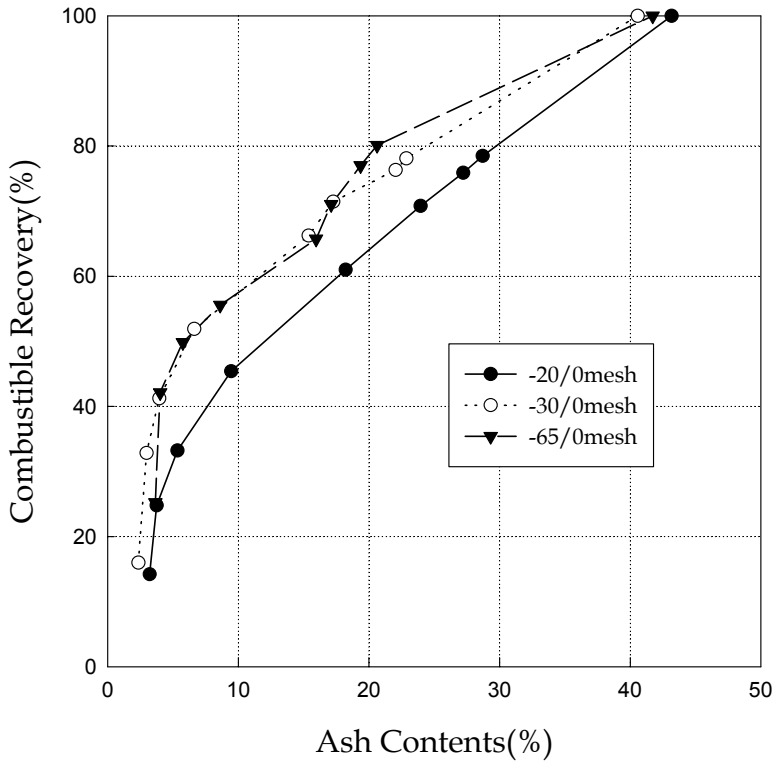

Figure 70 Effects of particle size on the separation performance of the bench-scale TES unit.

Detailed testing on the POC - TES unit was carried out using pulverizer reject material from the Glen Lyn power plant. The mill rejects were crushed to below 2 mm and then dry screened to

produce different feeds. Tests were carried out using feeds of two different size classes, i.e., 28 x 70 mesh and minus 28 mesh.

The initial test work focused on (i) feed size distribution, (ii) electrode design and (iii) electrode configuration. Initial test results showed that better separations could be made with the bench-scale unit than with the POC-scale unit. By a process of elimination, it was concluded that the vertical recycle conveyor was grinding the feed material via attrition. This resulted in dust coatings on both the coal and refuse particles that would not accept a differential charge at the turbocharger.

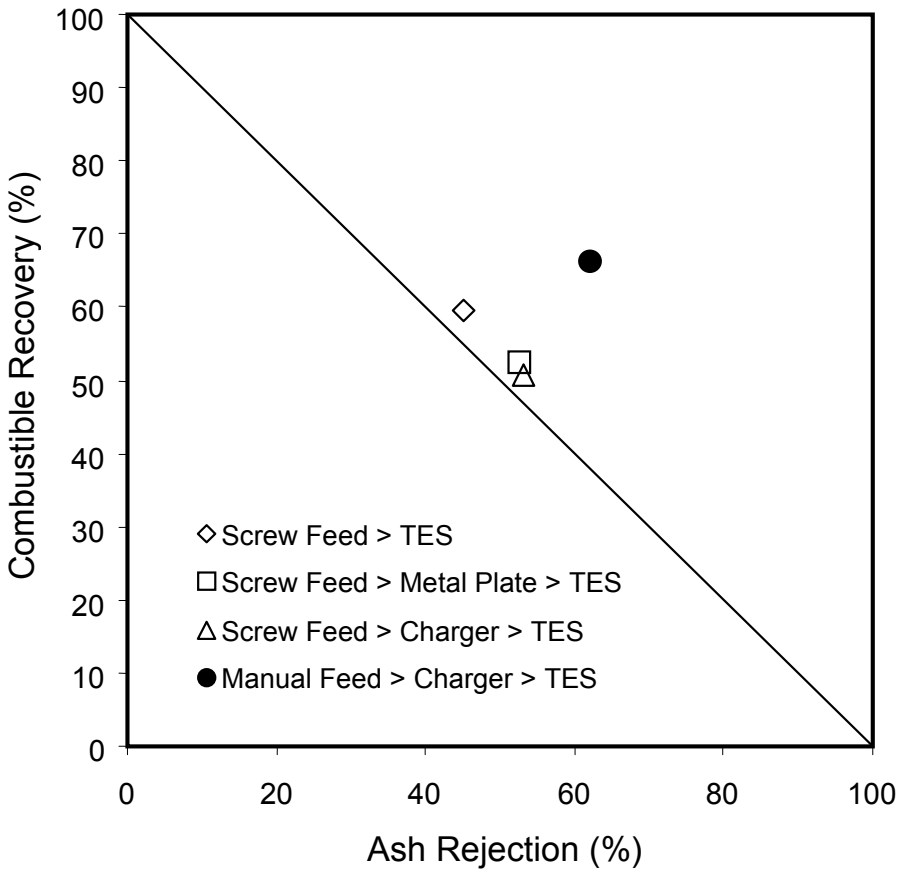

Figure 71. Effects of different feed handling procedures on separation performance.

Figure 71 provides a comparison of the test results obtained from the tests conducted with and without the recycle screw. In the first three experiments, the feed coal was passed through the vertical recycle screw as would be necessary during routine operation. The discharge from the recycle was then either (i) fed directly into the TES without passing through the turbocharger, (ii) fed across a grounded metal plate to remove any residual charge before passing into the TES, or (iii) fed to the turbocharger before passing into the TES. As shown, poor separation results were obtained in all three cases.

As shown in Figure 71, much improved separation results were obtained by bypassing the recycle screw. Until this problem was corrected, the recycle screw was taken out of operation and the unit was operated as a batch process whereby the feed was hand fed directly into the turbocharger.

In light of the encouraging results obtained by manual feeding, two series of tests were conducted to evaluate the effectiveness of the proposed electrode systems for upgrading the minus-28-mesh sample from the Glen Lyn plant. In the first series of experiments, the rotating cylindrical electrodes were evaluated (see Figure 72a). The second series of tests were conducted using screen electrodes mounted directly over the cylindrical electrodes (see Figure 72b). In both series of experiments, the coal product from the initial separation step (i.e., rougher stage) was subjected to two additional stages of upgrading (i.e., cleaner stage and recleaner stage) to produce higher quality products. Likewise, the reject sample from the rougher stage was reprocessed (scavenger stage) in an attempt to recover additional organic matter. For reference, diagrams illustrating the different stages of upgrading are provided in Figure 73 and Figure 74 for the cylindrical electrodes and screen electrodes, respectively.

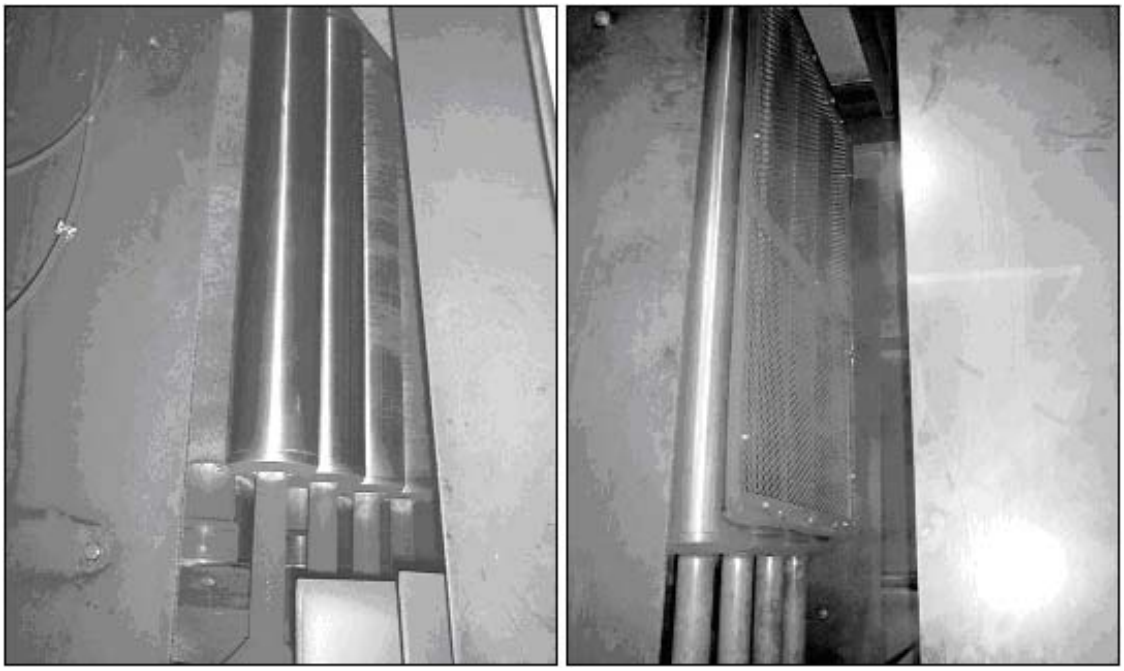

(a) (b)

Figure 72. Photographs of the cylindrical (a) and screen electrode (b) configurations evaluated in the TES test program.

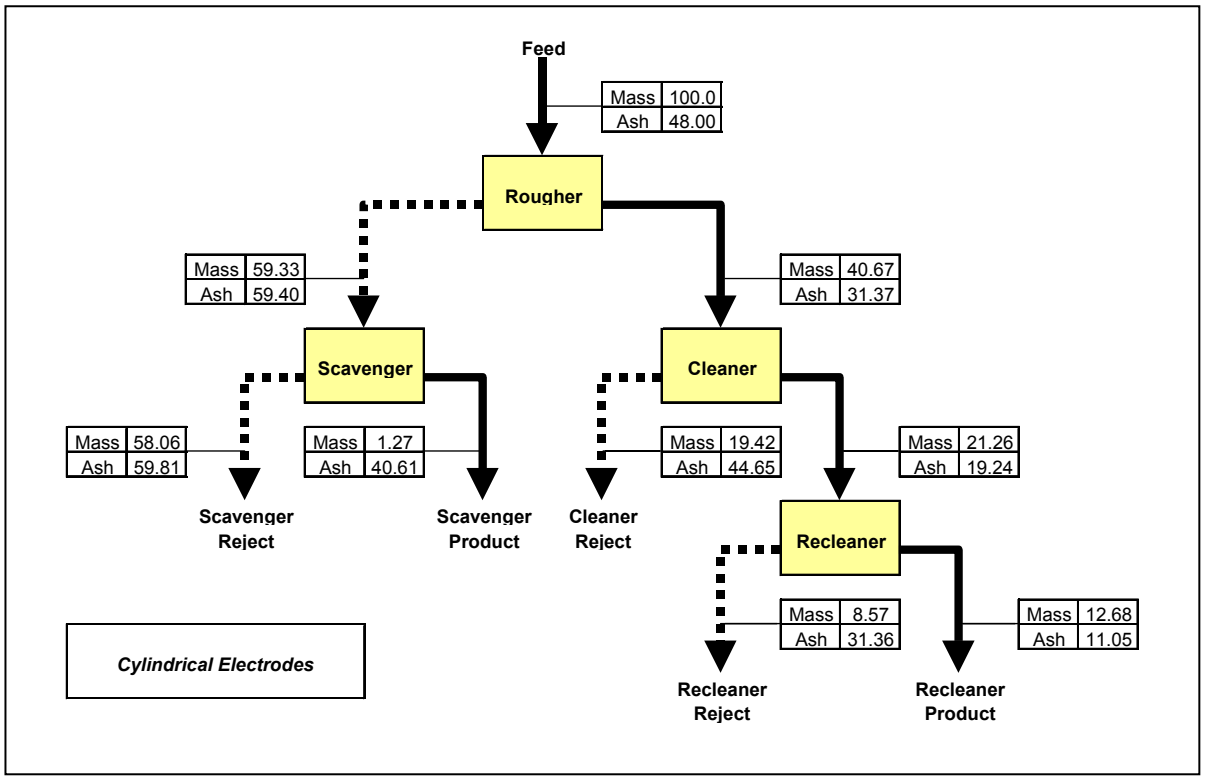

Figure 73. Multi-stage flowsheet used for the evaluation of the cylindrical electrode system.

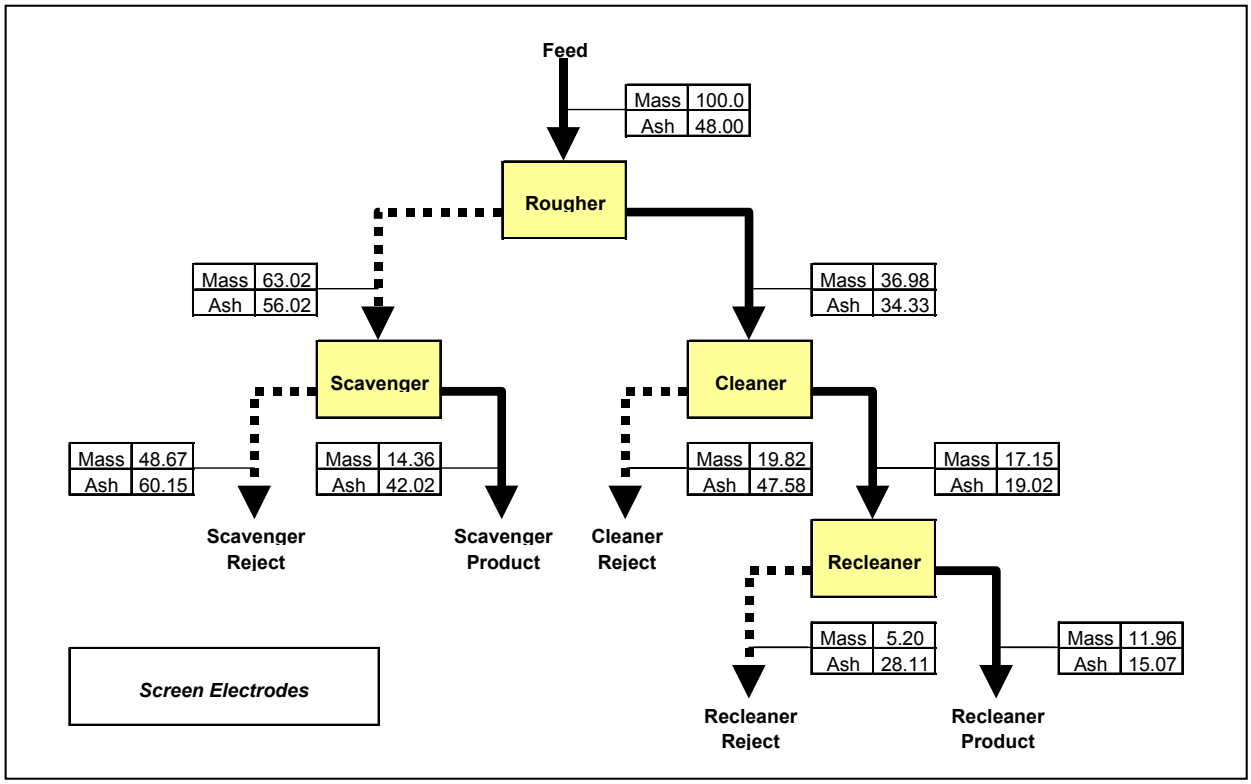

Figure 74 Multi-stage flowsheet used for the evaluation of the screen electrode system .

The separation results obtained from the comparison tests conducted using the different electrode systems are summarized in Figure 75 (yield-ash curve) and Figure 76 (recovery-rejection curve). The test data suggest that the two electrode systems are very similar in terms of performance. Both configurations reduced the feed ash by more than half (48% to 20%) after just two stages of cleaning. In fact, somewhat poorer yields were obtained using the screen electrode system. However, a careful review of the laboratory test conditions indicated that the tests conducted using the screen electrodes were carried out at a much higher relative humidity (50% versus 32%) and lower temperature (48º F versus 72º F) than those performed using the cylindrical electrodes.

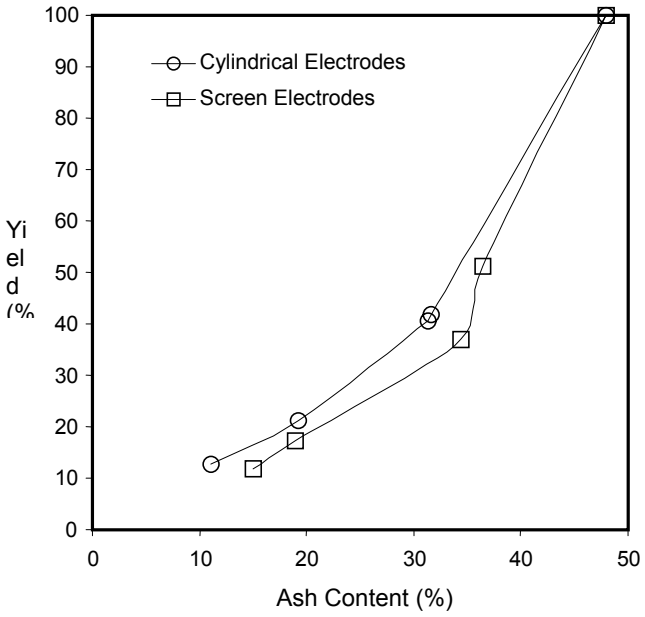

Figure 75. Yield-ash data obtained from the comparison tests conducted using the cylindrical electrode and screen electrode systems.

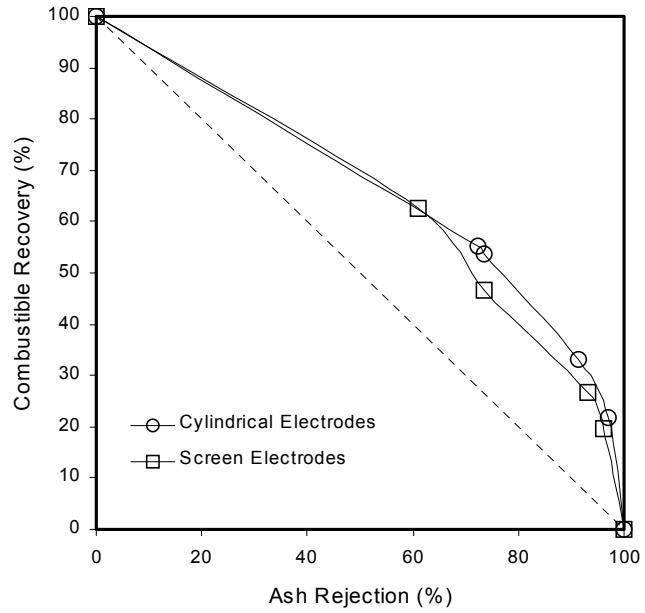

Figure76. Recovery-rejection data obtained from the comparison tests conducted using the cylindrical electrode and screen electrode systems

As demonstrated previously on the bench scale, conditions of higher humidity and lower temperature are detrimental to the electrostatic separation process. It should also be noted that the separation results described above were achieved without the use of a recycled middlings product due to the grinding problems caused by the vertical screw conveyor. Previous test work indicates that the middlings recycle stream can further improve the separation performance by optimizing recovery and clean coal quality.

It was concluded that the pilot-scale tests gave results substantially inferior to the bench-scale test results. The reasons for the discrepancy were considered to be as follows:

- The bench-scale test unit was equipped with screen electrodes, while the pilot-scale test unit was made of drum-type electrodes equipped with self-cleaning brushes. The latter is Carpco's patented design and the former is the invention made as part of the current project.
- The pilot-scale unit was equipped with a recycle loop, using a screw conveyer. In addition to the excessive grinding caused by this conveyer, it was thought that the difference in the material of the screw (stainless steel) and the casing (PVC) was causing a conflict in charging. One type of particles became positively charged by the stainless steel, while the PVC tubing was causing them to become negatively charged.
- The particle size of the feed may have been too large for the pilot-scale tests. Owing to its size, large particles may fall too fast to be captured by the electrodes. Furthermore, the potential gradient in the pilot-scale unit is lower than that in the laboratory unit due to the large separation distances between the electrodes.
- In the pilot-scale unit, it was difficult to change the electrode positions. This was particularly the case with the cylindrical electrodes of Carpco's design, which are bulky.

- In the bench-scale unit, particles were charged while they were being fed and recycled through a PVC tubing pneumatically (i.e., by blowing a stream of compressed air). In the pilot-scale unit, particles were charged by means of a turbocharger shown previously in Figures 58 and 62. In this latter unit, the particles present in the feed and recycle streams were agitated by means of Plexiglas blades. The particles were thrown against the inner wall (Plexiglas cylinder) of the charger by the impeller and then swirl downward. The particles acquired surface charge while being in contact with the Plexiglas wall. An advantage of using the dynamic mixer was that it was not necessary to us a large volume of gas to move the particles through the recycle loop.

The above problems were addressed as follows.

- The Carpco's cylindrical electrodes were replaced by a set of screen electrodes. Two engineers from Carpco spent one week in Blacksburg to assist in the replacement procedure.
- The screw conveyer was replaced by a bucket elevator.
- The particle size of the feed was reduced to -35 mesh from -28 mesh.
- The turbo-charger was modified to install blades in two layers (see Figure 58).

This modified system was used in all subsequent testwork with the POC unit.

6.2.4 Effects of Electrode/Splitter Position

The first series of detailed tests were conducted by changing the configuration of the electrodes relative to the feed point and the splitter locations at the bottom. Figure 77 is a schematic representation of the configuration. The data given in Figure 78 and Table 3 show the test results obtained using the minus-35-mesh Glen Lyn mill reject samples. Also shown for

comparison are the results obtained on the minus-28-mesh fraction. The results are given in Figure 78 and were obtained with the following configuration: Dcf=203 mm (8 -s), Daf=178 mm (7-inches), and Das=80 mm (3.15-inches), while Dcs was varied in the range of 0 to 60 mm (2.37-inches).

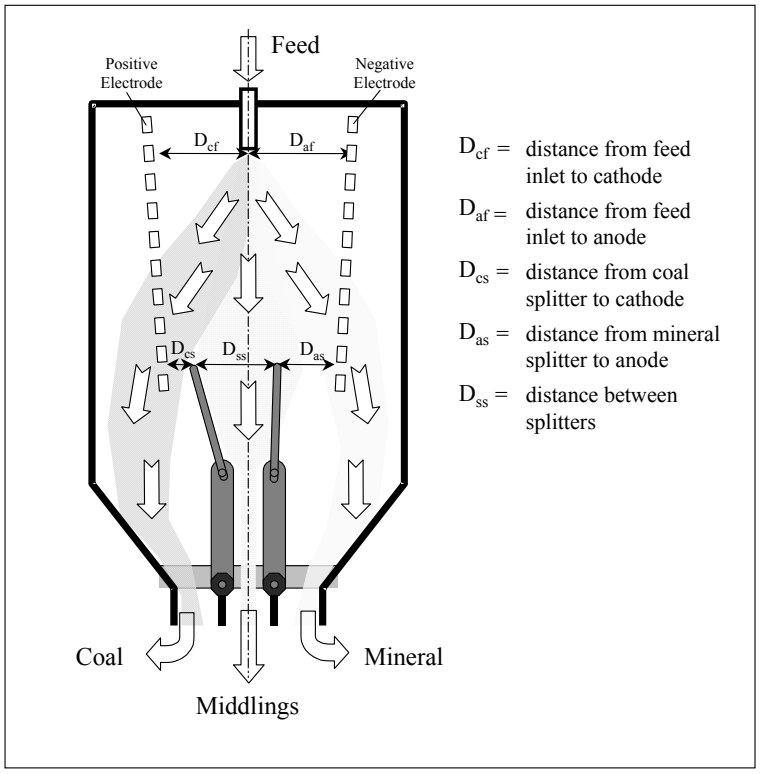

Figure 77. Schematic showing the dimensions used to specify the positions of the TES electrodes and splitters.

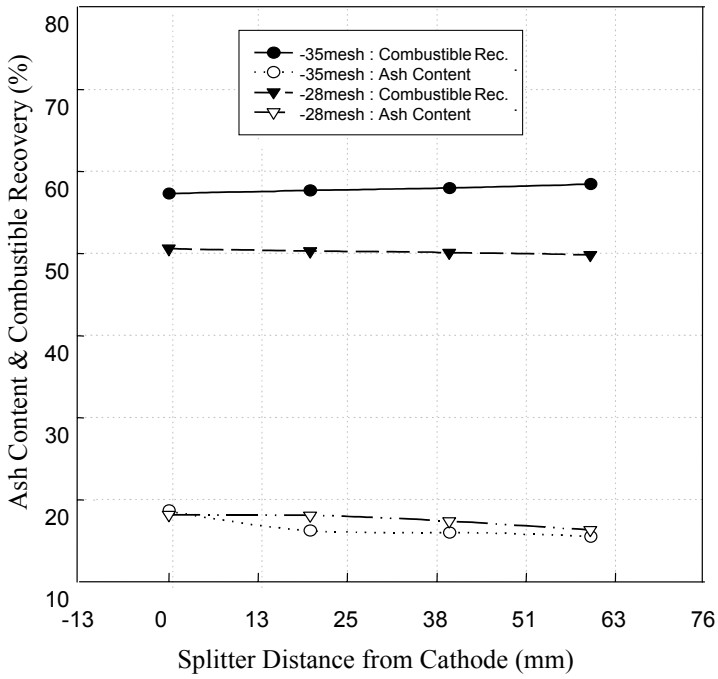

Figure 78 The results of the POC-scale triboelectrostatic separation tests conducted on the mill reject sample from Glen Lyn Power Plant, Virginia. The sample was pulverized to 28 mesh x 0 and 35 mesh x 0 prior to the pilot-scale tests. The results are plotted as a function of the distance (D_{cs}) between the cathode and splitter, which controls the amount of middlings recycled.

Table 3. Results of the POC-scale triboelectrostatic separation tests conducted on the mill reject from Glen Lyn Power Plant, Virginia, by changing splitter position (D_{cs}).

Particle Size (mesh)	Splitter Position, D_{cs} (mm)	Product				Combustible Recovery (%)
		Yield (% wt.)		Ash (% wt.)		
		Clean Coal	Reject	Clean Coal	Reject	
35 x 0	0	37.6	62.4	18.7	63.5	57.3
	25	36.7	63.3	16.2	64.3	57.7
	40	36.8	63.2	16.0	64.6	58.0
	60	36.9	63.1	15.5	64.9	58.4
28 x 0	0	32.4	67.6	18.1	61.6	50.5
	25	32.2	67.8	18.1	61.5	50.2
	40	31.8	68.2	17.4	61.6	50.1
	60	31.2	68.8	16.3	61.7	49.8

The results (ash content and combustible recovery) have been plotted versus the distance between the cathode and the splitter (D_{cs}) at the bottom. Ash-forming minerals move toward the cathode, while clean coal particles move toward the anode, which is consistent with the results of the bench-scale test work reported earlier. Because of the feed composition, the amount of the ash-forming minerals reporting to the cathode was considerably larger than the amount of coal reporting to the anode. Therefore, controlling the amount of the ash-forming minerals (tailings) reporting to the product stream controlled the amount of the middlings recycled. For this reason, the tests were conducted by varying the distance (D_{cs}) between the cathode and the splitter. As D_{cs} was increased, the amount of the middlings recycled was reduced. The results show that as the amount of the recycled material decreased, the ash content was decreased, as some of the middlings reported to the clean coal product. However, the changes in recovery due to recycling were minimal. The results given in Figure 78 and Table 3 suggest that there is no need to recycle the middlings stream for the sample tested in this series. This finding may indicate that the separation is as good as it can be in the first pass. The results also showed that the minus-35-mesh particles gave a higher recovery than the minus-28-mesh particles. A possible explanation may be that the coarse particles may fall too fast to be attracted by the electrodes.

6.2.5 Effects of Applied Potential

Figure 79 and Table 4 show the results obtained on the minus-35-mesh sample with the following electrode configurations: D_{cf}=203 mm (8 -s), D_{af}=178 mm (7-inches), D_{as}=80 mm (3.15-inches), and D_{cs}=60 mm (2.36-inches). At this configuration, the amount of the middlings recycled was minimal. The potential difference between the two electrodes was varied in the range of 20 to 100 kV. The results showed that coal recovery decreased with increasing electrode potential difference, which seemed surprising. A possible explanation could have been that the charge of the coal particles was substantially higher than that of the ash-forming

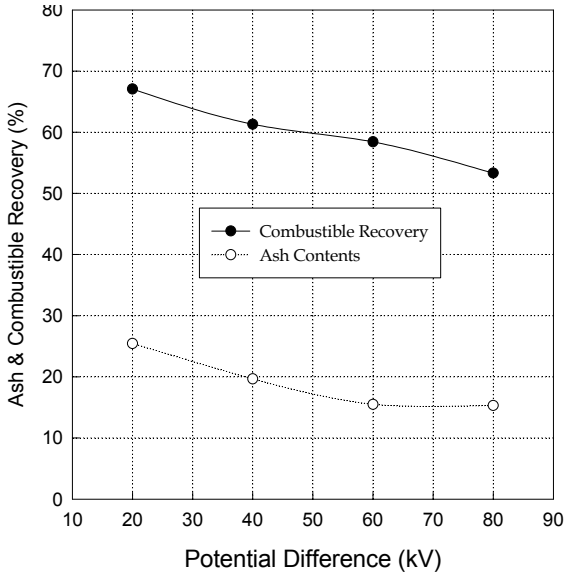

Figure 79 The results of the pilot-scale triboelectrostatic separation tests conducted on the mill reject sample (35 mesh x 0) from Glen Lyn Power Plant, Virginia. The tests were conducted by changing the potential difference between the cathode and anode.

Table 4 Results of the POC-scale triboelectrostatic separation tests conducted on the mill reject (35 mesh x 0) from Glen Lyn Power Plant, Virginia, by changing the potential difference between the cathode and anode at a potential difference of 60 kV.

Potential Difference (kV)	Product				Combustible Recovery (%)
	Yield (%wt)		Ash (% wt)		
	Clean Coal	Reject	Clean Coal	Reject	
20	48.0	52.1	25.5	66.2	67.1
40	40.7	59.3	19.7	65.2	61.3
60	36.9	63.1	15.5	64.9	58.4
80	33.6	66.4	15.3	62.5	53.3

minerals, as has been found in Task 3.1 (Charger Tests). At low potentials, highly charged coal particles could have been recovered in preference to the weakly charged ash-forming minerals, resulting in high recoveries. As the potential difference was increased, weakly charged ash particles and some of the middlings were then pulled toward the cathode, causing a decrease in recovery. Decreasing ash content observed with decreasing recovery can be attributed to the loss of middlings to the cathode.

6.2.6 Effects of Charger Speed

Figure 80 and Table 5 show the results obtained using the minus 35 mesh feed by changing the rotation speed of the impeller in the turbocharger. The electrode and splitter were configured as follows: Dcf=203 mm (8 -s), Daf=178 mm (7-inches), Dcs=60 mm (2.36-inches), and Das=80 mm (3.15-inches). These dimensions are the same as the case with the results given in Figure 77. All of the tests were conducted at 60 kV of potential difference between the electrodes. As shown, combustible recovery increased with increasing impeller speed, which suggests that the coal recovery increased with increasing charge of the coal particles. As shown in Task 3.1 (Charger Tests), the charge of the coal particles increased with increasing impeller speed of the turbo charger. The combustible recovery increased from 50 to 59%, with little changes in ash contents. These results suggest that proper design of the charger is important for improving the recovery. The results shown in Figure 80 and Table 5 were obtained using two impellers in the turbocharger.

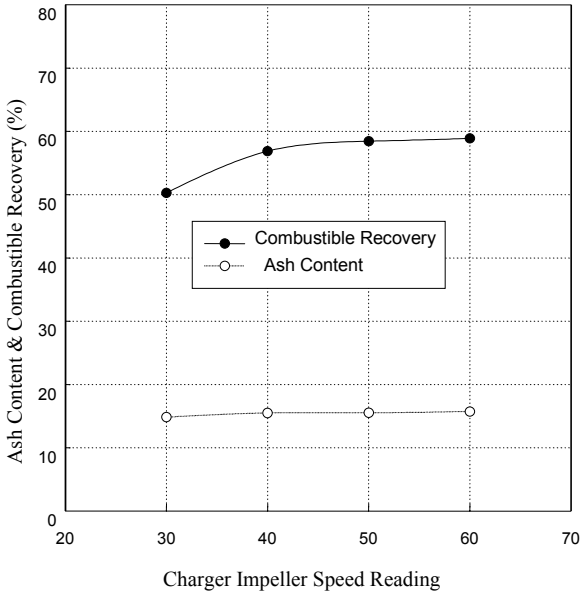

Figure 80. The results of the pilot-scale triboelectrostatic separation tests conducted on the mill reject sample (35 mesh x 0) from Glen Lyn power plant, Virginia. The sample was pulverized to 28 mesh x 0 and 35 mesh x 0 prior to the pilot-scale tests. The tests were conducted by changing the impeller speed of the Turbocharger.

Table 5. Results of the POC-scale triboelectrostatic separation tests conducted on the mill reject (35 mesh x 0) from Glen Lyn Power Plant, Virginia, by changing the impeller speed of the turbocharger.

Charger Speed Reading	Product				Combustible Recovery (%)
	Yield (%wt)		Ash (%wt)		
	Clean Coal	Reject	Clean Coal	Reject	
20	31.3	68.7	14.8	62.1	50.2
40	35.9	64.1	15.5	64.1	56.9
60	36.9	63.1	15.5	64.9	58.4
80	37.3	67.8	15.7	65.1	58.9

6.2.7 Comparative Testing of Bench-Scale and POC-Scale Units

Further comparative testing was carried out between the modified POC circuit and the bench-scale unit. The feed to both units consisted of Glen Lyn mill rejects crushed to minus-35-mesh. In the case of the bench–scale tests, the feed ash was progressively increased by the addition of high-ash reject material. The bench-scale tests were carried out under the following conditions:

- Potential Difference = 30 kV
- Charger Speed = 30-35 rpm
- Clean Coal Splitter = 51 mm (2-inches) from the cathode
- Reject Splitter = 110 mm (4.3-inches) from the anode
- Potential Difference = 30 kV
- Charger Speed = 50 rpm
- Relative Humidity = 18-25%

The comparative test results obtained from the bench-scale and POC-scale test runs are summarized in Tables 6 and 7.

The test data show that the POC–scale unit was still giving lower combustible recovery results than the bench–scale unit. It was noted that in both test series the higher the feed ash, the lower the combustible recoveries. Also, in both levels of testing, the reject ash generally remained constant and was relatively independent of the feed ash.

One major difference between the two units is the material of construction of the screen electrodes. The bench–scale electrodes were aluminum and the POC were mild steel. In order to establish if the different materials of construction had a significant influence on the performance, a series of tests were carried out on the POC unit fitted with aluminum screen electrodes. In addition, the POC unit was modified to include a feed chute that extended into the area between

Table 6. Results of the Bench-Scale Triboelectrostatic Separation Tests Conducted on the Mill Reject (35 mesh x 0) from Glen Lyn Power Plant, Virginia.

Feed Ash (%)	Clean Yield (%)	Reject Yield (%)	Clean Ash (%)	Reject Ash (%)	Combustible Recovery (%)
34.10	58.79	41.21	12.30	65.20	78.24
40.45	55.55	44.45	16.00	71.00	78.35
46.21	47.53	52.47	24.00	66.33	67.16
49.11	41.45	58.55	24.48	66.55	61.52

Table 7. Results of the POC-Scale Triboelectrostatic Separation Tests Conducted on the Mill Reject (35 mesh x 0) from Glen Lyn Power Plant, Virginia.

Feed Ash (%)	Clean Yield (%)	Reject Yield (%)	Clean Ash (%)	Reject Ash (%)	Combustible Recovery (%)
31.74	52.24	47.76	14.50	50.60	65.44
32.40	50.89	49.11	15.03	50.40	63.97
35.56	37.51	62.49	13.17	49.00	50.54

*Splitter Position: Dcs = 51 mm (from cathode); Dca = 109 mm (from anode)

the electrodes. It was considered that a shortened feed chute would allow an increased exposure time of the feed particles to the electrode surfaces and thus give them more time to be directed to the correct side of the unit.

The experimental results obtained from the POC-scale test runs using mild steel and aluminum electrodes and long and short feeder are summarized in Figure 81 and Tables 8 and 9.

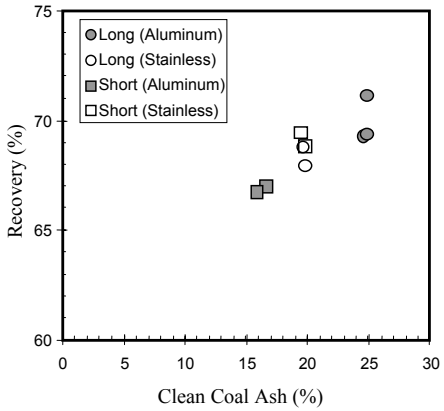

Figure 81 Grade vs. recovery curve showing the effects of feeder length and electrode material on separation performance.

Table 8. Results of the POC-Scale Triboelectrostatic Separation Tests Conducted on the Mill Rejects (35mesh x 0) from Glen Lyn Power Plant, Virginia –Comparing Stainless Steel with Aluminum Electrodes. (Unit Operated with a Long Feeder).

Test Run	Electrode Type	Clean Coal Yield (%)	Reject Yield (%)	Feed Ash (%)	Clean Coal Ash (%)	Reject Ash (%)	Combustible Recovery (%)
1	Stainless	49.55	50.45	41.48	19.76	62.81	67.94
2	Stainless	50.23	49.77	41.27	19.59	63.15	68.77
3	Aluminum	54.62	45.38	40.54	24.59	59.74	69.28
4	Aluminum	54.69	45.31	40.8	24.89	60.00	69.38
5	Aluminum	56.75	43.25	40.02	24.84	59.94	71.12

Table 9. Results of the POC-Scale Triboelectrostatic Separation Tests Conducted on the Mill Rejects (35mesh x 0) from Glen Lyn Power Plant, Virginia –Comparing Stainless Steel with Aluminum Electrodes. (Unit Operated with a Short Feeder).

Test Run	Electrode Type	Clean Coal Yield (%)	Reject Yield (%)	Feed Ash (%)	Clean Coal Ash (%)	Reject Ash (%)	Combustible Recovery (%)
1	Stainless	51.34	48.66	40.36	19.37	62.51	69.41
2	Stainless	50.78	49.22	40.8	19.77	62.5	68.82
3	Aluminum	47.45	52.55	40.93	16.6	62.9	67.00
4	Aluminum	47.04	52.96	40.95	16.16	62.97	66.79

The following conclusions were drawn from the above test work:

- In general, the longer electrodes tended to provide a higher recovery and higher ash than the shorter electrodes. However, the separation occurred in a much shorter period of time when the shorter feeder was used. The faster separation kinetics were attributed to the longer exposure in electrostatic field made possible by the use of the shorter feeder.
- When using the standard long feeder, the data suggest that aluminum electrodes provide a higher clean-coal recovery (and correspondingly higher clean-coal ash) than the stainless steel electrodes. However, when using the shorter feeder, the reverse trend was observed, i.e., the stainless steel electrodes provided a higher clean-coal recovery and ash than the aluminum electrodes.

In order to further verify the findings that the bench-scale unit produces superior results when compared to POC-scale unit, an additional series of bench-scale and POC-scale tests were conducted using a run-of-mine coal sample from the Moss No. 3 preparation plant. The test data, which are summarized in Table 10, show that the bench-scale unit did indeed attain a higher combustible recovery (69-71% versus 50-57%), lower clean coal ash (15.2-15.4% versus 18.1-19.0%), and higher separation efficiency (40.1-41.1% versus 23.4-27.7%) than the POC-scale unit. Several modifications were planned to improve the separation performance of the POC-scale unit and are described below.

Table 10 Results of POC tests conducted on Intermediate products (Sample # 1 & 2) from Shawville Power Plant. Single stage rotating paddle charger.

Sample Origin	Sampling Point	Size	% Ash				% Wt Yield	% Recovery
			Feed	Clean	Reject	Middlings		
Shawville Jan-01	# 1 Sampling Port	35 x 0 Natural	28.38	24.86	31.09	0	43.41	45.5
			29.38	27.66	31.32	0	53.01	54.3
Shawville Jan-01	# 2 Sampling Port	35 x 0 Natural	24.47	22.41	29.41	0	70.41	72.3
			24.23	22.91	24.91	0	79.71	81.1
Shawville Oct-00	# 1 Sampling Port	35 x 0 Ground	30.98	16.05	38.65	42.73	33.91	41.2
			30.84	15.66	38.61	42.62	34.01	41.5
Shawville Jan-01	# 2 Sampling Port	35 x 0 Natural	24.52	9.7	28.22	34.6	19.98	15.88
			25.52	9.35	28.29	35.0	14.63	11.57
			24.52	12.73	27.91	30.88	22.33	18.45

6.2.8 POC-Scale Modifications

In light of the superior performance of the bench-scale unit, several modifications were made to the POC-scale separator. These modifications include:

- An improved turbocharger was constructed.
- The tribocharger used to date has been constructed of several different materials (i.e., Plexiglas shell and housing, copper plate in the conical part of the chute, and glass in the vertical feed distributor). Since these materials have different work functions, the surface charge created by contact with one type of material may be cancelled when the particle contacts another type of material. The charger and feed chute were rebuilt entirely of Plexiglas to avoid this problem.
- Up to this point in the test program the discharge from the turbocharger has fallen by gravity to the electric field below. The bench-scale unit utilizes a pneumatic system to transport material and to disperse particles before they enter the separator's electric field.

A nitrogen injection system that will help disperse the charged particles was installed on the POC unit.

Following a project review it was decided that the testing of reject collected from the Raymond Mill pyrite traps was proving to be unsatisfactory for several reasons. It was therefore decided to test other materials in the mine /power plant supply chain including raw coal and Raymond Mill intermediate products.

Comparative bench-scale tests were subsequently carried out using samples of Moss No. 3 coal, Glen Lyn and Possum Point mill rejects, and Shawville intermediate mill products. As standard practice, bench-scale tests are conducted to evaluate the cleaning potential of all test samples prior to conducting POC-scale tests. Most of the bench-scale tests were conducted by charging the feed particles using a pneumatic tube charger in series with a two-stage horizontal rotary charger.

6.2.9 Testing of Moss No. 3 Coal

Bench-scale TES tests were carried out to compare the results obtained when treating "natural" fines to those obtained when treating "freshly pulverized" fines. In these tests, the sample of natural fines was prepared by screening a run-of-mine coal sample from the Moss No. 3 preparation plant to obtain a 35 mesh x 0 fraction. The sample of freshly pulverized fines was prepared by crushing coarse lumps of coal from the Moss No. 3 preparation plant down to a topsize of 35 mesh. Each of the two 35 mesh x 0 samples were passed separately through the bench-scale separator and the resultant products collected and analyzed. Each test was run in duplicate so that the experimental repeatability could be determined.

The results of the bench-scale comparison tests are summarized in Table 11. The data indicate that the separation efficiencies obtained with the naturally occurring fines were slightly superior to those obtained with the freshly pulverized fines by approximately five percentage

points (45.2-46.8% versus 40.1-40.9%). Although the freshly pulverized sample gave slightly higher recoveries (69.9-71.3% versus 65.4-68.9%), this improvement was more than offset by the higher ash content of the clean coal products obtained when treating the freshly pulverized sample (14.2-13.6% versus 15.2-15.4%).

Table 11. Comparison of test data obtained using "natural" and "freshly pulverized" fines from the Moss No. 3 preparation plant.

Size Fraction	% Ash			% Yield	Combustible % Recovery
	Feed	Clean	Reject		
Natural -35 mesh	33.97	14.19	56.30	53.00	68.90
	33.78	13.56	54.05	50.10	65.30
Whole Coal Ground to -35 mesh	29.84	15.24	50.83	59.00	71.00
	29.87	15.38	49.81	57.90	69.90

Table 12. Summary of test results obtained using mill "reject" from the Possum Point Power Plant.

Size Fraction	% Ash			% Yield	Combustible % Recovery
	Feed	Clean	Reject		
Natural -35 mesh rejects	61.50	51.11	72.05	50.00	64.00
	61.26	44.37	71.73	38.30	55.00
Natural -35 mesh rejects mixed with -35 mesh feed coal	45.65	28.77	59.75	46.00	60.00
	45.98	27.43	59.84	42.10	56.60
	37.83	18.86	55.41	48.00	63.00
	38.01	18.05	54.85	45.80	60.05

6.2.10 Testing of Raymond Mill Reject

Several bench-scale tests were conducted using "reject" material from the Virginia Power Possum Point power plant located in Manassas, Virginia. The mill reject, which was collected from the pyrite trap of the Raymond mill pulverizer, was screened to remove 35-mesh oversize material prior to being fed to the bench-scale separator. Unfortunately, the ash content of the

minus-35-mesh feed was found to be very high (i.e., >60% ash). Therefore, a second series of tests were carried out using artificially prepared feeds with a lower ash content. The artificial feeds were created by blending a small amount of low-ash mill feed coal that had been crushed to minus-35-mesh with the high-ash minus-35-mesh mill reject. Two artificial feed samples, i.e., 46% ash and 38% ash, were prepared in this manner.

Table 12 summarizes the results of the tests conducted using the minus-35-mesh reject material and the two artificial feed samples. The original high-ash reject material showed little reduction in ash content. In this particular case, the ash content was reduced from 61.5-61.3% down to 51.1-44.4%. The separation efficiencies for these tests ranged from 22.1-27.2%. In contrast, the best separation results were obtained with the artificial feed mixture that had an ash content of approximately 38%. In this case, the feed was cleaned down to 18.1-18.9% ash at a recovery of 60.5-62.8%. The separation efficiency for this series of tests was 38.8%. As expected, the results obtained using the artificial mixture with the 46% ash content was between those obtained with the high-ash (61%) reject material and low-ash (38%) artificial mixture.

6.2.11 Testing of Raymond Mill Intermediate Products

The use of mill reject material as feed for the TES process was determined to be inappropriate due to the high ash content of this stream. Therefore, samples of "intermediate" products were taken from within the grinding chamber of the Raymond mill at the Shawville power plant. Figure 82 shows the general layout of the mill and the specific locations of the four sampling ports installed along the height of the grinding chamber. Samples were collected from each of the sampling points and were subjected size and ash analyses.

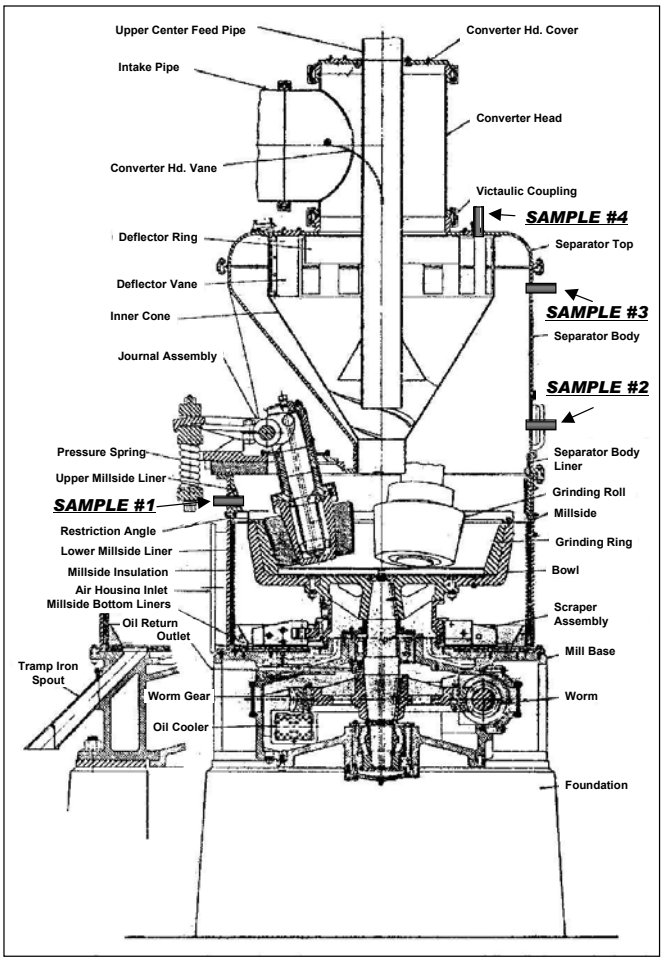

Figure 82. Detailed schematic of the Raymond mill showing the location of sampling ports for the collection of intermediate products.

Figure 83 shows the ash content of the intermediate products collected from each of the four sampling ports. Because of the inherent segregation of particles within the mill classifier, the sample taken near the bottom of the mill (Sample #1) possessed a much higher ash content than the sample taken near the top of the mill (Sample #4). However, the ash content of each of the four intermediate products was significantly lower than that of the reject material collected from the pyrite trap. The lower ash content and finer size distribution make the intermediate products a more attractive source of feed coal for the TES process.

Three sets of bench-scale tests were conducted to evaluate the cleanability of the intermediate products collected as a function of mill height. In each set of tests, the samples were dry screened into several different size fractions before being tested. For the first sample (Sample #1), the size fractions included 35 x 48 mesh, 14 x 100 mesh, 100 x 200 mesh, and 48 mesh x 0. The next two samples (Samples #2 and #3) were screened into 35 x 100 mesh and 28 mesh x 0 fractions. The final sample (Sample #4), which was obtained from the top of the mill, was not tested because of its very low ash content (i.e., 14.1% ash).

The results of the tests conducted with the first intermediate product (Sample #1) is summarized in Table 13. In general, the test data do not follow any discernable trend, perhaps because of the large variability in the ash contents of the different size fractions in the feed. However, the data do suggest that the "by-zero" material (i.e., 48 mesh x 0) provided a higher recovery (60-64%), lower clean coal ash (14-16%), and higher separation efficiency (31-33%) than the screened fractions in which the finest material had been removed. This finding is important since it suggests that the intermediate feed material need not be "dedusted" prior to being fed to the TES process.

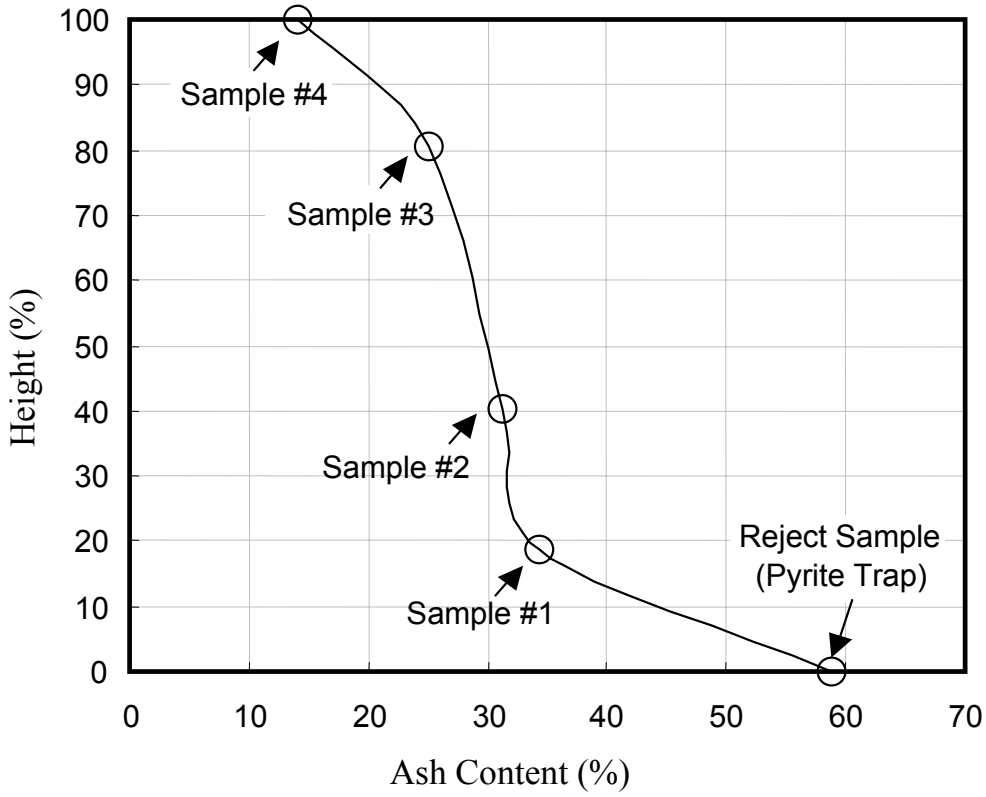

Figure 83. Effect of sample port position (measured in terms of percentage of grinding chamber height) on the ash content of the intermediate product.

Table 13. Results of bench-scale tests conducted on an intermediate product (Sample #1) from the Shawville Power Plant.

Test No.	Size Fraction Mesh	% Ash			% Yield	% Recovery
		Feed	Clean	Reject		
1	14 x100	32.23	24.4	37.62	40.8	45.5
2	35 x 48	42.35	25.46	51.97	46.9	46.9
3	48 x 0	27.37	14.73	40.94	60.8	60.8
4	48 x 0	27.25	15.66	41.11	63.1	63.1
5	100 x 200	24.61	17.03	32.23	55.2	55.2

Table 14. Results of bench-scale tests conducted on an intermediate product (Sample #2) from the Shawville Power Plant.

Test No.	Size Fraction Mesh	% Ash			% Yield	% Recovery
		Feed	Clean	Reject		
1	28 x 0	34.15	23.37	44.94	50.1	58.3
2	35 x 100	35.59	23.03	44.1	40.4	48.2

Table 15. Results of bench-scale tests conducted on an intermediate product (Sample #3) from the Shawville Power Plant.

Test No.	Size Fraction Mesh	% Ash			% Yield	% Recovery
		Feed	Clean	Reject		
1	28 x 0	25.2	13.3	38.3	52.4	60.7
2	35 x 100	26.7	10.1	40.04	44.5	54.6

The bench-scale data for tests conducted using Samples #2 and #3 are summarized in Tables 14 and 15. The data obtained with these samples also indicated that higher recoveries could be obtained using the "by-zero" samples (28 mesh x 0). In addition, the recovery values were generally consistent with those obtained using Sample #1. However, the ash contents of the products obtained for the by-zero fractions of Samples #2 and #3 were slightly higher than those obtained using the 35 x 100 mesh fraction.

6.2.12 Comparison of Charging Systems

Two additional series of bench-scale tests were carried out to compare the effectiveness of the pneumatic charging and the turbo-charging systems. In order to compare the two

chargers, tests were carried out using Sample #1 from the Shawville Raymond mill. Four different circuit configurations were evaluated in the test program, i.e.:

1. The TES unit fed directly with no charger.
2. The feed passing through the pneumatic charger only.
3. The feed passing through the rotary charger only.
4. The feed passing through both the pneumatic charger and rotary charger.

Figure 84 shows simplified schematics of the four different charger configuration evaluated in this study. The dashed lines in the figure represent streams that were transferred manually (by hand) during each test run.

The results of the charger comparison tests are summarized in Table 16. The data indicate that there is virtually no separation when no charger was employed. The average separation efficiency obtained with the pneumatic charger was slightly higher than that obtained with the rotary charger (20.1% versus 14.8%). It is also worth noting that the pneumatic charger provided a high recovery (65%) and poor clean coal ash (25.4%), while the rotary charger provided a low recovery (23%) and good clean coal ash (13.7%). Although the best separation efficiency (27%) was obtained by combining both the pneumatic and rotary chargers in series, this two-stage configuration produced too low of a recovery (49%) and reject ash (43%) to be commercially viable.

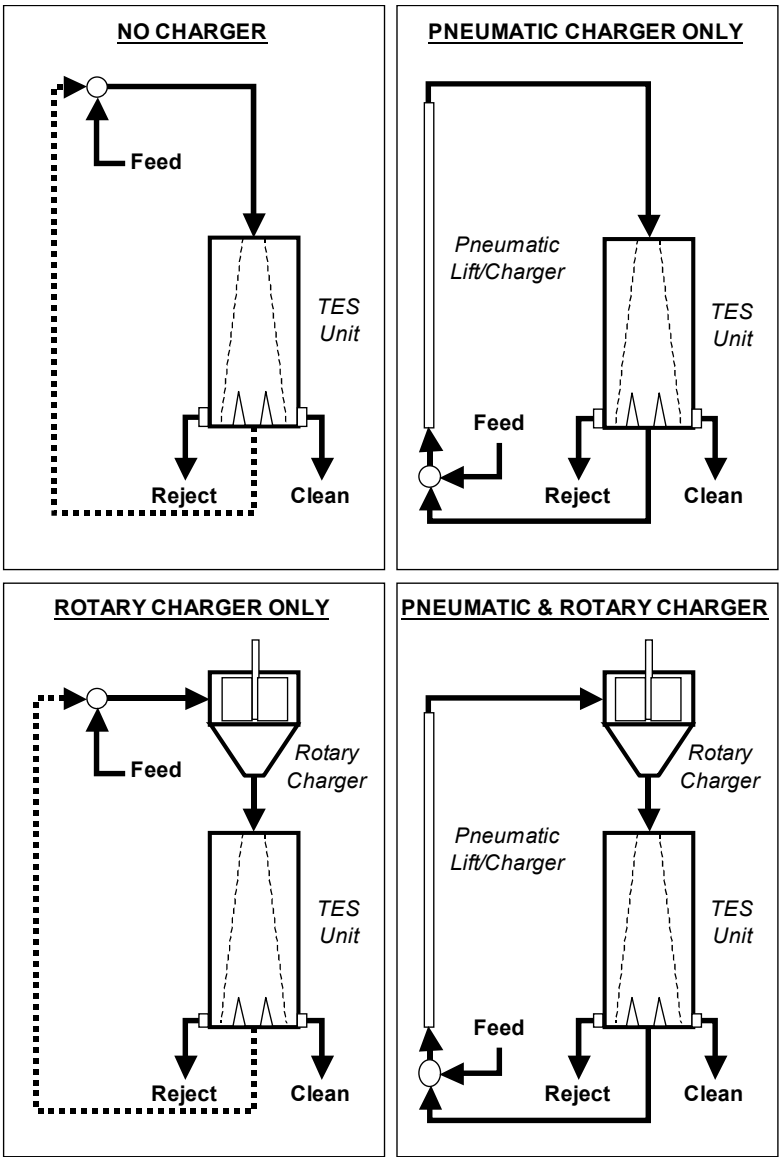

Figure 84 Schematics representation of the four different charger configuration for separator performance study.

Table 16. Effect of charger configuration on the performance of the bench-scale separator (Sample #1, 28 mesh x 0).

No Charger

Test Run	Ash Content (%)			Yield (%)	Combustible Recovery (%)	Efficiency (%)
	Feed	Clean	Reject			
1	31.23	16.92	31.72	3.3	4.0	2.2
2	31.11	16.76	30.60	---	---	---
Mean	31.17	16.84	31.16	---	---	---

Pneumatic Charger Only

Test Run	Ash Content (%)			Yield (%)	Combustible Recovery (%)	Efficiency (%)
	Feed	Clean	Reject			
1	33.05	25.49	43.38	57.7	64.3	19.7
2	33.02	25.20	43.87	58.1	64.9	20.5
Mean	33.04	25.35	43.63	57.9	64.6	20.1

Rotary Charger Only

Test Run	Ash Content (%)			Yield (%)	Combustible Recovery (%)	Efficiency (%)
	Feed	Clean	Reject			
1	30.90	13.65	35.00	19.2	24.0	15.5
2	30.90	13.79	34.52	17.5	21.8	14.0
Mean	30.90	13.72	34.76	18.3	22.9	14.8

Both Pneumatic & Rotary Charger

Test Run	Ash Content (%)			Yield (%)	Combustible Recovery (%)	Efficiency (%)
	Feed	Clean	Reject			
1	33.02	17.83	42.83	39.2	48.1	27.0
2	33.02	18.55	43.21	41.3	50.2	27.0
Mean	33.02	18.19	43.02	40.3	49.2	27.0

6.2.13 Effect of Electrode Shielding

It was noted that the strength of the electrostatic field was constrained by the onset of arcing between the surfaces of the oppositely charged electrodes. To prevent this problem, a series of bench-scale tests were carried out using screen electrodes that were "shielded" by

covering the screen wires with a plastic spray-on coating. Two series of tests were carried out, the first using the rotary charger only and the second using both the pneumatic and rotary chargers in series.

Table 17 shows the results obtained with the shielded and unshielded electrodes. In all cases, the shielded electrodes provided a superior level of performance when compared to the unshielded electrodes. For the tests conducted with the rotary charger only, the shielded electrodes increased the average recovery from 22.9% to 34.3% with essentially no change in the clean coal ash content (13.7% versus 13.6%). Likewise, the shielded electrodes improved the average recovery for the tests conducted with the two chargers in series from 49.2% to 62.7%.

In fact, the shielded electrode test increased the reject ash content by approximately 3%, clean coal yield by 9-12%, combustible recovery by 11-13%, and separation efficiency by 5-8%. Since the electrode potential was held constant in all tests, the improved level of performance obtained with the coated electrodes is believed to be due to prevention of accidental charge reversal. The charge reversal occurs when selectively charged particles collide with uncoated electrodes fabricated from copper or steel wires. The plastic shielding insulates the electrodes and prevents the particles from making contact with the conducting surfaces, thereby preventing charge reversal. Therefore, the coated electrodes (i) allow higher field strengths to be tested without of risk of arcing and (ii) minimize the likelihood of charge reversal caused by particles colliding with the uncoated electrode conductors.

Table 17. Effect of electrode shielding (plastic coating) on the performance of the bench-scale separator (Sample #1, 28 mesh x 0).

Rotary Charger – No Shielding

Test Run	Ash Content (%)			Yield (%)	Combustible Recovery (%)	Efficiency (%)
	Feed	Clean	Reject			
1	30.90	13.65	35.00	19.2	24.0	15.5
2	30.90	13.79	34.52	17.5	21.8	14.0
Mean	30.90	13.72	34.76	18.3	22.9	14.8

Rotary Charger – With Shielding

Test Run	Ash Content (%)			Yield (%)	Combustible Recovery (%)	Efficiency (%)
	Feed	Clean	Reject			
1	31.05	13.85	37.83	28.3	35.3	22.7
2	31.30	13.38	37.71	26.3	33.2	22.0
Mean	31.18	13.62	37.77	27.3	34.3	22.3

Pneumatic & Rotary Charger – No Shielding

Test Run	Ash Content (%)			Yield (%)	Combustible Recovery (%)	Efficiency (%)
	Feed	Clean	Reject			
1	33.02	17.83	42.83	39.2	48.1	27.0
2	33.02	18.55	43.21	41.3	50.2	27.0
Mean	33.02	18.19	43.02	40.3	49.2	27.0

Pneumatic & Rotary Charger – With Shielding

Test Run	Ash Content (%)			Yield (%)	Combustible Recovery (%)	Efficiency (%)
	Feed	Clean	Reject			
1	31.23	18.00	45.73	52.3	62.3	32.2
2	31.57	18.09	46.57	52.7	63.0	32.9
Mean	31.40	18.05	46.15	52.5	62.7	32.5

Figure 85 provides a graphical summary of the test results obtained with the different charging and electrode systems. As shown, the shielded electrodes (designated by an asterisk) gave a superior recovery-ash curve to that obtained using the uncoated electrodes. It is also obvious from this plot that the pneumatic charger gives a high recovery/low ash product, while the rotary charger gives a low recovery/high ash product. The data point obtained by combining the two chargers in series represents a compromise between these two operating extremes.

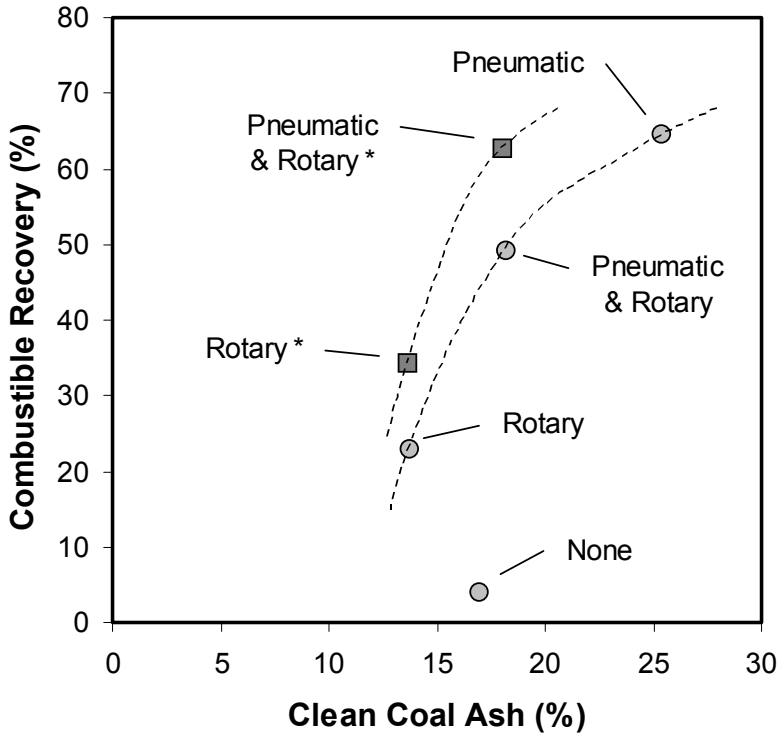

Figure 85 Summary of test results obtained using different charging systems (pneumatic and rotary) and electrode configurations (shielded and unshielded). An asterisk is used to designate tests with the shielded electrodes.

6.2.14 Supplementary Testing

A series of bench-scale tests were carried out on intermediate samples to establish the optimum particle size of the feed material. The mesh size fractions used in the testing were 14 x 0,

20 x 0, 28 x 0, 35 x 0 and 48 x 0. The results are shown in Table 18. The conclusion reached was that the 35 x 0 size fraction gave the best overall results at a reasonable clean coal ash.

A new charger was installed in the POC unit. It consisted of two sets of driven paddles set in series and mounted in a rectangular box, as shown in Figure 86. The samples tested were Shawville intermediate products from the No 1 and No 2 sampling ports of the 633 Raymond Mill as shown in Figure 82. The results are shown in Appendix E, Table E1. The results were not encouraging and a second stage charger of the same design was added. The results of the POC tests using the second stage charger are shown in Appendix E, Table E2 and it can be seen that there was still no significant improvement.

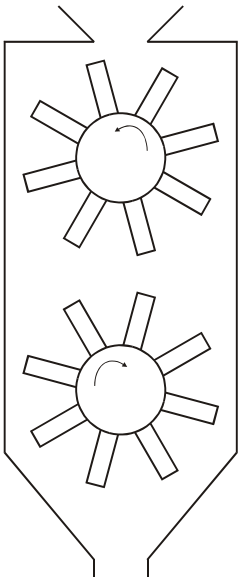

Figure 86 POC-scale turbocharger used in conjunction with the POC-scale TES unit.

A series of tests were carried out to confirm the superiority of coated (shielded) screen electrodes over regular (metal) screen electrodes. Tests were carried out on the 35 x 0, 35 x 70 and 70 x 0 size fractions from sample Port # 1 and the results are shown in Table 19. The coated electrodes were considered to give superior performance due to the ability to produce a superior clean coal ash, although the regular screen electrodes showed higher combustible recoveries and

separation efficiencies. The test results on sample port # 2 material as shown in Table 20 demonstrated that regular screen electrodes are marginally better than the coated electrodes.

Although samples are routinely heated prior to testing, it was decided to apply a heating tape at the feed pipe to the charger. The results for sample port #1 and 2 are shown in Table 21

Comparative data for unheated feed is shown in Tables 19 and 20. The heated samples show a small increase in separation performance on the 35 x 0 size fraction. It was decided therefore to continue using the heating system.

A series of tests were carried out to establish the optimum electrode distance from the centerline. All previous testing has been carried out where the electrodes were 3 cm equidistant from the centerline. Two series of tests were performed where the positive electrode and the negative electrode were moved to 1cm of the centerline. The results are shown in Table 22 and 23 respectively. When the positive electrode (coal side) was moved to 1 cm of the centerline there was a slight deterioration in the separation as shown in Table 22. At the reverse setting with the negative electrode (reject side) set at 1cm, there was a deterioration in the quality of the clean coal product on the 35 x 0 fraction from sample port #1 and some improvement in the separation of the 70 x 0 fraction from sample port # 2 as shown in Table 23. The general conclusion was that there was no benefit in moving the electrodes closer to the centerline.

Table 18. Results of bench-scale tests conducted on sized intermediate products from Shawville power plant (633 Raymond Mill, Sample Ports # 1 & 2).

Sampling Point	Electrode Position		Size	% Ash			% Wt Yield	% Comb.	Separation
	Reject	Coal	(Mesh)	Feed	Clean	Reject		Recovery	Efficiency
# 1 Sampling			14 x 0	40.95	34.21	42.08	14.36	16.0	14.75
Port	3cm	3cm		39.89	33.91	42.85	33.11	36.4	35.57
# 2 Sampling	3cm	3cm	14 x 0	27.84	13.93	34.71	33.06	39.4	41.22
Port				28.21	19.91	34.95	44.81	50.0	55.52
# 1 Sampling	3cm	3cm	20 x 0	36.06	33.51	39.14	54.71	56.9	59.38
Port				35.74	34.04	39.37	68.11	69.9	75.02
# 2 Sampling	3cm	3cm	20 x 0	25.91	20.12	35.03	61.17	65.9	82.70
Port				25.61	20.52	35.27	65.49	70.0	90.19
# 1 Sampling	3cm	3cm	28 x 0	34.44	31.52	35.41	24.94	26.0	25.64
Port				34.02	31.52	35.41	35.73	37.1	37.19
# 2 Sampling	3cm	3cm	28 x 0	25.91	19.51	32.11	49.21	53.5	60.98
Port				25.65	20.03	32.85	56.16	60.4	71.93
# 1 Sampling	3cm	3cm	35 x 0	29.67	24.01	34.01	43.40	46.9	49.75
Port				29.67	26.95	36.74	72.22	75.0	89.42
# 2 Sampling	3cm	3cm	35 x 0	24.12	14.61	33.23	48.93	55.1	67.40
Port				24.12	14.73	33.15	49.02	55.1	67.38
# 1 Sampling	3cm	3cm	48 x 0	22.97	12.93	28.98	37.45	42.3	47.24
Port				22.97	14.34	29.55	43.26	48.1	55.65
# 2 Sampling	3cm	3cm	48 x 0	20.79	9.28	29.97	44.37	50.8	63.96
Port				20.79	11.65	29.56	48.97	54.6	69.62

Table 19. Results of bench-scale tests conducted on sized intermediate products from Shawville power plant (633 Raymond Mill (Sample Port # 1), comparison of regular and shielded screens.

Screen	Electrode Position		Size	% Ash			% Wt Yield	% Comb.	Separation
Type	Reject	Coal	(Mesh)	Feed	Clean	Reject		Recovery	Efficiency
Regular	3cm	3cm	35 x 0	37	27	51	58.33	67.6	80.41
				37	22	49	44.44	55.0	58.86
			35 x70	45	36	57	57.14	66.5	72.38
				45	33	55	45.45	55.4	55.56
			70 x 0	34	20	48	50.00	60.6	70.59
				34	20	47	48.15	58.4	66.56
Coated (Shielded)	3cm	3cm	35 x 0	37	17	49	37.50	49.4	49.66
				37	18	50	40.63	52.9	54.90
			35 x70	45	22	56	32.35	45.9	40.26
				45	26	55	34.48	46.4	42.15
			70 x 0	34	18	45	40.74	50.6	53.92
				34	18	46	42.86	53.2	57.98

Table 20. Results of bench-scale tests conducted on sized intermediate products from Shawville power plant, 633 Raymond Mill (Sample Port # 2), comparison of regular and shielded screens.

Screen Type	Electrode Position		Size (Mesh)	% Ash			% Wt Yield	% Comb. Recovery	Separation Efficiency
	Reject	Coal		Feed	Clean	Reject			
Regular	3cm	3cm	35 x 0	29	14	40	42.31	51.2	58.36
				29	14	40	42.31	51.2	58.36
			35 x70	35	20	44	37.50	46.2	47.14
				35	23	43	40.00	47.4	49.14
			70 x 0	26	12	37	44.00	52.3	62.62
				26	14	37	47.83	55.6	68.06
Coated (Shielded)	3cm	3cm	35 x 0	29	13	38	36.00	44.1	47.17
				29	13	39	38.46	47.1	51.72
			35 x70	35	14	44	30.00	39.7	37.71
				35	16	43	29.63	38.3	36.40
			70 x 0	26	13	36	43.48	51.1	60.20
				26	14	36	45.45	52.8	62.94

Table 21. Results of bench-scale tests conducted on sized intermediate products from Shawville power plant, 633 Raymond Mill (Sample Ports # 1 & 2), feed continuously heated with heating tape.

Operating Parameters	Electrode Position		Size (Mesh)	% Ash			% Wt Yield	% Comb. Recovery	Separation Efficiency
	Reject	Coal		Feed	Clean	Reject			
Sample Port # 1	3cm	3cm	35 x 0	37	16.86	50.56	40.24	53.10	54.98
				37	19.19	51.79	45.37	58.19	63.50
Coated Screen									
			35 x70	45	21.89	55.2	30.60	43.46	37.53
Heated Feed				45	21.4	55.67	31.14	44.49	38.52
			70 x 0	34	16.64	45.86	40.59	51.26	54.75
				34	18.58	46.67	45.11	55.64	61.91
			35 x 0	29	11.96	41.73	42.76	53.02	61.53
Sample Port # 2	3cm	3cm		29	13.69	39.2	39.98	48.61	54.05
Coated Screen			70 x 0	26	12.77	36.87	45.10	53.17	63.96
				26	13.72	36.92	47.07	54.88	66.84
Heated Feed									

.

In order to improve the separation the reject was reprocessed as a second stage and the two clean coal products combined. The 35 x 0 size fraction was tested in this manner and the results are shown in Table 24. As expected there is significant improvement in yield, recovery and separation efficiency. However the reject ash remains low and the cost implications of a two-stage separation may not prove economical. A further two-stage test was carried out with both electrodes set at 1 cm from the centerline. The results as shown in Table 25, indicate that the clean coal product contained too high an ash level to be acceptable.

Table 22. Results of bench-scale tests conducted on sized intermediate products from Shawville power plant, 633 Raymond Mill (Sample Ports # 1 & 2), feed continuously heated with heating tape. Electrode position adjusted.

Operating Parameters	Electrode Position		Size (Mesh)	% Ash			% Wt Yield	% Comb. Recovery	Separation Efficiency
	Reject	Coal		Feed	Clean	Reject			
Sample Port # 1	3cm	1cm	35 x 0	37	17.66	51.18	42.30	55.3	58.52
				37	17.63	50.26	40.64	53.1	55.20
Coated Screen									
			70 x 0	34	15.79	44.99	37.64	48.0	49.80
Heated Feed				34	15.65	44.99	37.46	47.9	49.56
			35 x 0	29	13.35	40.8	42.99	52.5	60.48
Sample Port # 2	3cm	1cm		29	13.45	40.31	42.11	51.3	58.53
Coated Screen			70 x 0	26	12.46	35.48	41.18	48.7	56.20
Heated Feed				26	12.41	35.9	42.15	49.9	58.19

Table 23. Results of bench-scale tests conducted on sized intermediate products from Shawville power plant, 633 Raymond Mill (Sample Ports # 1 & 2), feed continuously heated with heating tape. Electrode position adjusted.

Operating Parameters	Electrode Position		Size (Mesh)	% Ash			% Wt Yield	% Comb. Recovery	Separation Efficiency
	Reject	Coal		Feed	Clean	Reject			
Sample Port # 1	1 cm	3 cm	35 x 0	37	21.71	50.9	47.62	59.2	65.51
				37	20.53	50.95	45.86	57.8	63.15
Coated Screen									
			70 x 0	34	16.08	46.45	40.99	52.1	56.01
Heated Feed				34	15.57	46.33	40.08	51.3	54.62
			35 x 0	29	15.29	41.53	47.75	57.0	68.38
Sample Port # 2	1 cm	3 cm		29	16.07	41.8	49.75	58.8	71.70
Coated Screen			70 x 0	26	13.01	36.79	45.37	53.3	64.20
Heated Feed				26	13.13	36.98	46.04	54.0	65.48

Table 24. Results of bench-scale tests conducted on sized intermediate products from Shawville power plant, 633 Raymond Mill (Sample Ports # 1 & 2), feed continuously heated with heating tape. 2-Stage separation-reject scavenging.

Operating Parameters	Electrode Position		Size (Mesh)	% Ash			% Wt Yield	% Comb. Recovery	Separation Efficiency
	Reject	Coal		Feed	Clean	Reject			
			35 x 0						
Sample Port # 1	3 cm	3 cm	Stage 1	36.54	17.25	50.83	42.56	55.5	59.20
			Stage2	50.83	29.01	56.12	19.51	28.2	21.54
Heated Feed			Combined	36.54	19.70	56.12	53.8	68.0	82.57
Coated Screen			Stage 1	36.54	17.31	51.12	43.12	56.2	60.33
			Stage2	51.12	28.18	53.79	10.43	15.3	10.97
			Combined	36.54	18.62	53.79	49.1	62.9	72.21
			35 x 0						
Sample Port # 2	3 cm	3 cm	Stage 1	33.75	15.76	45.26	39.02	49.6	52.32
			Stage2	45.26	19.76	50.31	16.53	24.2	18.37
Heated Feed			Combined	33.75	16.58	50.31	49.1	61.8	73.19
			Stage 1	33.75	15.74	45.23	38.93	49.5	52.17
			Stage2	45.23	19.71	50.26	16.46	24.1	18.30
			Combined	33.75	16.55	50.26	49.0	61.7	72.95

Table 25. Results of bench-scale tests conducted on sized intermediate products from Shawville power plant, 633 Raymond Mill (Sample Ports # 1 & 2), feed continuously heated with heating tape. 2-Stage separation-reject scavenging.

Operating Parameters	Electrode Position		Size (Mesh)	% Ash			% Wt Yield	% Comb. Recovery	Separation Efficiency
	Reject	Coal		Feed	Clean	Reject			
Sample Port # 1			35 x 0						
	1 cm	1 cm	Stage 1	36.54	22.58	48.03	45.15	55.1	59.34
Coated Screen			Stage2	48.03	35.22	52.96	27.79	34.6	30.64
Heated Feed			Combined	36.54	25.77	52.96	60.4	70.6	87.53
Sample Port # 2									
	1 cm	1 cm	Stage 1	36.54	24.01	47.8	47.33	56.7	61.92
Coated Screen			Stage2	47.8	33.74	54.09	30.91	39.2	34.98
Heated Feed			Combined	36.54	26.50	54.09	63.6	73.7	94.16

6.3 Conclusions – POC TES Unit Test Program

Four different feed samples were used for the POC TES unit test program. These feed samples include: (i) Glen Lyn Raymond Mill Rejects (feed ash ≈ 42-45%), (ii) Moss 3 Raw Coal, (iii) Possum Point Raymond Mill Rejects (iv) Shawville Raymond Mill Intermediate Products.

A series of tests were conducted to determine the influence of electrode position on combustible recovery and product ash content. The test results obtained from this series of tests were similar to the results obtained from the drum-type bench-scale TES unit under bias-feeding conditions. It was concluded that biasing the feeding point or relative electrode position does not make a significant difference in separation efficiency.

Relative humidity plays an important role in the particle charging process and triboelectrostatic separation. Combustible recovery and ash rejection remain relatively constant when the relative humidity is held below about 50%. On the other hand, the combustible recovery begins to deteriorate as the relative humidity is increased to 60%. A further increase in relative humidity to 70% causes a sharp decrease in recovery with little change in the ash content of the clean coal product.

Initial test results showed that better separations could be made with the bench-scale unit than with the POC-scale unit under identical test conditions. By a process of elimination, it was concluded that the vertical recycle conveyor was grinding the feed material via attrition. This resulted in dust coatings on both the coal and refuse particles that would not accept a differential charge at the turbocharger. In addition, the particle charging procedures used in the bench-scale TES unit is different from that of POC-scale TES unit. Therefore, 1) the recycle screw conveyor was replaced with bucket elevator, 2) turbo-charger was modified to install blades in two layers

for the POC unit, and 3) screen electrode was installed to replace the original cylindrical electrodes.

A series of tests were conducted on the POC unit to evaluate the relative position of electrode and splitter settings. The results show that as the amount of the recycled material decreased, the ash content was decreased, as some of the middlings reported to the clean coal product. However, the changes in recovery due to recycling were minimal. The results also suggest that there is no need to recycle the middlings stream for the sample tested in this series. This finding may indicate that the separation is as good as it can be in the first pass. The results also showed that the minus-35mesh particles gave a higher recovery than the minus 28 mesh particles. A possible explanation may be that the coarse particles may fall too fast to be attracted by the electrodes.

The effect of applied potential showed that coal recovery decreased with increasing electrode potential difference, which seemed surprising. A possible explanation could have been that the charge of the coal particles was substantially higher than that of the ash-forming minerals. At low potentials, highly charged coal particles could have been recovered in preference to the weakly charged ash-forming minerals, resulting in high recoveries. As the potential difference was increased, weakly charged ash particles and some of the middlings were then pulled toward the cathode, causing a decrease in recovery. Decreasing ash content observed with decreasing recovery can be attributed to the loss of middlings to the cathode.

Test results suggest that proper design of the charger is important for improving the combustible recovery and separation efficiency. Combustible recovery increased with increasing impeller speed, which suggests that the coal recovery increased with increasing charge of the coal particles.

Test results showed that the shielded electrodes, i.e., coated electrode surface or laminated electrode, provided a superior level of performance when compared to the unshielded electrodes. For the tests conducted with the rotary charger only, the shielded electrode test increased the reject ash content by approximately 3%, clean coal yield by 9-12%, recovery by 11-13%, and separation efficiency by 5-8%. The improved level of performance obtained with the coated electrodes is believed to be due to prevention of accidental charge reversal. The charge reversal occurs when selectively charged particles collide with uncoated electrodes fabricated from copper or steel wires. The plastic shielding insulates the electrodes and prevents the particles from making contact with the conducting surfaces, thereby preventing charge reversal. Therefore, the coated electrodes (i) allow higher field strengths to be tested without of risk of arcing and (ii) minimize the likelihood of charge reversal caused by particles colliding with the uncoated electrode conductors.

Feed samples from several mill rejects in conjunction with different particle charging procedures were employed to evaluate the separation efficiency of the POC TES unit. The test results indicate that there is virtually no separation when no charger was employed. The average separation efficiency obtained with the pneumatic charger was slightly higher than that obtained with the rotary charger. It is also worth noting that the pneumatic charger provided a high recovery and poor clean coal ash, while the rotary charger provided a low recovery and good clean coal ash. Although the best separation efficiency was obtained by combining both the pneumatic and rotary chargers in series, this two-stage configuration produced too low of a recovery (49%) and reject ash (43%) to be commercially viable.

Task 7 – Analysis/Characterization

Each of the samples collected during the project were subjected to a variety of laboratory analyses. This included a proximate analysis consisting of the determination of moisture, volatile matter, ash and fixed carbon. The determination of sulfur content was also completed for selected samples. ASTM procedures were utilized for all laboratory analyses.

In order to evaluate the overall reliability of the sampling and analysis procedures, the raw test data was analyzed using the TECHBAL material balance program. This program examines the overall circuit to determine whether the mass flow rate of each component entering and leaving each unit operation within the circuit is equivalent. If minor discrepancies are noted, the program adjusts the measured values until all of the component mass flows are externally and internally consistent (using a routine that minimizes the sum of squares of the differences between the measured and adjusted values). Little or no adjustment suggests that the data set is reliable. Because all material flows are considered in the material balance routines, the adjusted set of data is generally considered to be of higher reliability than the unadjusted data set. In the present work, test data that did not material balance well were considered to be inconsistent and/or unreliable and were eliminated from the data set.

Task 8 – Process Evaluation

Sub-Task 8.1 – Technical Evaluation

8.1.1 Objectives

The primary objective is to prepare a technical evaluation will include:

- a summary of all major experimental data, engineering analyses, computations and test results,
- a review of the scale-up procedures and the reliability of these procedures, and
- a listing of deficiencies and lessons learned.

Sub-Task 8.2 – Economic Evaluation

After completing Subtasks 3.1, 3.2, and 6.2, technical and economic evaluations were performed to establish the overall potential of the proposed TES technology for upgrading fine coal. Virginia Tech assumed the responsibility of compiling the raw test data. The technical evaluation included an overview of all major experimental data, engineering analyses, computations and test results. The economic evaluation included an estimation of total capital and operating costs for the full-scale installation of the proposed circuitry and a cost-benefit analysis that specifies the expected return on the investment. The results of the technical evaluations are discussed in previous sections of this report (i.e., Subtasks 3.1, 3.2, and 6.2). The findings of the economic evaluations are discussed in Subtask 8.2.

8.2.1 Objectives

The objective of this task was to conduct the economic analyses necessary to evaluate the economic viability of the TES process. Experimental results obtained during the testing of the

Raymond Mill reject sample were used to provide the necessary operating data for the economic analyses. The performance data and supporting economic calculations are summarized in Appendix F of this report. The analyses assume that the proposed TES circuit would be a placed into operation as a "green-field" installation. For the purpose of this study, the feed rate to the TES unit was estimated to be 4% of the feed rate to the pulverizer. The plant was assumed to operate for three 8-hour shifts per day for 360 days per year, i.e., 8640 hrs/yr. The circuit was assumed to have an on-line availability of 95% (8208 operating hrs/yr.) and a life span of 20 years.

Estimation of Capital Costs

In order to estimate the capital costs of the proposed circuits, preliminary scale-up projections were made for the TES unit. These calculations indicated that two full-scale separators with 10 ft wide electrode plates would be required to achieve the desired production rates. A specific capacity of 500 lb/hr per ft of separator width was assumed. The cost of the TES unit, including as associated instrumentation and controls, was estimated to be $105,000 each. An additional $11,500 and $22,500 were required for each of the two units to cover costs associated with the purchase of the turbocharger system and high-voltage power supply, respectively. The scale-up projections and cost estimates for the TES unit are based on a new unit design that provides a significantly higher throughput capacity than the design evaluated in the present work. The new design was not available for testing during the project test dates.

In addition to the TES separator and charger, several ancillary operations were also included in the listing of capital costs. These included a feed collection bin ($2,500), secondary pulverizer ($28,000), protection sieve ($2,000), feed transfer conveyor ($15,000), rotary feed distributor ($5,500), clean coal transfer conveyor ($12,500 each x 2), reject collection bin

($2,500), reject transfer conveyor ($12,500), flue gas blower ($2,500) for inerting, and miscellaneous instrumentation ($18,500). An additional capital outlay of $35,000 was allocated to cover costs associated with electrical services and ductwork. The total capital cost of the plant equipment was calculated to be $427,000. The total installed cost was estimated by multiplying the total equipment cost by an installation cost factor of 1.0. Local fabricators often use this rule-of-thumb estimation procedure for green-field installations. Other costs considered in the capital estimation included a 5% fee for engineering/permitting and an overhead rate of 10%.

Estimation of Operating Costs

Annual operating costs were estimated for power consumption, equipment maintenance, personnel and miscellaneous consumables (i.e., reagents, lubricants, etc.). Electrical power consumption was estimated for the TES unit and ancillary operations. The major power consumers included the secondary pulverizer (50 kW), rotary feed distributor (3 kW), clean coal transfer conveyors (7-8 kW per conveyor), turbocharger unit (42 kW), TES unit (14 kW) and flue gas blower (3 kW). For these unit operations, a power load factor of 80% was used to estimate actual power requirements, while a power factor of 15% was used for instrumentation systems. Power costs were estimated at an industrial rate of $0.04/kW-hr. Based on these values, the total power cost for the proposed circuitry was estimated to be $47,616 per year.

The plant staff was assumed to consist of a one operator ($50,000/yr) for 10% of each working shift. Personnel benefits were estimated as 50% of the base salary. Total salaries/wages were estimated to be $22,500 per year. Annual equipment maintenance costs were estimated as 10% of the total capital cost of the proposed circuitry (i.e., $42,700 per year). Consumables included lubricants ($328/yr) and replacement wear plates for the turbocharger

($13,133/year). As such, the total operating and maintenance costs were estimated to be $126,277 per year.

Cost-Benefit Analysis

The final step in the economic analysis of the TES circuit involved the completion of the cost-benefit analysis. Profitability was established on the basis of an internal rate-of-return after all costs of conducting business were covered (e.g., income taxes, cost of capital, etc.). A detailed cost-benefit analysis was conducted for each circuit over an effective life span of 20 years with an inflation rate of 3%. Tax payments were estimated using a standard 7-year depreciation period and 38% corporate tax rate. A straight-line depreciation schedule was assumed in each case. A discount rate of 10% was assumed in calculating the net present value on the capital investment.

In the cost-benefit analysis, the market value of the coal was pro-rated based on variations in the heating value. The energy premium/penalty was calculated on the basis of the base coal price times the net fractional change above or below a contract specification of 29.08 MJ/kg (12,500 Btu/lb.). This pricing structure, which accounts for variations in both ash and moisture contents, is common for steam market contracts. The assessment of the sulfur premium/penalty was based on an empirical expression established from a survey of spot-market coal prices. Although this pricing structure was somewhat arbitrary and subject to day-to-day variations, it was deemed to be reasonably adequate for the degree of accuracy needed in the present work. A coal value of $30 per ton of as-received clean coal was assumed (at 29.08 MJ/kg or 12,500 Btu/lb.). Coal transportation costs were assumed to average $20 per ton of clean coal. Savings in transportation costs associated with reductions in ash and/or moisture were passed directly to the utility as profit. The as-received moisture content of the coal product

was assumed to be constant at 7% throughout the analysis. For convenience, the coal pricing schedule was reported in terms of $/ton and $/MM Btu for three separate bases, i.e., clean coal dry, clean coal as-received and raw coal dry. As a result, the net value of the coal recovered by the TES process was calculated by subtracting the energy and sulfur premiums/penalties from the base coal price (FOB) plus transportation costs.

Table 26 shows the utility internal rate-of-return (expressed as a percentage) and payback period (expressed in years) realized by the utility. These values have been calculated as a function of the percentage of debt carried forward by the utility during the project lifespan. In the first analysis, it was assumed that no debt was carried forward (i.e., no loan was necessary to cover the capital expenditure) and all capital costs were covered from internal funds provided by the utility. In this case, an internal rate of return of 24.6% was obtained with a corresponding payback of 4.2 years. As should be expected, the internal rate of return increases as less utility funds are used to cover the capital expenses. For example, if 50% of the capital funds are borrowed, the internal rate of return increases to 42.6% (compared to 24.6% when no funds are borrowed). This value approaches infinity when 100% of the fixed capital costs are borrowed. On the other hand, the payback period increases from approximately 4.2 years when no funds are borrowed to 5.8 years by borrowing 100% of the required capital funds.

In summary, the cost-benefit analyses conducted in the present work indicate that a "green-field" installation of the TES circuit would offer a reasonably attractive rate of return (25%-75%) when compared to the alternative existing practice of discarding the pulverizer reject material. However, the payback period on the capital investment would be relatively long (i.e., 4-6 years). Furthermore, these margins would be expected to improve as additional market premiums become available for lower ash and lower sulfur coal products. The introduction of

new legislative restrictions associated with the emissions of trace elements (particularly mercury) may also provide new incentives for utilizing this technology in the future.

Table 26. Summary of the TES cost-benefit analysis

Percentage of Fixed Capital Borrowed	Internal Rate of Return (%)	Payback Period (years)
0	24.58	4.22
25	30.65	4.53
50	42.55	4.89
75	77.67	5.31
100	---	5.80

References

Agus, M., Carbini, P., Cicu, R. and Ghiani, M. 1990. Triboelectric Coal Cleaning and Desulfurization with the Turbocharger Separator. *3rd Int. Conf. Proc. And Util. Of High Sulfur Coals*. Amsterdam: Elsevier Science Publishers.

Blacktin, S.C. and Robinson, H. (1931). Safety in Mines Research Board Paper, no. 71. London. Carpenter, J.H. (1951). U.S. Patent 2,548,711.

Carta, M., Carbini, P., Ciccu, R., Del Fa, C., Ghiani, M. and Rossi, G. (1982). Beneficiation Methods for Coal Desulphurization. In A.M. Al Taweel (ed.), Proc. CIC Coal Symp. 64th (pp. 164).

Carbini, P, Carta, M., Ciccu R., Del Fa, C,. Ghiani, M. and Rossi, G. (1982). Beneficiation Methods for Coal Desulphurization. Proc. CIC Coal Symp. 64th.

Finseth D.H., Newby, T. and Elstrodt, R. (1993). Dry Electrostatic Separation of Fine Coal, 5th Int. Conf. Proc. and Util. of High Sulfur Coals. Amsterdam: Elsevier Science Publishers.

Fricke, G. (1977). The Use of Electrostatic Separation Processes in the Beneficiation of Crude Potassium Salts. Phosphorus Potassium, 90.

Fuhrmann, J. (1977/1978). Contact Electrification of Dielectric Solids. Electrostatics, 4, 109-118.

Gaudin, A.M. (1971). The Principles of Electrical Processing with Particular Application to Electrostatic Separation. Miner. Sci. Engng., 3, 46-57.

Gidapow, D., Wasan, D., Saxena, S., Gupta, R. and Mukherjee, A. (1987). Electrostatic Desulfurization of Coal in Fluidized Beds and Conveyors. AIChE Symposium (Series No. 255), 83, 74-85.

Harper, W.R. (1967). Contact and Frictional Electrification. London: Oxford University Press.

Henry, P.S.H. (1957). Br. J. Appl. Phys., 4(Suppl. 2), S6.

Inculet, I.I., Quigley, R.M., Bergougnow, M.A. and Brown, J.D. (1980). Electrostatic Beneficiation of Hat Creek Coal in the Fluidized State. The Canadian Mining & Metallurgical Bulletin, 73, 51-61.

Inculet, I.I., Bergougnow, M.A. and Brown, J.D. (1982). Electrostatic Beneficiation of Coal. In Y.A. Liu (Ed.), Physical Cleaning of Coal. New York: Marcel Dekker, Inc.

Kelly, E.G. and Spottiswood, D.J. (1989). The Theory of Electrostatic separation: A Review part II. Particle Charging. Minerals Engineering, 2(2), 193-205.

Kittaka, S., Masui, N. and Murata, Y. (1979). A Method for Measuring the Charging Tendency of Powder in Pneumatic Conveyance through Metal Pipes. J. Electrostatics, 6, 181-190.

Krupp, H. (1971). Physical Models of the Static Electrification of Solids. In Static Electrification Conference Series No. 11 (pp.1), Bristol, Great Britain Institute of Physics.

Lowell, J. (1977). The Role of Material Transfer in Contact Electrification. J. Phys. D: Appl. Phys., 10, L233-L235.

Lowell, J. and Rose-Innes, A.C. (1980). Contact Electrification. Advanced in Physics, 29(6), 947-1023.

Mazuda, S. Toragushi, M., Takahashi, T. and Haga, K. (1983). Electrostatic Beneficiation on Coal Using a Cyclone-Tribocharger. IEEE Transactions on Industry Applications, IA-19(5), 789-793.

Mazumder, M.K., Ware, R. E., Yokoyama, T. Rubin, B. and Kamp, D. (1981). Measurement of Particle size and Electrostatic Charge Distributions on Toners Using E-SPART Analyzer. IEEE Trans. Ind. Appl., 27(4), 611-619.

Montgomery, D.J. (1959). Solid State Physics, 9, 139.

Nieh, S. and Nguyen, T. (1987). Measurement and Control of Electrostatic Charges on Pulverized Coal in a Pneumatic Pipeline. Particulate Science and Technology, 5, 115-130.

Pounder, C. (1977). The Quest for a Charging Mechanism to the End of the 19th Century. J. Electrostatics, 3, 389-394.

Rich, S.R. (1986). U.S. Patent 4,627,579.

Robinson, M. (1969). In H.A. Pohl (Ed.), Dielectrophoretic and Electrophoretic Deposition. Cambridge: Electrochem Soc.

Ruckdeschel, F.R. and Hunter, L.P. (1977). J. Appl. Phys., 48, 4898.

Salanek, W.R., Paton, A. and Clark, D.T. (1976). J. Appl. Phys., 47, 144.

Seanor, D.A. (1972). In K.C. Frisch and A.V. Patsis (Eds.), Electrical Properties of Polymers. Westport, Connecticut: Technomic Publication.

Schaefer, J.L., Stencel, J.M. and Ban, H. (1994). Triboelectrostatic Dry Coal Cleaning. Proc. 11th Int. Annual Pittsburgh. Coal Conf., Pittsburgh, USA.

Shaw, P.E. (1917). Proc. R. Soc., 94, 16.

Vick, F.A. (1953). Static Electrification: Theory of Contact Electrification. In British Journal of Applied Physics: Supplement No. 2(pp. S1). London: The Institute of Physics.

List of Acronyms and Abbreviations

CCMP	Center for Coal and Minerals Processing
POC	Proof of Concept
RSM	Response Surface Methodology
Tribo	Triboelectrostatic
TES	Tribo Electrostatic Separator
FFT	Fast Fourier Transformation
VSTAT	Vertical Static Separator
AEP	American Electric Power
NETL	National Energy Technology Laboratory

Appendices

APPENDIX A – BENCH-SCALE CHARGER TEST DATA

Test conditions and experimental testing matrix for each of the operating parameters included in the parametric study of particle charging mechanism

Variables	Test Conditions		
	High (+1)	Normal (0)	Low (-1)
Air velocity (m/sec), Vg	1.90	1.15	0.40
Feed Rate (kg/min), Vf	0.40	0.25	0.10
Particle Size (μm), Dp	283.50	198.00	112.50
Ash (%)	20	13	6

	Coded Conditions				Actual Operating Conditions				Results
Run	**Vg**	**Vf**	**Dp**	**Ash**	**Vg (m/sec)**	**Vf**	**Dp (μm)**	**Ash (%)**	**Charge**
1	1	1	0	0	1.90	0.40	198.00	13	6.31E-06
2	1	0	-1	-1	1.90	0.25	112.50	6	9.45E-06
3	1	0	0	1	1.90	0.25	198.00	20	5.44E-06
4	-1	0	1	0	0.40	0.25	283.50	13	7.01E-07
5	0	1	0	1	1.15	0.40	198.00	20	7.70E-07
6	0	0	1	1	1.15	0.25	283.50	20	1.86E-06
7	-1	0	0	1	0.40	0.25	198.00	20	3.65E-07
8	0	0	-1	1	1.15	0.25	112.50	20	2.94E-06
9	0	1	0	-1	1.15	0.40	198.00	6	2.41E-06
10	0	0	1	-1	1.15	0.25	283.50	6	6.46E-07
11	0	1	1	0	1.15	0.40	283.50	13	1.11E-06
12	0	0	0	0	1.15	0.25	198.00	13	3.45E-06
13	-1	-1	0	0	0.40	0.10	198.00	13	8.16E-07
14	0	-1	0	-1	1.15	0.10	198.00	6	4.80E-06
15	1	-1	0	-1	1.90	0.10	198.00	6	1.28E-05
16	-1	0	-1	0	0.40	0.25	112.50	13	1.88E-07
17	-1	1	0	0	0.40	0.40	198.00	13	1.71E-07
18	0	0	0	0	1.15	0.25	198.00	13	3.63E-06
19	1	0	1	0	1.90	0.25	283.50	13	1.05E-06
20	0	-1	-1	0	1.15	0.10	112.50	13	2.97E-06
21	-1	-1	0	1	0.40	0.10	198.00	20	6.55E-07
22	0	0	-1	0	1.15	0.25	112.50	13	1.64E-06
23	0	0	0	0	1.15	0.25	198.00	13	3.30E-06
24	-1	0	0	-1	0.40	0.25	198.00	6	3.73E-07
25	1	-1	0	0	1.90	0.10	198.00	13	8.02E-06
26	1	0	-1	0	1.90	0.25	112.50	13	5.37E-06
27	0	-1	1	0	1.15	0.10	283.50	13	1.09E-06

APPENDIX B – BENCH-SCALE SEPARATOR TESTS

Work functions for a variety of different materials used to construct tribochargers for the particle charging mechanism study

Materials	Work Functions (eV)
Chromium	4.50[a]
Copper	4.65[a]
Stainless Steel	4.69[c]
Copper-Nickel Alloy	4.70[b]
Polyvinylchloride (PVC)	5.13[d]
Nickel	5.22[a]
Aluminum	5.42[c]
Polytetrafluoroethylene (Teflon)	5.75[d]

(a) from H.B.Michaelson, in *CRC Handbook of Chemistry and Physics*, CRC press, Boca Raton, (1995-6).
(b) from I.I.Inculet, Electrostatic Mineral Separation, Wiley, New York, (1984).
(c) from R.Gupta et al., Powder Tech., 75 (1993) 79-87.
(d) from D.A.Seanor, in *Electrical Properties of Polymers*, K.Frisch and A.Patsis (eds.), (1972) 37-58.

APPENDIX C – MULTI-STAGE SEPARATION FLOWSHEET

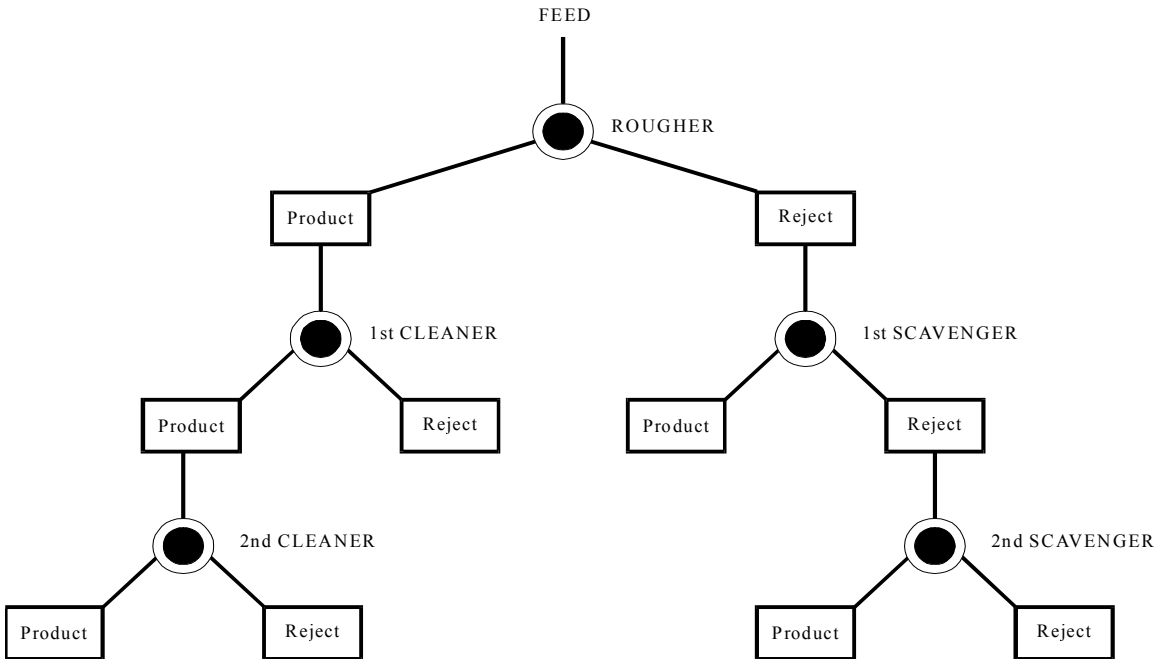

APPENDIX D: POC FLOWSHEETS AND MASS BALANCES

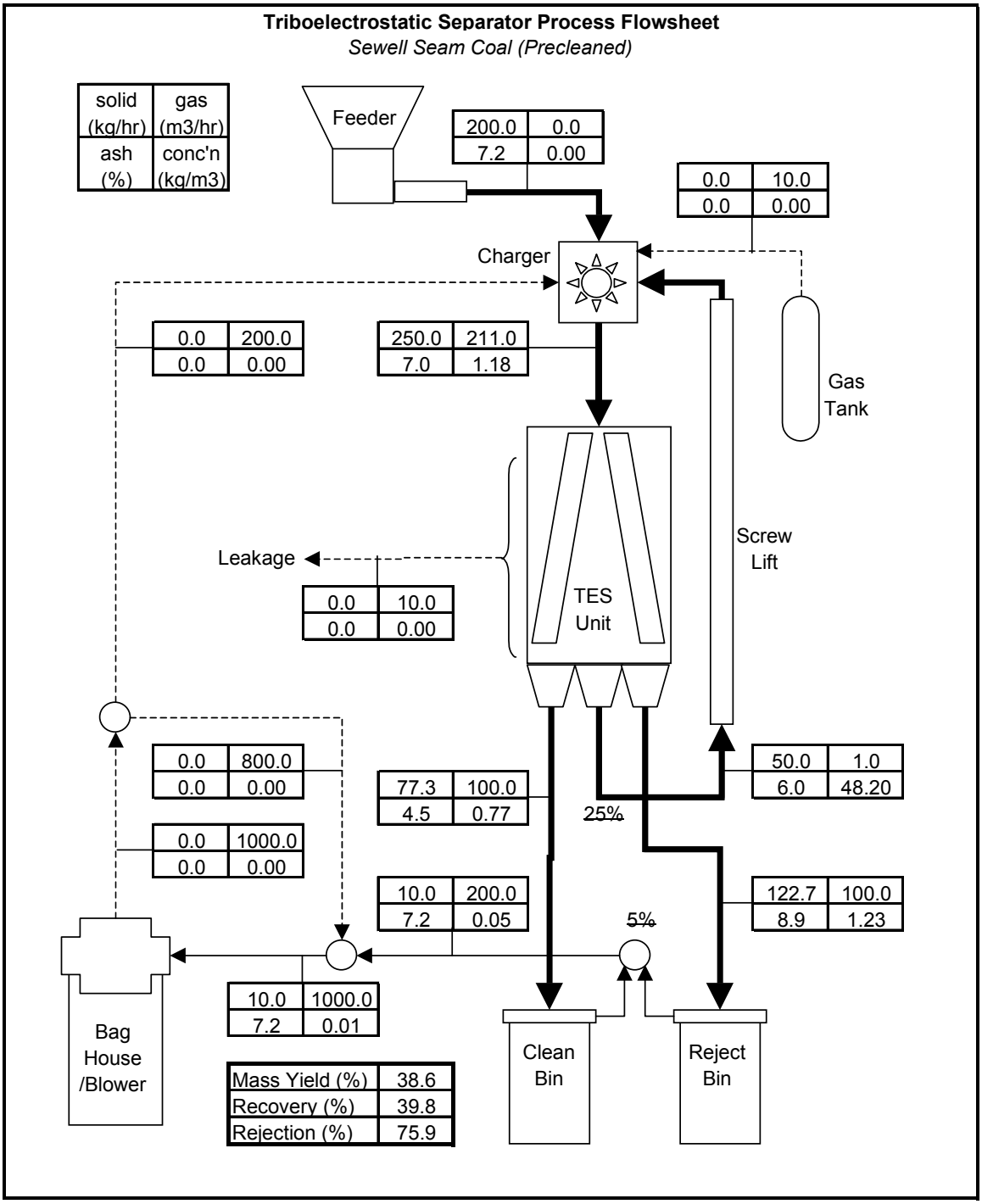

Figure D1. POC flowsheet and mass balance for the precleaned Sewell Seam coal (metric units).

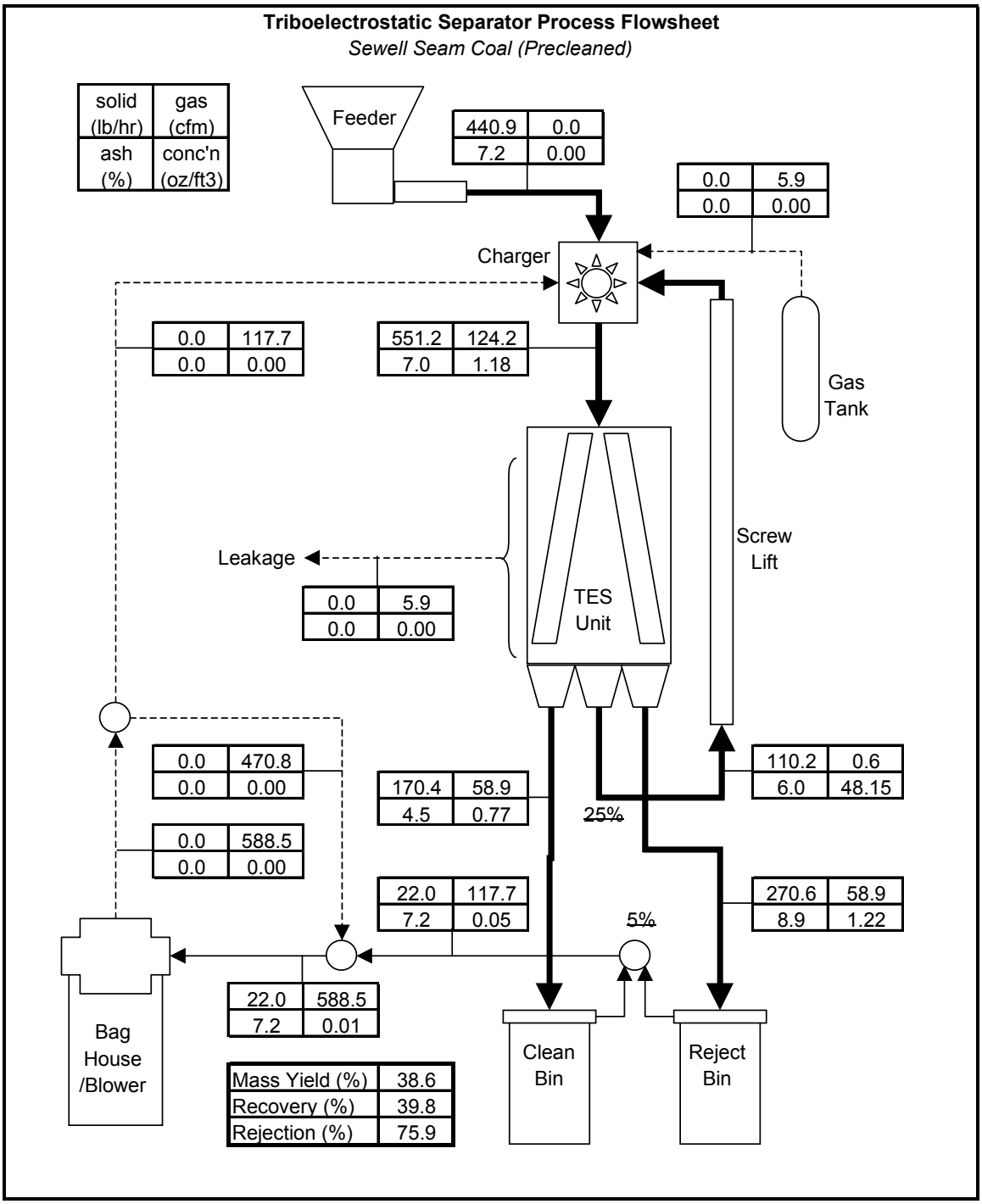

Figure D2. POC flowsheet and mass balance for the precleaned Sewell coal (English units).

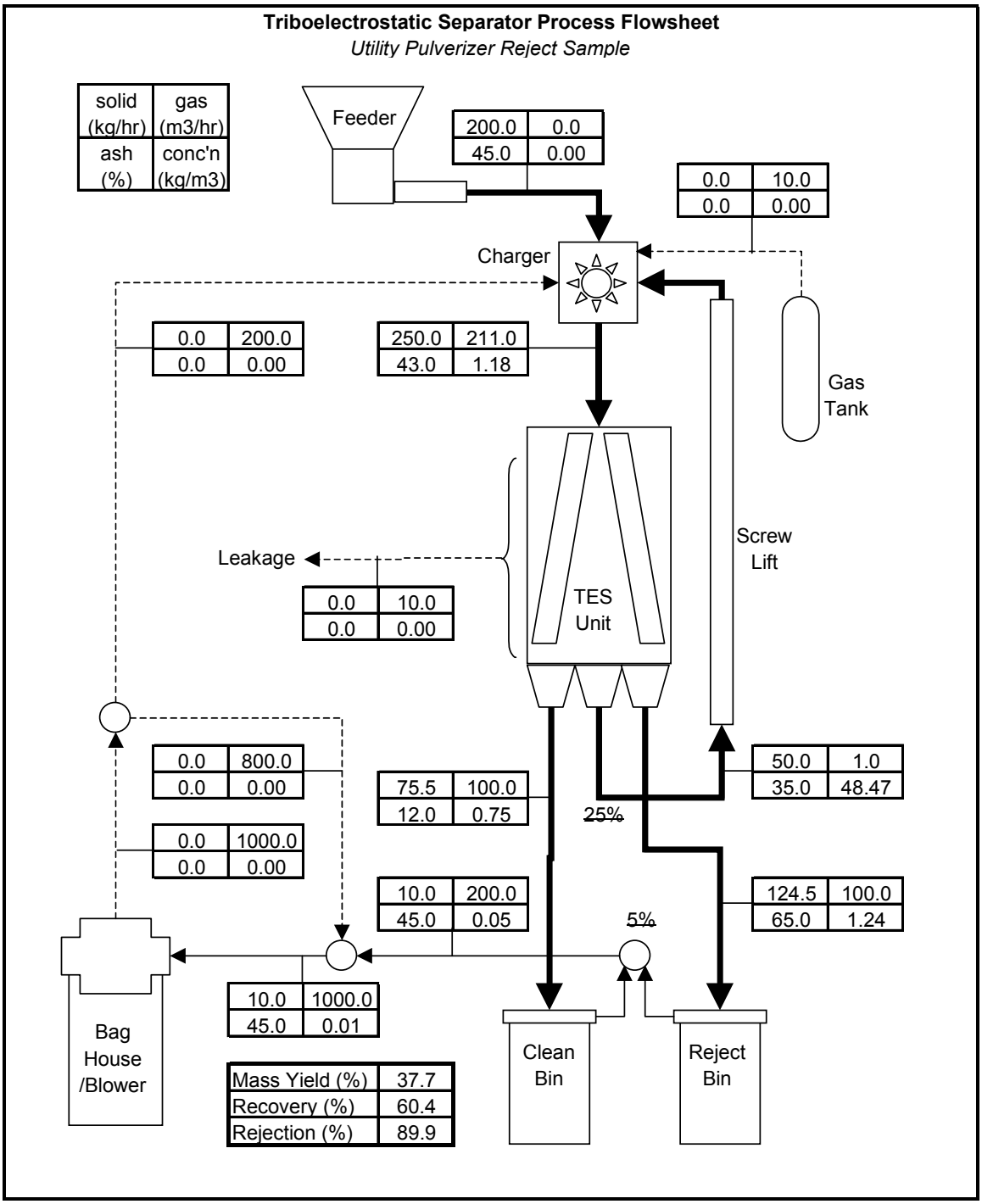

Figure D3. POC flowsheet and mass balance for the utility pulverizer sample (metric units).

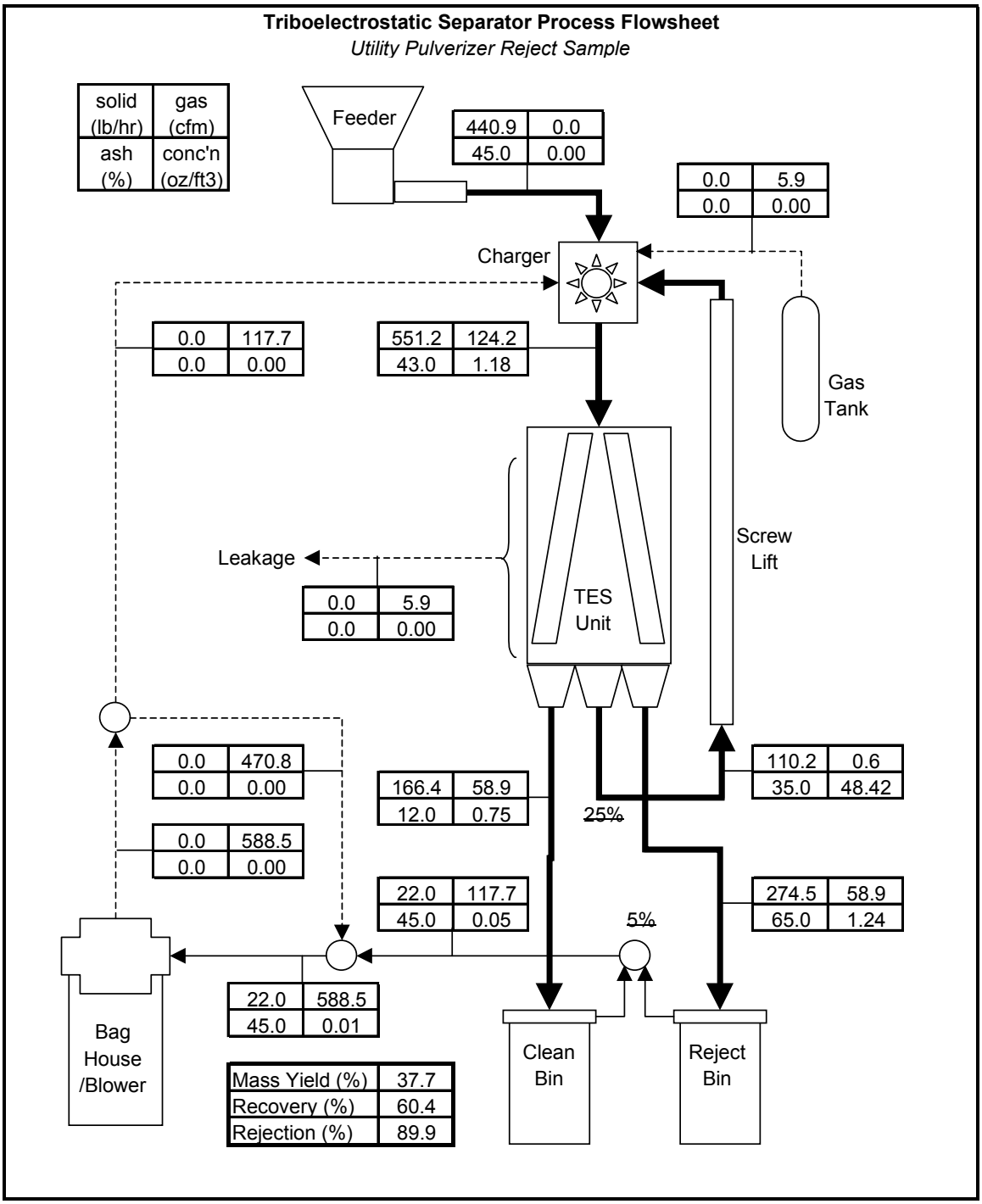

Figure D4. POC flowsheet and mass balance for the utility pulverizer sample (English units).

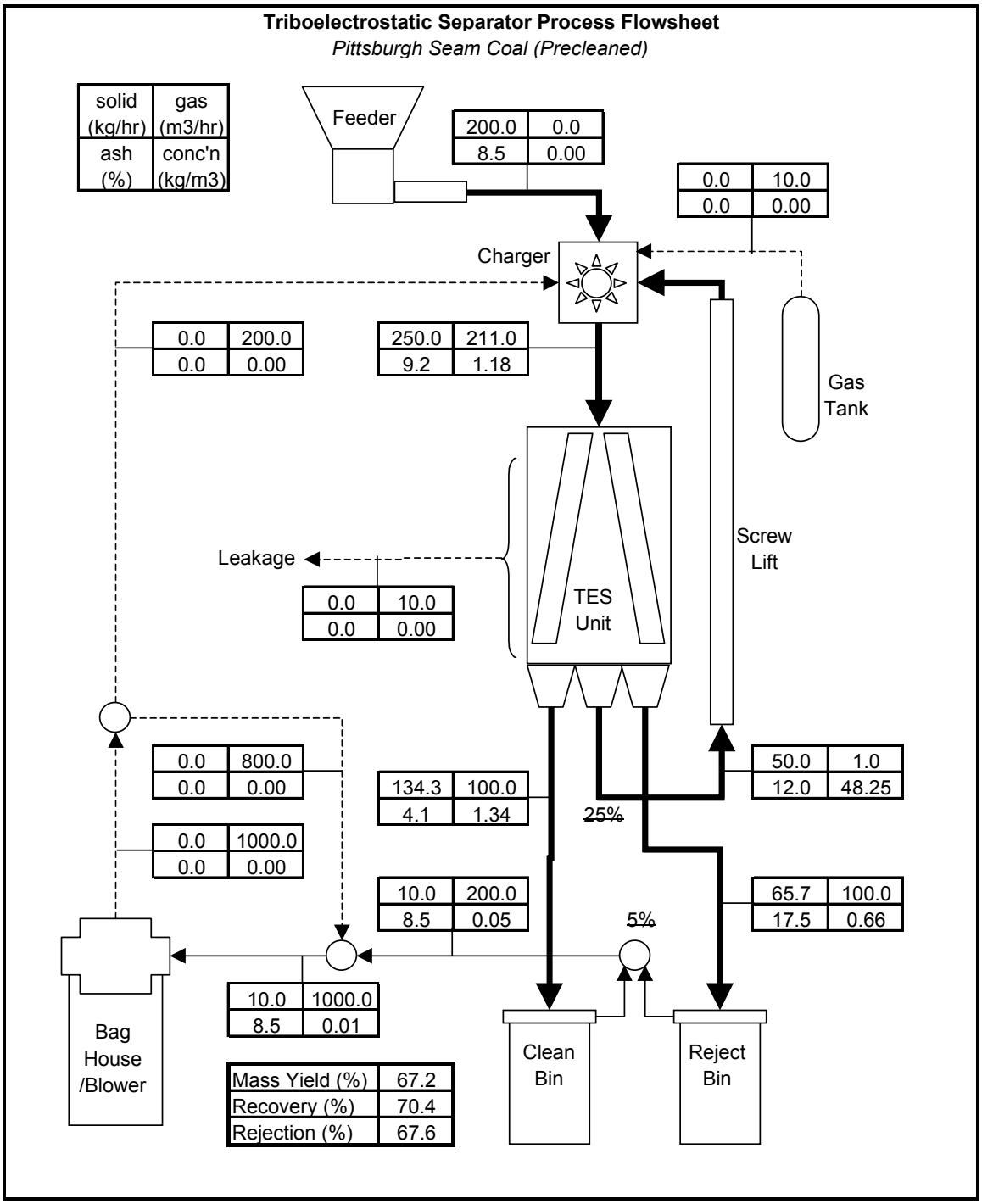

Figure D5. POC flowsheet and mass balance for the Pittsburgh No. 8 coal (metric units).

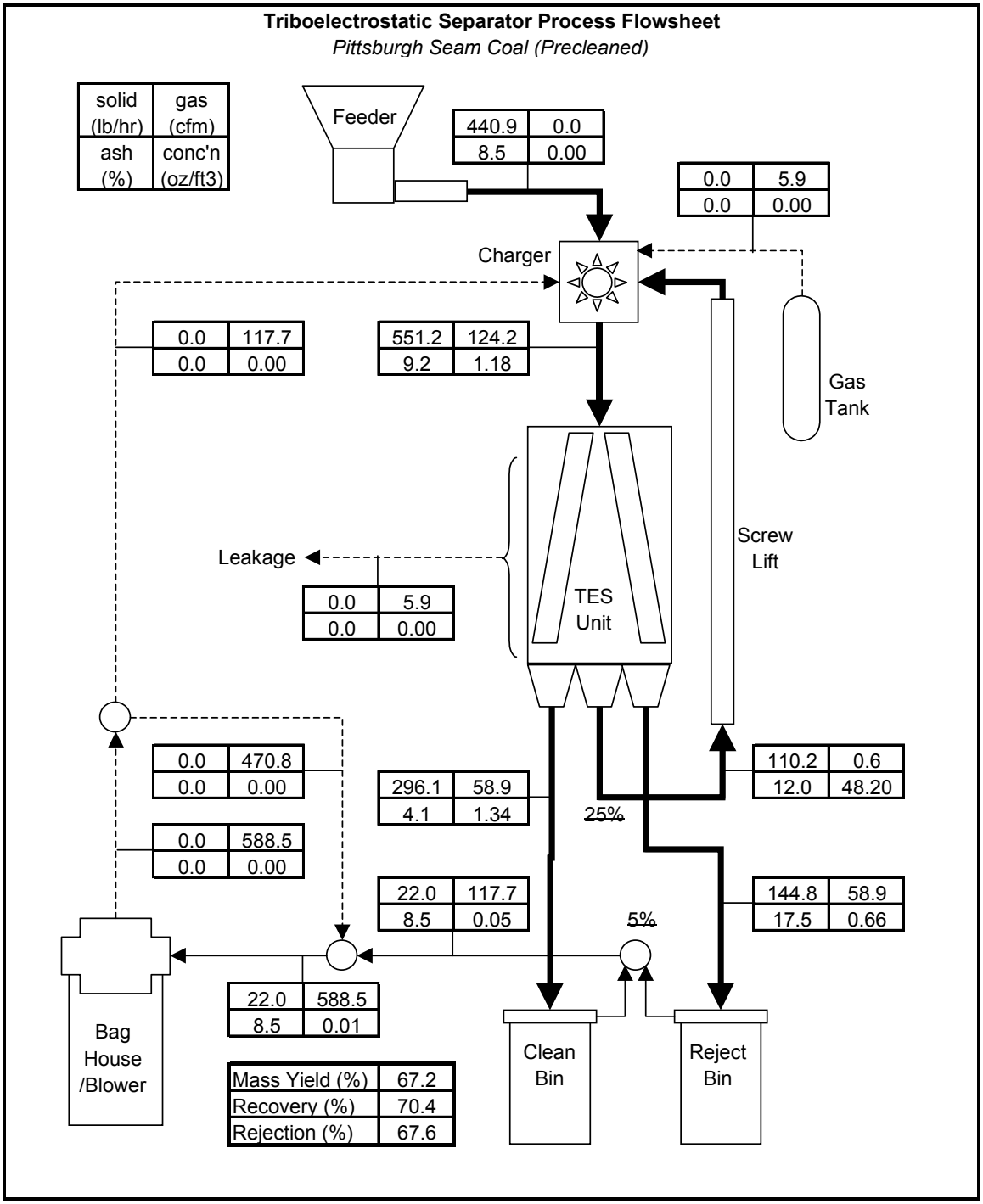

Figure D6. POC flowsheet and mass balance for the Pittsburgh No. 8 coal (English units).

APPENDIX E – POC-TEST DATA

Table E1. Results of POC tests conducted on intermediate products (Sample #1 & 2) from Shawville Power Plant. Single-stage rotating paddle charger.

Sample Origin	Sampling Point	Size	% Ash				% Wt Yield	% Comb. Recovery
			Feed	Clean	Reject	Middlings		
Shawville Jan-01	# 1 Sampling Port	35 x 0 Natural	28.38	24.86	31.09	0	43.41	45.5
			29.38	27.66	31.32	0	53.01	54.3
Shawville Jan-01	# 2 Sampling Port	35 x 0 Natural	24.47	22.41	29.41	0	70.41	72.3
			24.23	22.91	24.91	0	79.71	81.1
Shawville Oct-00	# 1 Sampling Port	35 x 0 Ground	30.98	16.05	38.65	42.73	33.91	41.2
			30.84	15.66	38.61	42.62	34.01	41.5
Shawville Jan-01	# 2 Sampling Port	35 x 0 Natural	24.52	9.7	28.22	34.6	19.98	15.88
			25.52	9.35	28.29	35.0	14.63	11.57
			24.52	12.73	27.91	30.88	22.33	18.45

Table E2. Results of POC tests conducted on intermediate products (Sample #1 & 2) from Shawville Power Plant. Two-stage rotating paddle charger.

Sample Origin	Sampling Point	Size	% Ash				% Wt Yield	% Comb. Recovery
			Feed	Clean	Reject	Middlings		
Shawville Jan-01	# 1 Sampling Port	35 x 0 Ground	35.13	29.37	39.87	44.49	45.1	49.2
			35.2	27.67	40.39	44.60	40.8	45.5
			36.33	28.28	38.65	44.35	22.4	25.2
Shawville Jan-01	# 2 Sampling Port	35 x 0 Natural	29.69	11.78	31.05	44.24	7.1	72.31

APPENDIX F – ECONOMIC ANALYSIS BACK-UP DATA

Raymond Mill Reject Sample

OPERATING DATA:

Utility Feed Rate (tph):	100	Operating Shifts/Day:	3
Raymond Mill Reject (%):	4	Operating Hours/Shift:	8
TES Feed Rate (tph):	4.0	Operating Days/Year:	360
Circuit Availability (%):	95	Operating Time (hr/yr):	8208
TES Capacity (lb/hr/ft):	500		
TES Total Width (ft)	16		
TES Units Required:	2		

Product Stream	Mass Yield (%)	Ash Assay (%)	Comb. Assay (%)	Sulfur Assay (%)	Energy Assay (Btu/lb)
Clean Coal	36.84	15.50	84.50	0.80	12253
Reject	63.16	64.90	35.10	0.80	5090
Feed	100.00	46.70	53.30	0.80	7729

Product Stream	Mass Recovery (%)	Ash Recovery (%)	Comb Recovery (%)	Sulfur Recovery (%)	Energy Recovery (%)
Clean Coal	36.84	12.23	58.41	36.84	58.41
Reject	63.16	87.77	41.59	63.16	41.59
Feed	100.00	100.00	100.00	100.00	100.00

Product Stream	Production Rate (tph)	Ash Rate (tph)	Comb. Rate (tph)	Sulfur Rate (tph)	Energy Rate (MM Btu/hr)
Clean Coal	1.47	0.23	1.25	0.01	36.11
Reject	2.53	1.64	0.89	0.02	25.72
Feed	4.00	1.87	2.13	0.03	61.83

Product Stream	Production Rate (tpy)	Ash Rate (tpy)	Comb. Rate (tpy)	Sulfur Rate (tpy)	Energy Rate (MM Btu/yr)
Clean Coal	12096	1875	10221	97	296412
Reject	20736	13458	7278	166	211072
Feed	32832	15333	17499	263	507484

Product Stream	SO2 Rate (tph)	SO2 Rate (tpy)	lb Ash per MM Btu	lb Sulfur per MM Btu	lb SO2 per MM Btu
Clean Coal	0.024	193.5	12.7	0.65	1.31
Reject	0.040	331.8	127.5	1.57	3.14
Feed	0.064	525.3	60.4	1.04	2.07

Raymond Mill Reject Sample

ESTIMATION FACTORS:

Installation Cost Factor:	1.00	Overhead Rate (%):	10
Maintenance Cost Factor:	0.10	Engineering/Permits (%):	5
Power Fee ($/KW-hr):	0.040	Circuit Life (yrs):	20

EQUIPMENT:

Equipment Description	Number of Units	Unit Equipment Cost ($)	Equipment Cost ($)	Unit Power (HP)	Total Power (HP)	Load Factor (%)	Power Required (KW)
Feed Collection Bin	1	$2,500	$2,500	0	0	0	0.00
Secondary Pulverizer	1	$28,000	$28,000	85	85	80	50.73
Protection Sieve	1	$2,000	$2,000	0	0	0	0.00
Feed Transfer Conveyor	1	$15,000	$15,000	12	12	80	7.16
Rotary Feed Distributor	1	$5,500	$5,500	5	5	80	2.98
Coal Transfer Conveyor	2	$12,500	$25,000	15	30	80	17.90
Reject Collection Bin	1	$2,500	$2,500	0	0	0	0.00
Reject Transfer Conveyor	1	$12,500	$12,500	12	12	80	7.16
TES Turbocharger	2	$11,500	$23,000	35	70	80	41.78
TES Separator	2	$105,000	$210,000	0	0	0	0.00
Power Supply	2	$22,500	$45,000	12	24	80	14.32
Flue Gas Blower	1	$2,500	$2,500	5	5	80	2.98
Piping/Chutes	1	$35,000	$35,000	0	0	0	0.00
Instrumentation	1	$18,500	$18,500	0.05	0.05	15	0.01

Total Equipment Cost ($)	$427,000	Total	243.05	Total	145.0
Installation Cost ($)	$427,000			Power Cost ($/yr)	$47,616
Overhead Cost ($)	$42,700				
Engineering/Permiting Cost ($)	$21,350				
Maintenance Cost ($/yr)	$42,700				

Raymond Mill Reject Sample

CONSUMABLES:

Item Description	Unit Cost ($/lb)	Dosage (lb/t feed)	Dosage (lb/t conc)	Unit Cost ($/t feed)	Unit Cost ($/t conc)	Annual Cost ($)
Lubricants	$0.10	0.10	0.27	$0.01	$0.03	$328
Contact Plates	$0.80	0.50	1.36	$0.40	$1.09	$13,133
Subtotal	**	0.60	1.63	$0.41	$1.11	$13,461

PERSONNEL:

Position Description	Salary ($/yr)	Benefits (%)	Benefits ($/yr)	Utilization Factor	Number Shifts	Annual Cost ($)
Operator	$50,000	50	$25,000	0.1	3	$22,500
					Total ($/yr)	$22,500

O&M COSTS:

Maintenance Cost ($/yr):	$42,700
Power Cost ($/yr):	$47,616
Consumables Cost ($/yr):	$13,461
Personnel Cost ($/yr):	$22,500
Total O&M Cost ($/yr):	$126,277
Total O&M Cost ($):	$2,525,534

FIXED COSTS:

Equipment Cost ($):	$427,000
Installation Cost ($):	$427,000
Overhead ($):	$42,700
Engineering Cost ($):	$21,350
Total Fixed Cost ($):	$918,050
Total FIxed Cost ($/yr):	$45,903

TOTAL COSTS:

Annual ($/yr)	$172,179
Clean Coal ($/ton)	$14.23
Raw Coal ($/ton)	$5.24
Total ($)	$3,443,584

Raymond Mill Reject Sample

COAL QUALITY SPECIFICATIONS:

	Clean Coal		Feed Coal
	Dry	As-Received	Dry
Ash (%):	15.50	14.42	46.70
Sulfur (%):	0.80	0.74	0.80
Heat Value (Btu/lb):	12253	11395	7729
Emission (lb SO2/MM Btu)	1.31	1.31	2.07
Moisture (%):	0.00	7.00	0.00

LEVELIZED COST/PRICE SCHEDULE:

	Clean Coal Basis (dry)		Clean Coal Basis (ar)		Raw Coal Basis (dry)	
	($/ton)	($/MM Btu)	($/ton)	($/MM Btu)	($/ton)	($/MM Btu)
Coal Pricing:						
Base Coal Price (FOB)	$32.26	$1.316	$30.00	$1.316	$11.88	$0.769
Btu Price Adjustment	($4.75)	($0.194)	($4.42)	($0.194)	($1.75)	($0.113)
Sulfur Penalty	($2.00)	($0.082)	($1.86)	($0.082)	($0.74)	($0.048)
Net Market Price (FOB)	$25.50	$1.041	$23.72	$1.041	$9.40	$0.608
Transportation Cost:	$21.51	$0.878	$20.00	$0.878	$7.92	$0.513
TES Production Cost:	$14.23	$0.581	$13.24	$0.581	$5.24	$0.339
Net Coal Value:	$32.78	$1.34	$30.48	$1.34	$12.08	$0.78

Raymond Mill Reject Sample

LOAN INFORMATION:

Capital Amount ($):	$918,050
Debt Carried (%):	0
Loan Carried ($):	$0
Loan Duration (yrs):	20
Interest Rate (%):	6

INFLATION FACTORS:

O&M Cost (%):	3
Coal Price (%):	3

Year	Loan Cost ($)	Principal Cost ($)	Interest Cost ($)	Principal/ Loan Ratio (%)	O&M Cost ($)	Total Cost ($)
0	$0	$0	$0	N/A	$0	$0
1	$0	$0	$0	N/A	$126,277	$126,277
2	$0	$0	$0	N/A	$130,065	$130,065
3	$0	$0	$0	N/A	$133,967	$133,967
4	$0	$0	$0	N/A	$137,986	$137,986
5	$0	$0	$0	N/A	$142,126	$142,126
6	$0	$0	$0	N/A	$146,389	$146,389
7	$0	$0	$0	N/A	$150,781	$150,781
8	$0	$0	$0	N/A	$155,304	$155,304
9	$0	$0	$0	N/A	$159,964	$159,964
10	$0	$0	$0	N/A	$164,762	$164,762
11	$0	$0	$0	N/A	$169,705	$169,705
12	$0	$0	$0	N/A	$174,797	$174,797
13	$0	$0	$0	N/A	$180,040	$180,040
14	$0	$0	$0	N/A	$185,442	$185,442
15	$0	$0	$0	N/A	$191,005	$191,005
16	$0	$0	$0	N/A	$196,735	$196,735
17	$0	$0	$0	N/A	$202,637	$202,637
18	$0	$0	$0	N/A	$208,716	$208,716
19	$0	$0	$0	N/A	$214,978	$214,978
20	$0	$0	$0	N/A	$221,427	$221,427
Total	$0	$0	$0	---	$3,393,103	$3,393,103

Raymond Mill Reject Sample

TAX INFORMATION:

Depr. Period (yrs): 7

Income Tax (%): 38

Year	Gross Revenue ($)	O&M Cost ($)	Interest Deduction ($)	Depreciation Deduction ($)	Net Taxable Income ($)	Income Tax ($)
0	$0	$0	$0	$0	$0	$0
1	$396,454	$126,277	$0	$131,150	$139,027	$52,830
2	$408,347	$130,065	$0	$131,150	$147,132	$55,910
3	$420,598	$133,967	$0	$131,150	$155,481	$59,083
4	$433,216	$137,986	$0	$131,150	$164,080	$62,350
5	$446,212	$142,126	$0	$131,150	$172,937	$65,716
6	$459,599	$146,389	$0	$131,150	$182,059	$69,183
7	$473,387	$150,781	$0	$131,150	$191,456	$72,753
8	$487,588	$155,304	$0	$0	$332,284	$126,268
9	$502,216	$159,964	$0	$0	$342,252	$130,056
10	$517,282	$164,762	$0	$0	$352,520	$133,958
11	$532,801	$169,705	$0	$0	$363,095	$137,976
12	$548,785	$174,797	$0	$0	$373,988	$142,116
13	$565,248	$180,040	$0	$0	$385,208	$146,379
14	$582,206	$185,442	$0	$0	$396,764	$150,770
15	$599,672	$191,005	$0	$0	$408,667	$155,293
16	$617,662	$196,735	$0	$0	$420,927	$159,952
17	$636,192	$202,637	$0	$0	$433,555	$164,751
18	$655,278	$208,716	$0	$0	$446,561	$169,693
19	$674,936	$214,978	$0	$0	$459,958	$174,784
20	$695,184	$221,427	$0	$0	$473,757	$180,028
Total	$10,652,861	$3,393,103	$0	$918,050	$6,341,708	$2,409,849

Raymond Mill Reject Sample

FINANCIAL DATA:

Discount Rate (%) 10

Year	Cash Inflow ($)	Capital Purchase ($)	O&M Cost ($)	Loan Cost ($)	Income Tax ($)	Net Cash ($)
0	$0	$918,050	$0	$0	$0	($918,050)
1	$396,454	$0	$126,277	$0	$52,830	$217,347
2	$408,347	$0	$130,065	$0	$55,910	$222,372
3	$420,598	$0	$133,967	$0	$59,083	$227,548
4	$433,216	$0	$137,986	$0	$62,350	$232,879
5	$446,212	$0	$142,126	$0	$65,716	$238,371
6	$459,599	$0	$146,389	$0	$69,183	$244,027
7	$473,387	$0	$150,781	$0	$72,753	$249,852
8	$487,588	$0	$155,304	$0	$126,268	$206,016
9	$502,216	$0	$159,964	$0	$130,056	$212,196
10	$517,282	$0	$164,762	$0	$133,958	$218,562
11	$532,801	$0	$169,705	$0	$137,976	$225,119
12	$548,785	$0	$174,797	$0	$142,116	$231,873
13	$565,248	$0	$180,040	$0	$146,379	$238,829
14	$582,206	$0	$185,442	$0	$150,770	$245,994
15	$599,672	$0	$191,005	$0	$155,293	$253,374
16	$617,662	$0	$196,735	$0	$159,952	$260,975
17	$636,192	$0	$202,637	$0	$164,751	$268,804
18	$655,278	$0	$208,716	$0	$169,693	$276,868
19	$674,936	$0	$214,978	$0	$174,784	$285,174
20	$695,184	$0	$221,427	$0	$180,028	$293,729
Total	$10,652,861	$918,050	$3,393,103	$0	$2,409,849	$3,931,859

FINANCIAL SUMMARY:

Total Net Income ($):	$10,652,861
Total Net Payout ($):	$6,721,002
Total Net Profit ($):	$3,931,859
Internal Rate of Return:	24.58%
Net Present Value:	$1,075,134
Payback Period (yrs):	4.22

Raymond Mill Reject Sample

LOAN INFORMATION:

Capital Amount ($):	$918,050
Debt Carried (%):	25
Loan Carried ($):	$229,513
Loan Duration (yrs):	20
Interest Rate (%):	6

INFLATION FACTORS:

O&M Cost (%):	3
Coal Price (%):	3

Year	Loan Cost ($)	Principal Cost ($)	Interest Cost ($)	Principal/ Loan Ratio (%)	O&M Cost ($)	Total Cost ($)
0	$0	$0	$0	N/A	$0	$0
1	$20,010	$6,239	$13,771	31.18	$126,277	$146,287
2	$20,010	$6,614	$13,396	33.05	$130,065	$150,075
3	$20,010	$7,010	$13,000	35.03	$133,967	$153,977
4	$20,010	$7,431	$12,579	37.14	$137,986	$157,996
5	$20,010	$7,877	$12,133	39.36	$142,126	$162,135
6	$20,010	$8,349	$11,660	41.73	$146,389	$166,399
7	$20,010	$8,850	$11,160	44.23	$150,781	$170,791
8	$20,010	$9,381	$10,629	46.88	$155,304	$175,314
9	$20,010	$9,944	$10,066	49.70	$159,964	$179,974
10	$20,010	$10,541	$9,469	52.68	$164,762	$184,772
11	$20,010	$11,173	$8,836	55.84	$169,705	$189,715
12	$20,010	$11,844	$8,166	59.19	$174,797	$194,806
13	$20,010	$12,554	$7,455	62.74	$180,040	$200,050
14	$20,010	$13,308	$6,702	66.51	$185,442	$205,452
15	$20,010	$14,106	$5,904	70.50	$191,005	$211,015
16	$20,010	$14,953	$5,057	74.73	$196,735	$216,745
17	$20,010	$15,850	$4,160	79.21	$202,637	$222,647
18	$20,010	$16,801	$3,209	83.96	$208,716	$228,726
19	$20,010	$17,809	$2,201	89.00	$214,978	$234,988
20	$20,010	$18,877	$1,133	94.34	$221,427	$241,437
Total	$400,199	$229,513	$170,686	---	$3,393,103	$3,793,301

Raymond Mill Reject Sample

TAX INFORMATION:

Depr. Period (yrs): 7

Income Tax (%): 38

Year	Gross Revenue ($)	O&M Cost ($)	Interest Deduction ($)	Depreciation Deduction ($)	Net Taxable Income ($)	Income Tax ($)
0	$0	$0	$0	$0	$0	$0
1	$396,454	$126,277	$13,771	$131,150	$125,256	$47,597
2	$408,347	$130,065	$13,396	$131,150	$133,736	$50,820
3	$420,598	$133,967	$13,000	$131,150	$142,481	$54,143
4	$433,216	$137,986	$12,579	$131,150	$151,501	$57,570
5	$446,212	$142,126	$12,133	$131,150	$160,804	$61,105
6	$459,599	$146,389	$11,660	$131,150	$170,399	$64,752
7	$473,387	$150,781	$11,160	$131,150	$180,296	$68,512
8	$487,588	$155,304	$10,629	$0	$321,655	$122,229
9	$502,216	$159,964	$10,066	$0	$332,187	$126,231
10	$517,282	$164,762	$9,469	$0	$343,051	$130,359
11	$532,801	$169,705	$8,836	$0	$354,259	$134,618
12	$548,785	$174,797	$8,166	$0	$365,822	$139,012
13	$565,248	$180,040	$7,455	$0	$377,752	$143,546
14	$582,206	$185,442	$6,702	$0	$390,062	$148,224
15	$599,672	$191,005	$5,904	$0	$402,763	$153,050
16	$617,662	$196,735	$5,057	$0	$415,870	$158,030
17	$636,192	$202,637	$4,160	$0	$429,395	$163,170
18	$655,278	$208,716	$3,209	$0	$443,352	$168,474
19	$674,936	$214,978	$2,201	$0	$457,757	$173,948
20	$695,184	$221,427	$1,133	$0	$472,624	$179,597
Total	$10,652,861	$3,393,103	$170,686	$918,050	$6,171,022	$2,344,988

Raymond Mill Reject Sample

FINANCIAL DATA:

Discount Rate (%) 10

Year	Cash Inflow ($)	Capital Purchase ($)	O&M Cost ($)	Loan Cost ($)	Income Tax ($)	Net Cash ($)
0	$229,513	$918,050	$0	$0	$0	($688,538)
1	$396,454	$0	$126,277	$20,010	$47,597	$202,570
2	$408,347	$0	$130,065	$20,010	$50,820	$207,453
3	$420,598	$0	$133,967	$20,010	$54,143	$212,478
4	$433,216	$0	$137,986	$20,010	$57,570	$217,650
5	$446,212	$0	$142,126	$20,010	$61,105	$222,971
6	$459,599	$0	$146,389	$20,010	$64,752	$228,448
7	$473,387	$0	$150,781	$20,010	$68,512	$234,083
8	$487,588	$0	$155,304	$20,010	$122,229	$190,045
9	$502,216	$0	$159,964	$20,010	$126,231	$196,011
10	$517,282	$0	$164,762	$20,010	$130,359	$202,151
11	$532,801	$0	$169,705	$20,010	$134,618	$208,467
12	$548,785	$0	$174,797	$20,010	$139,012	$214,966
13	$565,248	$0	$180,040	$20,010	$143,546	$221,652
14	$582,206	$0	$185,442	$20,010	$148,224	$228,531
15	$599,672	$0	$191,005	$20,010	$153,050	$235,607
16	$617,662	$0	$196,735	$20,010	$158,030	$242,887
17	$636,192	$0	$202,637	$20,010	$163,170	$250,375
18	$655,278	$0	$208,716	$20,010	$168,474	$258,078
19	$674,936	$0	$214,978	$20,010	$173,948	$266,001
20	$695,184	$0	$221,427	$20,010	$179,597	$274,150
Total	$10,882,373	$918,050	$3,393,103	$400,199	$2,344,988	$3,826,033

FINANCIAL SUMMARY:

Total Net Income ($):	$10,882,373
Total Net Payout ($):	$7,056,340
Total Net Profit ($):	$3,826,033
Internal Rate of Return:	30.65%
Net Present Value:	$1,168,009
Payback Period (yrs):	4.53

Raymond Mill Reject Sample

LOAN INFORMATION:

Capital Amount ($):	$918,050
Debt Carried (%):	50
Loan Carried ($):	$459,025
Loan Duration (yrs):	20
Interest Rate (%):	6

INFLATION FACTORS:

O&M Cost (%):	3
Coal Price (%):	3

Year	Loan Cost ($)	Principal Cost ($)	Interest Cost ($)	Principal/ Loan Ratio (%)	O&M Cost ($)	Total Cost ($)
0	$0	$0	$0	N/A	$0	$0
1	$40,020	$12,478	$27,542	31.18	$126,277	$166,297
2	$40,020	$13,227	$26,793	33.05	$130,065	$170,085
3	$40,020	$14,021	$25,999	35.03	$133,967	$173,987
4	$40,020	$14,862	$25,158	37.14	$137,986	$178,006
5	$40,020	$15,754	$24,266	39.36	$142,126	$182,145
6	$40,020	$16,699	$23,321	41.73	$146,389	$186,409
7	$40,020	$17,701	$22,319	44.23	$150,781	$190,801
8	$40,020	$18,763	$21,257	46.88	$155,304	$195,324
9	$40,020	$19,889	$20,131	49.70	$159,964	$199,983
10	$40,020	$21,082	$18,938	52.68	$164,762	$204,782
11	$40,020	$22,347	$17,673	55.84	$169,705	$209,725
12	$40,020	$23,688	$16,332	59.19	$174,797	$214,816
13	$40,020	$25,109	$14,911	62.74	$180,040	$220,060
14	$40,020	$26,616	$13,404	66.51	$185,442	$225,461
15	$40,020	$28,212	$11,807	70.50	$191,005	$231,025
16	$40,020	$29,905	$10,115	74.73	$196,735	$236,755
17	$40,020	$31,700	$8,320	79.21	$202,637	$242,657
18	$40,020	$33,601	$6,418	83.96	$208,716	$248,736
19	$40,020	$35,618	$4,402	89.00	$214,978	$254,998
20	$40,020	$37,755	$2,265	94.34	$221,427	$261,447
Total	$800,398	$459,025	$341,373	---	$3,393,103	$4,193,500

Raymond Mill Reject Sample

TAX INFORMATION:

Depr. Period (yrs): 7

Income Tax (%): 38

Year	Gross Revenue ($)	O&M Cost ($)	Interest Deduction ($)	Depreciation Deduction ($)	Net Taxable Income ($)	Income Tax ($)
0	$0	$0	$0	$0	$0	$0
1	$396,454	$126,277	$27,542	$131,150	$111,486	$42,365
2	$408,347	$130,065	$26,793	$131,150	$120,340	$45,729
3	$420,598	$133,967	$25,999	$131,150	$129,482	$49,203
4	$433,216	$137,986	$25,158	$131,150	$138,922	$52,790
5	$446,212	$142,126	$24,266	$131,150	$148,670	$56,495
6	$459,599	$146,389	$23,321	$131,150	$158,738	$60,321
7	$473,387	$150,781	$22,319	$131,150	$169,136	$64,272
8	$487,588	$155,304	$21,257	$0	$311,027	$118,190
9	$502,216	$159,964	$20,131	$0	$322,121	$122,406
10	$517,282	$164,762	$18,938	$0	$333,582	$126,761
11	$532,801	$169,705	$17,673	$0	$345,422	$131,260
12	$548,785	$174,797	$16,332	$0	$357,656	$135,909
13	$565,248	$180,040	$14,911	$0	$370,297	$140,713
14	$582,206	$185,442	$13,404	$0	$383,360	$145,677
15	$599,672	$191,005	$11,807	$0	$396,860	$150,807
16	$617,662	$196,735	$10,115	$0	$410,812	$156,109
17	$636,192	$202,637	$8,320	$0	$425,234	$161,589
18	$655,278	$208,716	$6,418	$0	$440,143	$167,254
19	$674,936	$214,978	$4,402	$0	$455,556	$173,111
20	$695,184	$221,427	$2,265	$0	$471,492	$179,167
Total	$10,652,861	$3,393,103	$341,373	$918,050	$6,000,335	$2,280,127

Raymond Mill Reject Sample

FINANCIAL DATA:

Discount Rate (%) 10

Year	Cash Inflow ($)	Capital Purchase ($)	O&M Cost ($)	Loan Cost ($)	Income Tax ($)	Net Cash ($)
0	$459,025	$918,050	$0	$0	$0	($459,025)
1	$396,454	$0	$126,277	$40,020	$42,365	$187,793
2	$408,347	$0	$130,065	$40,020	$45,729	$192,533
3	$420,598	$0	$133,967	$40,020	$49,203	$197,408
4	$433,216	$0	$137,986	$40,020	$52,790	$202,420
5	$446,212	$0	$142,126	$40,020	$56,495	$207,572
6	$459,599	$0	$146,389	$40,020	$60,321	$212,869
7	$473,387	$0	$150,781	$40,020	$64,272	$218,314
8	$487,588	$0	$155,304	$40,020	$118,190	$174,074
9	$502,216	$0	$159,964	$40,020	$122,406	$179,826
10	$517,282	$0	$164,762	$40,020	$126,761	$185,739
11	$532,801	$0	$169,705	$40,020	$131,260	$191,815
12	$548,785	$0	$174,797	$40,020	$135,909	$198,059
13	$565,248	$0	$180,040	$40,020	$140,713	$204,475
14	$582,206	$0	$185,442	$40,020	$145,677	$211,068
15	$599,672	$0	$191,005	$40,020	$150,807	$217,840
16	$617,662	$0	$196,735	$40,020	$156,109	$224,798
17	$636,192	$0	$202,637	$40,020	$161,589	$231,946
18	$655,278	$0	$208,716	$40,020	$167,254	$239,287
19	$674,936	$0	$214,978	$40,020	$173,111	$246,827
20	$695,184	$0	$221,427	$40,020	$179,167	$254,570
Total	$11,111,886	$918,050	$3,393,103	$800,398	$2,280,127	$3,720,208

FINANCIAL SUMMARY:

Total Net Income ($):	$11,111,886
Total Net Payout ($):	$7,391,678
Total Net Profit ($):	$3,720,208
Internal Rate of Return:	42.55%
Net Present Value:	$1,260,885
Payback Period (yrs):	4.89

Raymond Mill Reject Sample

LOAN INFORMATION:

Capital Amount ($):	$918,050
Debt Carried (%):	75
Loan Carried ($):	$688,538
Loan Duration (yrs):	20
Interest Rate (%):	6

INFLATION FACTORS:

O&M Cost (%):	3
Coal Price (%):	3

Year	Loan Cost ($)	Principal Cost ($)	Interest Cost ($)	Principal/ Loan Ratio (%)	O&M Cost ($)	Total Cost ($)
0	$0	$0	$0	N/A	$0	$0
1	$60,030	$18,718	$41,312	31.18	$126,277	$186,307
2	$60,030	$19,841	$40,189	33.05	$130,065	$190,095
3	$60,030	$21,031	$38,999	35.03	$133,967	$193,997
4	$60,030	$22,293	$37,737	37.14	$137,986	$198,016
5	$60,030	$23,631	$36,399	39.36	$142,126	$202,155
6	$60,030	$25,048	$34,981	41.73	$146,389	$206,419
7	$60,030	$26,551	$33,479	44.23	$150,781	$210,811
8	$60,030	$28,144	$31,886	46.88	$155,304	$215,334
9	$60,030	$29,833	$30,197	49.70	$159,964	$219,993
10	$60,030	$31,623	$28,407	52.68	$164,762	$224,792
11	$60,030	$33,520	$26,509	55.84	$169,705	$229,735
12	$60,030	$35,532	$24,498	59.19	$174,797	$234,826
13	$60,030	$37,663	$22,366	62.74	$180,040	$240,070
14	$60,030	$39,923	$20,107	66.51	$185,442	$245,471
15	$60,030	$42,319	$17,711	70.50	$191,005	$251,035
16	$60,030	$44,858	$15,172	74.73	$196,735	$256,765
17	$60,030	$47,549	$12,481	79.21	$202,637	$262,667
18	$60,030	$50,402	$9,628	83.96	$208,716	$268,746
19	$60,030	$53,426	$6,603	89.00	$214,978	$275,007
20	$60,030	$56,632	$3,398	94.34	$221,427	$281,457
Total	$1,200,597	$688,538	$512,059	---	$3,393,103	$4,593,699

Raymond Mill Reject Sample

TAX INFORMATION:

Depr. Period (yrs): 7

Income Tax (%): 38

Year	Gross Revenue ($)	O&M Cost ($)	Interest Deduction ($)	Depreciation Deduction ($)	Net Taxable Income ($)	Income Tax ($)
0	$0	$0	$0	$0	$0	$0
1	$396,454	$126,277	$41,312	$131,150	$97,715	$37,132
2	$408,347	$130,065	$40,189	$131,150	$106,943	$40,638
3	$420,598	$133,967	$38,999	$131,150	$116,482	$44,263
4	$433,216	$137,986	$37,737	$131,150	$126,343	$48,010
5	$446,212	$142,126	$36,399	$131,150	$136,537	$51,884
6	$459,599	$146,389	$34,981	$131,150	$147,078	$55,890
7	$473,387	$150,781	$33,479	$131,150	$157,977	$60,031
8	$487,588	$155,304	$31,886	$0	$300,398	$114,151
9	$502,216	$159,964	$30,197	$0	$312,055	$118,581
10	$517,282	$164,762	$28,407	$0	$324,113	$123,163
11	$532,801	$169,705	$26,509	$0	$336,586	$127,903
12	$548,785	$174,797	$24,498	$0	$349,490	$132,806
13	$565,248	$180,040	$22,366	$0	$362,841	$137,880
14	$582,206	$185,442	$20,107	$0	$376,658	$143,130
15	$599,672	$191,005	$17,711	$0	$390,956	$148,563
16	$617,662	$196,735	$15,172	$0	$405,755	$154,187
17	$636,192	$202,637	$12,481	$0	$421,074	$160,008
18	$655,278	$208,716	$9,628	$0	$436,934	$166,035
19	$674,936	$214,978	$6,603	$0	$453,355	$172,275
20	$695,184	$221,427	$3,398	$0	$470,359	$178,736
Total	$10,652,861	$3,393,103	$512,059	$918,050	$5,829,649	$2,215,267

Raymond Mill Reject Sample

FINANCIAL DATA:

Discount Rate (%) 10

Year	Cash Inflow ($)	Capital Purchase ($)	O&M Cost ($)	Loan Cost ($)	Income Tax ($)	Net Cash ($)
0	$688,538	$918,050	$0	$0	$0	($229,513)
1	$396,454	$0	$126,277	$60,030	$37,132	$173,016
2	$408,347	$0	$130,065	$60,030	$40,638	$177,614
3	$420,598	$0	$133,967	$60,030	$44,263	$182,338
4	$433,216	$0	$137,986	$60,030	$48,010	$187,190
5	$446,212	$0	$142,126	$60,030	$51,884	$192,173
6	$459,599	$0	$146,389	$60,030	$55,890	$197,290
7	$473,387	$0	$150,781	$60,030	$60,031	$202,544
8	$487,588	$0	$155,304	$60,030	$114,151	$158,103
9	$502,216	$0	$159,964	$60,030	$118,581	$163,641
10	$517,282	$0	$164,762	$60,030	$123,163	$169,327
11	$532,801	$0	$169,705	$60,030	$127,903	$175,163
12	$548,785	$0	$174,797	$60,030	$132,806	$181,152
13	$565,248	$0	$180,040	$60,030	$137,880	$187,298
14	$582,206	$0	$185,442	$60,030	$143,130	$193,604
15	$599,672	$0	$191,005	$60,030	$148,563	$200,074
16	$617,662	$0	$196,735	$60,030	$154,187	$206,710
17	$636,192	$0	$202,637	$60,030	$160,008	$213,517
18	$655,278	$0	$208,716	$60,030	$166,035	$220,497
19	$674,936	$0	$214,978	$60,030	$172,275	$227,654
20	$695,184	$0	$221,427	$60,030	$178,736	$234,991
Total	$11,341,398	$918,050	$3,393,103	$1,200,597	$2,215,267	$3,614,382

FINANCIAL SUMMARY:

Total Net Income ($):	$11,341,398
Total Net Payout ($):	$7,727,016
Total Net Profit ($):	$3,614,382
Internal Rate of Return:	77.67%
Net Present Value:	$1,353,761
Payback Period (yrs):	5.31

Raymond Mill Reject Sample

LOAN INFORMATION:

Capital Amount ($):	$918,050
Debt Carried (%):	100
Loan Carried ($):	$918,050
Loan Duration (yrs):	20
Interest Rate (%):	6

INFLATION FACTORS:

O&M Cost (%):	3
Coal Price (%):	3

Year	Loan Cost ($)	Principal Cost ($)	Interest Cost ($)	Principal/ Loan Ratio (%)	O&M Cost ($)	Total Cost ($)
0	$0	$0	$0	N/A	$0	$0
1	$80,040	$24,957	$55,083	31.18	$126,277	$206,316
2	$80,040	$26,454	$53,586	33.05	$130,065	$210,105
3	$80,040	$28,041	$51,998	35.03	$133,967	$214,007
4	$80,040	$29,724	$50,316	37.14	$137,986	$218,026
5	$80,040	$31,507	$48,532	39.36	$142,126	$222,165
6	$80,040	$33,398	$46,642	41.73	$146,389	$226,429
7	$80,040	$35,402	$44,638	44.23	$150,781	$230,821
8	$80,040	$37,526	$42,514	46.88	$155,304	$235,344
9	$80,040	$39,777	$40,262	49.70	$159,964	$240,003
10	$80,040	$42,164	$37,876	52.68	$164,762	$244,802
11	$80,040	$44,694	$35,346	55.84	$169,705	$249,745
12	$80,040	$47,375	$32,664	59.19	$174,797	$254,836
13	$80,040	$50,218	$29,822	62.74	$180,040	$260,080
14	$80,040	$53,231	$26,809	66.51	$185,442	$265,481
15	$80,040	$56,425	$23,615	70.50	$191,005	$271,045
16	$80,040	$59,810	$20,229	74.73	$196,735	$276,775
17	$80,040	$63,399	$16,641	79.21	$202,637	$282,677
18	$80,040	$67,203	$12,837	83.96	$208,716	$288,756
19	$80,040	$71,235	$8,805	89.00	$214,978	$295,017
20	$80,040	$75,509	$4,531	94.34	$221,427	$301,467
Total	$1,600,796	$918,050	$682,746	---	$3,393,103	$4,993,898

Raymond Mill Reject Sample

TAX INFORMATION:

Depr. Period (yrs): 7

Income Tax (%): 38

Year	Gross Revenue ($)	O&M Cost ($)	Interest Deduction ($)	Depreciation Deduction ($)	Net Taxable Income ($)	Income Tax ($)
0	$0	$0	$0	$0	$0	$0
1	$396,454	$126,277	$55,083	$131,150	$83,944	$31,899
2	$408,347	$130,065	$53,586	$131,150	$93,547	$35,548
3	$420,598	$133,967	$51,998	$131,150	$103,482	$39,323
4	$433,216	$137,986	$50,316	$131,150	$113,764	$43,230
5	$446,212	$142,126	$48,532	$131,150	$124,404	$47,274
6	$459,599	$146,389	$46,642	$131,150	$135,417	$51,459
7	$473,387	$150,781	$44,638	$131,150	$146,817	$55,791
8	$487,588	$155,304	$42,514	$0	$289,770	$110,112
9	$502,216	$159,964	$40,262	$0	$301,990	$114,756
10	$517,282	$164,762	$37,876	$0	$314,644	$119,565
11	$532,801	$169,705	$35,346	$0	$327,749	$124,545
12	$548,785	$174,797	$32,664	$0	$341,324	$129,703
13	$565,248	$180,040	$29,822	$0	$355,386	$135,047
14	$582,206	$185,442	$26,809	$0	$369,955	$140,583
15	$599,672	$191,005	$23,615	$0	$385,052	$146,320
16	$617,662	$196,735	$20,229	$0	$400,698	$152,265
17	$636,192	$202,637	$16,641	$0	$416,914	$158,427
18	$655,278	$208,716	$12,837	$0	$433,725	$164,815
19	$674,936	$214,978	$8,805	$0	$451,154	$171,438
20	$695,184	$221,427	$4,531	$0	$469,227	$178,306
Total	$10,652,861	$3,393,103	$682,746	$918,050	$5,658,963	$2,150,406

Raymond Mill Reject Sample

FINANCIAL DATA:

Discount Rate (%) 10

Year	Cash Inflow ($)	Capital Purchase ($)	O&M Cost ($)	Loan Cost ($)	Income Tax ($)	Net Cash ($)
0	$918,050	$918,050	$0	$0	$0	$0
1	$396,454	$0	$126,277	$80,040	$31,899	$158,239
2	$408,347	$0	$130,065	$80,040	$35,548	$162,695
3	$420,598	$0	$133,967	$80,040	$39,323	$167,268
4	$433,216	$0	$137,986	$80,040	$43,230	$171,960
5	$446,212	$0	$142,126	$80,040	$47,274	$176,773
6	$459,599	$0	$146,389	$80,040	$51,459	$181,711
7	$473,387	$0	$150,781	$80,040	$55,791	$186,775
8	$487,588	$0	$155,304	$80,040	$110,112	$142,131
9	$502,216	$0	$159,964	$80,040	$114,756	$147,456
10	$517,282	$0	$164,762	$80,040	$119,565	$152,915
11	$532,801	$0	$169,705	$80,040	$124,545	$158,511
12	$548,785	$0	$174,797	$80,040	$129,703	$164,245
13	$565,248	$0	$180,040	$80,040	$135,047	$170,121
14	$582,206	$0	$185,442	$80,040	$140,583	$176,141
15	$599,672	$0	$191,005	$80,040	$146,320	$182,307
16	$617,662	$0	$196,735	$80,040	$152,265	$188,622
17	$636,192	$0	$202,637	$80,040	$158,427	$195,088
18	$655,278	$0	$208,716	$80,040	$164,815	$201,706
19	$674,936	$0	$214,978	$80,040	$171,438	$208,480
20	$695,184	$0	$221,427	$80,040	$178,306	$215,411
Total	$11,570,911	$918,050	$3,393,103	$1,600,796	$2,150,406	$3,508,557

FINANCIAL SUMMARY:

Total Net Income ($):	$11,570,911
Total Net Payout ($):	$8,062,354
Total Net Profit ($):	$3,508,557
Internal Rate of Return:	#DIV/0!
Net Present Value:	$1,446,637
Payback Period (yrs):	5.80